

BARC

NEWSLETTER



भाभा परमाणु अनुसंधान केंद्र
BHABHA ATOMIC RESEARCH CENTRE



IN THIS ISSUE

- Uncertainty Quantification of Contaminant Transport through Geological Repository using 2D Monte Carlo Simulation
- Development and Application of Radiotracer Technique for Online Leak Detection in High Pressure Heat Exchangers
- Design and Development of Weld Inspection Manipulator for Reactor Pressure Vessel of TAPS-1
- Machinery Protection System for Large Rotating Machines
- Development of DSP-based Signal Acquisition and Processing System for Extrinsic Fabry-Perot Interferometric (EFBI) Fiber Optics Sensors



In the Forthcoming Issue

- 1. Microwave Processing in Thorium Fuel Cycle**
G. K. Mallik
- 2. Emergent biofilm control strategies based on controlled release of antimicrobials: potential industrial and biomedical applications**
V. P. Venugopalan et al.
- 3. Atomic, molecular, and cluster physics with an indigenously developed supersonic molecular beam**
S.G. Nakhate, Sheo Mukund and Soumen Bhattacharyya
- 4. Synthetic and Structural Studies of Uranyl Complexes**
S. Kannan
- 5. Development of hybrid micro circuit based multi-channel programmable HV supply for BARC-pelletron experimental facility**
Manna, S. et al.
- 6. Xenon transport in uranium-10wt % zirconium alloy**
S. Kolay, et al.
- 7. Diffusion bonding of Nuclear Materials**
K. Bhanumurthy, et al.

CONTENTS

<i>Editorial Note</i>	ii
Interview with Shri Sekhar Basu, Director, BARC	iii
Brief Communications	
• Nodalization of Advanced Heavy Water Reactor Core for Efficient Spatial Control	viii
• Tele Distress Alarm Device	ix
• Studies on Separation and Purification of Fission ⁹⁹ Mo from Uranium Aluminium Alloy	x
• Spot Picker Robot	xi
Focus	
• Design and Development of Advanced Reactors <i>K.K. Vaze</i>	xii
Research Article	
• Uncertainty Quantification of Contaminant Transport through Geological Repository using 2D Monte Carlo Simulation <i>D.Datta, M. Pandey, Brij Kumar and P.S. Sharma</i>	1
Technology Development Articles	
• Development and Application of Radiotracer Technique for Online Leak Detection in High Pressure Heat Exchangers <i>H.J. Pant, V.K. Sharma, S. Goswami, J. Samantray and Gursharan Singh</i>	8
• Design and Development of Weld Inspection Manipulator for Reactor Pressure Vessel of TAPS-1 <i>H. Chatterjee, J.P. Singh, R. Ranjon, M.P. Kulkarni and R.J. Patel</i>	16
• Machinery Protection System for Large Rotating Machines <i>S.K. Jain, M. Kalra, Gaurav and D.A. Roy</i>	23
• Development of DSP-based Signal Acquisition and Processing System for Extrinsic Fabry-Perot Interferometric (EFBI) Fiber Optics Sensors <i>A. Rathod, S. Mishra, S. Ghildayal, S. Bahuguna, S. Dhage and S. Mukhopadhyay</i>	30
News and Events	
• Report on DAE-BRNS 4 th Interdisciplinary Symposium on Materials Chemistry (ISMS-2012)	36
• A Brief Report on National Seminar-cum-Workshop on "Water and Energy: Sustainability & Security for Future Needs"	37
• Report on the IPA Theme Meeting on Synergy in Physics and Industry (SPI-2013)	38
BARC Scientists Honoured	

Editorial Committee**Chairman**

Dr. S.K. Apte,
Associate Director, BMG

Edited by

Dr. K. Bhanumurthy
Head, SIRD

Associate Editors for this issue

Dr. A.P. Tiwari, RCnD
Dr. D.N. Badodkar, DRHR

Members

Dr. S.K. Apte, BMG
Dr. R.C. Hubli, MPD
Dr. D.N. Badodkar, DRHR
Dr. K.T. Shenoy, ChED
Dr. K. Bhanumurthy, SIRD
Dr. S. Kannan, FCD
Dr. A.P. Tiwari, RCnD
Dr. A.K. Tyagi, ChD
Mr. G. Venugopala Rao, APPD
Dr. C. Srinivas, PsDD
Dr. G. Rami Reddy, RSD
Dr. A.K. Nayak, RED
Dr. S.M. Yusuf, SSPD
Dr. S.K. Sandur, RB&HSD
Dr. S.C. Deokattey, SIRD

From the Editor's Desk

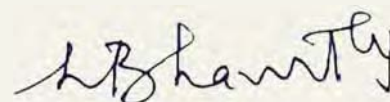
Dr. S.K. Apte, Associate Director, Bio-Medical Group has taken over as the New Chairman of the BARC Newsletter Editorial Committee. His contributions will further improve the quality and the content of the BARC Newsletter. In addition, few new members are added for the editorial committee and we look forward to work closely to enhance the quality of articles. I would like to place on record the excellent contributions of the members of the earlier editorial committee, Dr. N. Ramamoorthy, Mr. C.S.R. Prasad, Dr. Madangopal Krishnan, Dr. P. V. Varde, Mr. Avaneesh Sharma, Dr. S. K. Mukherjee, Dr. A. Vinod Kumar and Dr. Anand Ballal and also for bringing new ideas for enhancing the content of BARC Newsletter.

Welcome to the first issue of the BARC Newsletter for the year 2013.

In this issue, Director BARC wishes all the members of BARC fraternity good wishes for 2013 and also addresses the BARC Community through a series of questions put forth by the BARC Newsletter Editorial Committee members.

In this issue, we also cover Shri K.K. Vaze's article under the Group Directors contributions. His article traces research and development in BARC on Advanced Reactor Concepts with emphasis on Thorium utilization.

Apart from the above, Four Brief Communications and six articles are also featured in this issue.



Dr. K. Bhanumurthy
On behalf of the Editorial Committee

Interview with Shri Sekhar Basu, Director, BARC

Q.1: " You have recently taken over as Director, BARC. What would be your priorities in further enhancing the mandate of BARC?"

First of all, let me take this opportunity to wish all my colleagues a very happy and productive new year! I am glad of this opportunity provided by the BARC Newsletter Editorial Committee, to get my views across to the BARC fraternity, through this Question-Answer session.

R&D Programmes and projects at BARC are structured in 5-year time frames. At this stage of our programme, XI Plan activities are coming to an end and XII Plan work has been initiated. Our first priority is to complete the work taken up in the XI Plan at the earliest possible. We are also gearing-up for the new activities that have been proposed in the XII Plan, which include new reactors, accelerators, Indian Neutrino Observatory programme, reprocessing programme, etc. I would also like to see a multifold rise in our contribution to agriculture, food preservation, health care and desalination activities.

Q.2: What would be the flagship programmes of BARC, in keeping with its status as a premier institute of R&D for Nuclear Science & Technology?

Our flagship programmes include: the development of the Indian Pressurized Water Reactor, large scale accelerators, Indian Neutrino Observatory and large size nuclear recycle plants. Ongoing programmes of equal importance like the Advanced Heavy Water Reactor, BARC Vizag campus activities, etc. will also be pursued with equal vigour and emphasis.

Q.3: Can you tell us about the role of Research Reactors in BARC? What are our future plans in this direction?

As you are aware, Cirus and Apsara have been

decommissioned and today Dhruva, the AHWR Critical Facility and P4 are in operation. We are planning to construct a high flux reactor and a 125 MWe reactor at our Vizag campus under the XII Plan. We would also re-furbish the Apsara reactor for research activities in the Trombay campus. These reactors take forward our activities in the areas of Condensed Matter and Nuclear Physics studies, Production of radioisotopes, Studies on radiation stability of reactor materials to Shielding experiments, Neutron radiography and Development and testing of nuclear instrumentation.

Q.4: BARC is working on advanced reactors such as CHTR, AHWR and ADS. What are the advantages of these new reactor designs with special emphasis on utilizing Thorium?

A developing country like India requires increasing per capita electricity generation. In the near term fossil fuels, renewables and uranium (in closed cycle mode) will meet the energy requirement in the country. But in the long term, thorium-based reactors will meet our energy requirements. Multi faceted engineering and research activities are being pursued in BARC for better utilisation of Thorium in these advanced reactor concepts.

In order to use Thorium, it is essential to convert fertile thorium into fissile Uranium²³³ fuel. While the Advanced Heavy Water Reactor (AHWR) and the Compact High Temperature Reactor (CHTR) are essentially critical reactors, the ADS (Accelerator Driven System) is a sub-critical reactor. All these reactors use fertile thorium and convert it into fissile Uranium²³³ fuel. AHWR is designed to produce a substantial part of energy from Thorium. The interest in ADS for Thorium utilization is because of its efficient conversion into Uranium²³³ fissile fuel as compared to the critical reactors. ADS sub-critical reactors produce power by use of an external source

which comes from the interaction of high energy proton beam on the target. CHTR is being developed as a technology demonstrator for high efficiency hydrogen production, which is considered as a substitute for petroleum-based transport fuel. The AHWR is another innovative reactor designed for Thorium utilization which uses boiling light water as coolant and heavy water as moderator. It is designed to produce 300 MW(e) power and will prove to be a technology demonstrator for the Thorium fuel cycle. BARC has a comprehensive R&D programme to develop various technologies and subsystems related to ADS.

Q.5: Radioactive waste management is a major issue in public acceptance of nuclear energy as a clean alternative source of energy. What is the road map of BARC in this crucial area for the next 50 years?

Radioactive waste management programme is one of the earliest and major programmes of BARC and technologies related to handling of high level waste have matured over the years. Facilities for handling intermediate level waste, low level waste and solid wastes are operational at our sites at Trombay, Tarapur and Kalpakkam. A Pilot plant for Actinides separation from fission product in high level waste is coming up at Tarapur. In the long term, we will make arrangements for storage of separated fission products for 100 years or more on over ground facilities at the plant sites. Separated Actinides will be burnt in Accelerator Driven Systems/Fast Reactors. We would also like to complete our research work for underground repository, build one subsequently and make it available for storage of high level waste in the long term.

Q.6: How can we expand the outreach of BARC expertise in advanced areas of study, both in Basic as well as Applied Sciences? It is important that these programmes should address the students and also the non specialists.

The intricacies of nuclear science and technology are required to be explained in a simpler language for the benefit of all those who are not specialized in nuclear field. Our Senior Scientists are already working in this area to train the younger generation of Scientists who will in turn, disseminate this information to the public, in a simple language. In view of the fact that nuclear science and technologies and related applications are going to increase in a big way in the future, it is necessary that nuclear science and technology becomes a part of our School, College and University curriculum. We will work in this direction.

Q.7: How can we work towards bridging the gap between initial projections and final outcomes? Would incorporating a system of checks and balances tilt the scales in our favour? What steps do you propose in the speedy completion of projects?

For the type of projects and activities that we take up in the frontier areas of science and technology, some uncertainty about the end results and timeliness is expected. Our elaborate systems and procedures in the execution of projects can also result in some delay. We already have a system of checks and balances about implementation aspects through periodic progress reviews. However, there is certainly scope for improving our methodology and approach in achieving time-bound objectives, so that the option of foreclosing projects where there is no progress can also be exercised. It is also necessary to analyze the reasons for not achieving the final goals. This analysis will go a long way in the future planning of R&D activities at BARC.

Q.8: One of the major hurdles in initiating and completing projects on time is the present system of procurement of materials and equipment. What can be done to minimize delays?

Yes, at present contract management procedures for purchase and works, delay the execution of

projects and it is possible to improve on time and cost overruns, by modifying the contract management procedures. Even while remaining within the system, such changes are possible. However, contract management is not the only reason for delay and quite often there is scope for improvements in other related areas.

Q.9: How can we better utilize the time of research students, in the completion of regular R&D projects, given the present system restrictions?

Research students are the backbone of research in the University system and they significantly contribute to some of the key areas in our institutes also. Optimal contribution from research students in BARC is somewhat difficult because of security and infrastructural reasons as compared to smaller institutes within DAE, with lesser restrictions. We are trying to upgrade the infrastructure for improvement on this front.

Q.10: Colloquia and seminars are essential in communication of research findings in any field of study. How can we further encourage this activity among our Scientists and Engineers?

In BARC, Trombay Colloquia by eminent personalities has been a very effective means of communication within the scientific community. Colloquia and seminars are essential for exchange of information. However, the quality of such seminars must be judged by the papers presented and the discussions held. Our Scientists and Engineers should participate in select one or two seminars in their areas of specialization, in a year. In my opinion, this type of interaction should be with less number of participants and the presentations and discussions could be in a more focused manner.

Q.11: There is scarcity of drinking water in several villages of India. How can BARC technologies contribute in alleviating this problem?

We have two types of problems with regard to

drinking water, one related to contamination of available water with arsenic, fluoride, iron, etc. and the other problem is salinity. BARC has developed low cost technologies targeted for use by families, small communities and larger population in both the areas. Transfer of these technologies to many industrial units and private entrepreneurs has taken place and we are making continuous efforts in this direction.

Q.12: BARC has been at the forefront in the areas of Food preservation and in improving agricultural production in the country. Can you brief us about the R&D initiatives undertaken by BARC?

BARC has developed several food preservation technologies using irradiation and has also set up plants for this purpose. We have also helped the private sector in setting up plants for food and medical product irradiation. While continuing our research in this field, we are working towards application of these technologies on a much larger scale, so that food losses can be minimized through irradiation. In the area of nuclear agriculture, we have released around 40 crop varieties covering oil seeds, pulses, wheat, rice, etc. These varieties show high yield with low maturity period, disease-resistance and require less water and fertilizers. These seeds are in use in many states of India. However, there is a need for much larger scale of application of these technologies, so that common men benefit.

Q.13: Health care is a major concern in India. What are the strategies being pursued by BARC for providing health care benefits to the vast population in India?

BARC has developed radio-isotope based diagnostic and therapeutic equipment. These are very robust and can work continuously. Treatment cost is also low. We would like to popularize these equipment for use in smaller cities, where such health care facilities are not adequate. BARC has developed a

special class of radiolabelled molecules called “Radiopharmaceuticals”, which are used for diagnosis, management and treatment of many serious diseases ranging from cancer to cardiology to psychiatry, due to which several hundreds of patients have benefitted annually. Through its Radiation Medicine Centre (RMC) located at Parel, Mumbai, BARC offers both diagnostic and treatment facilities and services such as the Medical Cyclotron facility (the first of its kind in India), *In vitro* Nuclear Medicine services, *In vivo* Nuclear Medicine Services (Clinical, Scintigraphy, Radiopharmacy, and Radiation Safety Services) to patients. It also supplies radiopharmaceuticals to several hospitals in Mumbai such as Tata Memorial Hospital, Bombay Hospital, Hinduja Hospital among others. We have also developed a kit for detection of TB, where the cost of tests is low. While pursuing our research on the development of healthcare equipment, we aim to reduce the cost of treatment and thus reach the vast population of India.

Q.14: Innovation is at the core of Science & Technology. How can the pool of highly qualified Scientists and Engineers at BARC contribute to that end, so that the Scientific spirit of this institution attains global levels?

In BARC Scientists & Engineers are provided all possible freedom in continuing R&D in the areas of basic sciences, engineering sciences and technology development. The infrastructure available in multidisciplinary facilities provides the necessary impetus for innovation. In many areas of nuclear science and technology, we are at par with the achievements of developed countries and in some areas we are better off. I look forward to higher level of contributions from each one of my colleagues so that we can sustain our status as a leading institute and take it to great heights.

Q.15 : How can BARC further its goals through collaborative linkages with other R&D institutions,

academia and industry?

We already have strong collaborative linkages with premier institutes such as IITs, ICT, TIFR, IISc and others. We also have strong interactions with many central and state universities and MoUs with state governments in the area of Nuclear Science and Engineering. We have collaborative research projects funded by BRNS with practically all research institutions and academia. The scope of these collaborations can be expanded further. We are also open to the idea of an R&D forum for interaction with industry as well.

Q.16: What can BARC do in sensitizing public attitudes to the acceptance of nuclear energy as a viable, green alternative source of energy?

In the last 2-3 years, we have enhanced our efforts aimed at sensitizing the public about nuclear energy through all possible fora, from lectures in schools and colleges in remote areas to interactions with students, farmers and laymen. National symposia, conferences and annual meetings are organized with national science academia for dissemination of information on the benefits of nuclear energy.

Q.17: The BARC Newsletter has been the preferred channel of communication for BARC Scientists and Engineers for almost three decades now and in the last three years, it has undergone a major metamorphosis. Any suggestions to further improve it's quality and content?

The BARC Newsletter has been a vehicle of scientific communication within the BARC fraternity for more than three decades now. I am quite happy with the growing readership which has increased substantially after major structural changes in the format and content of the Newsletter. The Brief Communication Section, introduced last year, has become very popular with the young generation of our Scientists and Engineers. In my opinion, individual authors can quickly contribute their research and technical findings in a simple, non-technical language to

further enhance the readership.

Q.18: What is your future vision for BARC? Where do you see BARC 25 years from now?

BARC will continue to be a leader in nuclear science and technology at the global level. In 25 years, I would like to see an order of magnitude increase in the production of power from fast reactors, in which BARC would have contributed in many critical areas. I also hope to see the Indian Pressurized Water Reactors in operation in various parts of the country. The accelerator programme would have reached maturity and the Accelerator Driven System would be operational at our Vizag campus. The Indian

Neutrino Observatory would be built and attained full scope utilization by Indian scientists, students and academicians. Reprocessing programme would see multifold rise. Nuclear research would dominate the Indian scenario in the field of agriculture and food preservation. The benefits of these programmes would reach the common man through agricultural universities, seed corporations and progressive farmers. The healthcare sector also would see a large number of products based on BARC R&D. I would also like to see the Indian nuclear submarine fleet in operation.

I wish I could have worked in BARC for another 25 years. Thank you.”

Nodalization of Advanced Heavy Water Reactor Core for Efficient Spatial Control

(Electronics and Instrumentation Group)

Large nuclear reactors, like the Advanced Heavy Water Reactor, are susceptible to instabilities in spatial power distribution due to their loose neutron coupling. This puts forth a challenging requirement of spatial power control, in addition to the total power control requirements, in such reactors. This is generally accomplished through a tactful distribution of neutron detectors and reactivity control devices within the reactor core. However, optimization of the number and positions of such monitoring and control devices demands an extensive analysis of the reactor core based on control theoretic approach.

In order to analyze the spatial control requirements of the Advanced Heavy Water Reactor, a three-dimensional space-time kinetics model of the reactor has been developed within the framework of finite difference methods and multi-point kinetics. The model is incorporated with a simplified thermal hydraulics model of the main heat transport system, and reactivity feedbacks due to xenon and coolant void fraction have been considered. The number of zones into which the reactor core should be divided in order to accurately represent the core power distribution was optimized. Various nodalization schemes were worked out and compared in terms of steady state accuracy and control system characteristics such as stability, controllability and observability. Steady state accuracy was assessed by comparing the response of the model with that of accurate, higher order design models. The analysis revealed that the AHWR core should be divided into seventeen nodes, as shown in

Fig. 1, to accurately represent the control relevant characteristics as well as the steady state and transient behavior of the spatial power distribution of the reactor.

Further analysis of the model revealed that the AHWR is predominantly susceptible to two modes of instabilities in spatial power distribution, viz. first and second azimuthal modes respectively. Reactivity feedback due to coolant void fraction contributes slightly to the system stability, by introducing some amount of damping in the oscillatory response. Analysis reveals that complete control of the total power as well as spatial power distribution of the AHWR can be achieved by automatic control of four regulating rods, one in each quadrant of the reactor core, based on the feedback of total power and the quadrant core powers.

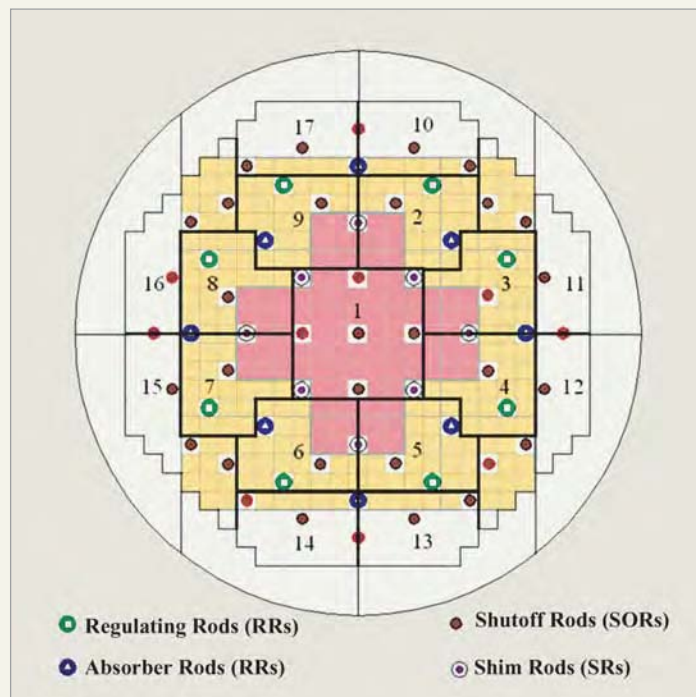


Fig. 1: AHWR Core

Tele Distress Alarm Device

(Electronics and Instrumentation Group)

Electronics Division, BARC has developed a compact and low cost Tele Distress Alarm Device named 'NIRBHAYA' to send information to near and dear ones including police in case of severe distress or fear of attack. The device can be carried in pocket or purse and requires a cell phone for its functionality. In case of need, a switch provided on the device is pressed. It automatically sends a signal on Bluetooth to the cell phone along with its GPS location. The software loaded on the cell phone sends pre-formatted message through SMS to pre-selected five cell phone numbers. These five phone numbers are user selectable. These can include phone numbers of parents, relatives, friends and police. The SMS message is also user defined and pre-formatted, which can be as follows. "I am X, female/male, aged Y years. I am in distress. I need urgent help. My location is latitude Lat and longitude Long." Once switch on the device is pressed, it continues to send its GPS location to the cell phone of the

person in distress every minute and the cell phone in turn transmits SMS again to the same five cell phones. Thus if the person is being kidnapped, the latest location will be available to the police. However, if kidnapper snatches the device and or the cell phone of the person, at least the last location from where he is kidnapped is known. The device can also be used in case the person gets heart attack or meets with an accident and needs immediate help.

The device is rugged and cannot be destroyed easily. The switch is located in such a way that it cannot get pressed accidentally. It has chargeable battery, which like any cell phone can be charged. There is a LED to indicate low battery voltage.

As almost everyone moving out of home carries a cell phone, the compact device in conjunction with the cell phone can provide necessary help in case of distress.



Studies on Separation and Purification of Fission ^{99}Mo from Uranium Aluminium Alloy

(Radiochemistry & Isotope Group)

^{99}Mo is the parent radioisotope of $^{99\text{m}}\text{Tc}$, which is considered as the workhorse of nuclear medicine. It is produced either by $^{98}\text{Mo}(n,\gamma)^{99}\text{Mo}$ reaction or by $^{235}\text{U}(n,f)^{99}\text{Mo}$. In the former route the low thermal neutron capture cross section (0.14 b) and low abundance of ^{98}Mo (24.1 %) yield low specific activity of ^{99}Mo ($< 1\text{Ci/g}$) thereby requiring large alumina column for $^{99\text{m}}\text{Tc}$ generators and resulting in large elution volumes for $^{99\text{m}}\text{Tc}$. On the other hand for the latter reaction the high fission cross section of $^{235}\text{U}(n_{\text{th}},f)$, coupled with the high fission yield of ^{99}Mo (6.1%), results in high specific activity of ^{99}Mo ($> 20,000\text{ Ci/g}$). Worldwide, there is a shortage in the supply of fission ^{99}Mo owing to the shutting down of the reactors and/or the complexities in the radiochemical separation process. As a part of the task force for development of the flow sheet for production of fission ^{99}Mo , a method has been developed for the separation of fission ^{99}Mo from irradiated uranium aluminium alloy.

The method involves dissolution of the irradiated target in 6 M NaOH, whereby only aluminium along with ^{99}Mo , ^{131}I and ^{103}Ru get into the solution with traces of ^{95}Zr , ^{95}Nb and ^{132}Te , while all other fission products, activation products (^{239}Np) and uranium remain in the solid residue. $\text{Al}(\text{OH})_3$ precipitation at lower pH (8-9) removed some of the impurities, e.g. ^{95}Zr , ^{95}Nb , ^{132}Te whereas AgI/AgIO_3 precipitation removed almost complete ^{131}I . ^{103}Ru was removed by addition of NaBiO_3 and evaporation to dryness. Subsequently ^{99}Mo was purified by precipitation as $\text{Mo-}\alpha\text{-benzoin oxime}$ followed by repeatedly washing with 0.1 M HNO_3 and dissolution in dilute NaOH. Organic impurities along with traces of iodine were separated by passing through silver coated activated charcoal. Final purification was carried out by anion exchange separation. ^{99}Mo is obtained with an overall recovery of 80% and the purity of the ^{99}Mo product was found to be in agreement with the US and European pharmacopoeia.

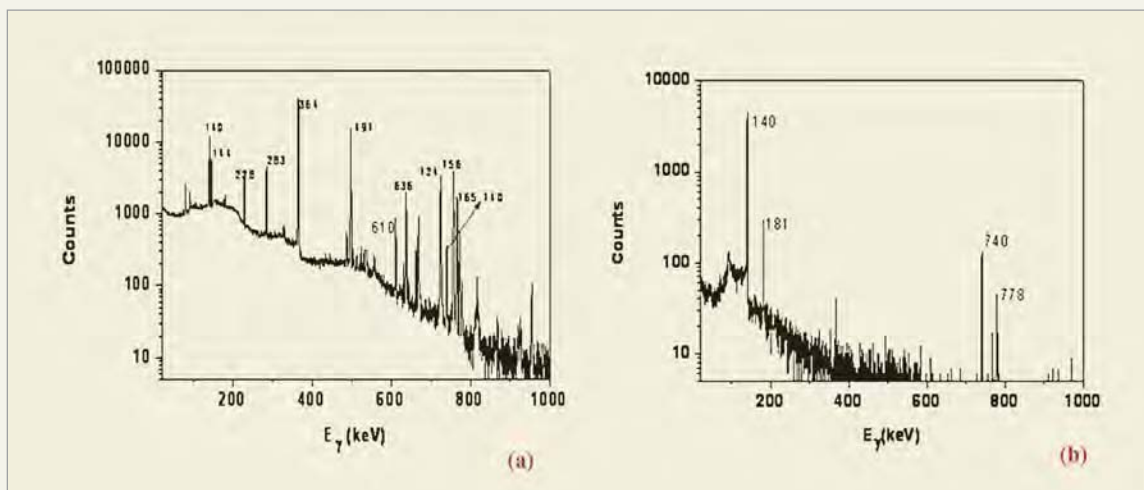


Fig. (1a): γ -ray spectrum of alkaline stock solution, (1b): γ -ray spectrum of purified ^{99}Mo

Spot Picker Robot

(Design, Manufacturing and Automation Group)

Spot picker robot is an indigenous three-axis robotic system designed for precise spot excision to accurately pick spots from 2D gel electrophoresis (2DGE). It transfers the picked protein into micro plates for analyzing protein expression. This finds application in protein research and developing new biomarkers and drugs.

The spot picker robot features the non-separable wavelet based novel imaging algorithm, better design of light illumination for detection of faint, irregular and overexposed protein spots in a non-linear background and generates more accurate reference coordinates of a dynamic protein object. Image resolution is of the order of 7 microns. The system includes a high performance solenoid controlled surgical grade protein spot excision tool and a novel wavelet based accurate positioning algorithm to reduce the effects of jerks on the system. Three-axis positioning is servo-controlled with necessary built-in software and hardware interlocks giving positional resolution of one micron and repeatability within ± 10 microns. This is achieved with the help of servomotors, high

resolution encoders, precision ball-screw drives, an advanced control system and a well damped table. Working gel image area is 160 x 180 mm. Fig. 1 shows the spot picker robot, Fig. 2 shows the spot cutter, Fig. 3 shows a typical 2D electrophoresis image analysis and Fig. 4 shows excision of protein spots.

The system acquires the image, analyzes it and presents the segmented result of protein spots to the user for automated picking of the system. However, system is also built with the provision of manual picking of the particular spot. The centroid coordinates of the spots in the image plane are converted into the robotic plane thus the robot cuts, picks and delivers the spots. After ultrasonic cleaning of the cutting tip, the robot picks the next spot and thus the cycle continues.

This robotic system is a low cost biomedical system which demonstrates state-of-the-art technology in precise positioning and powerful imaging algorithm in the field of proteomics. This system has been delivered to RMC, Parel for use.

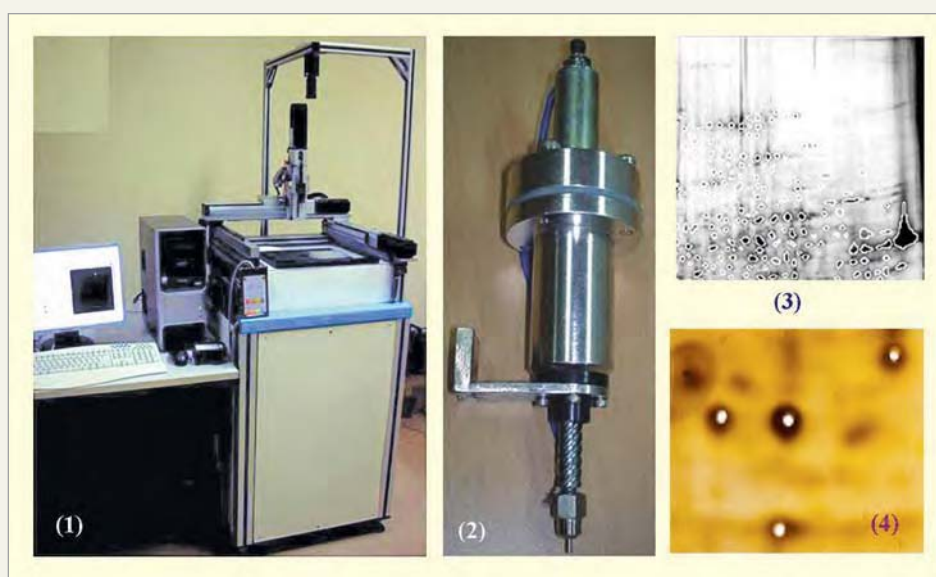


Fig.1: Spot picker robot, 2: Spot cutter, 3: 2DGE Image analysis, 4. Excision of protein spots

Design and Development of Advanced Reactors

K.K.Vaze

Reactor Design and Development Group

Abstract

Developing country like India requires increasing per capita electricity generation. Due to the depletion of fossil fuels and to meet this objective, the best option left for the country is utilisation of fissile fuels such as thorium which is in abundance. In addition to power requirements, the demand on fuel is also increasing in transport sector. Use of hydrogen as an alternate fuel will help to meet the demand. To meet these two objectives in particular, advanced heavy water reactors and high temperature reactors are being developed. Science and technology developments related to these reactors are discussed in this article.

Introduction

Reactor Design and Development Group is engaged in physics analysis of reactors, structural engineering and thermal hydraulic design of reactor components & systems and reactor fuels, experimental validation of design, development of passive safety systems and components, assessment of reactor safety in case of severe accident scenarios, providing technological solutions for life management of the ageing structures, system and components of operating reactors. Besides, it is also engaged in developing reactor technologies of future generation. The multifaceted engineering and research activities being pursued in the group to support such a wide range of programmes like Compact High Temperature Reactor (CHTR), Advanced Heavy Water Reactor (AHWR), and Life Management of Ageing structures, systems and Components of nuclear facilities are described in the subsequent paragraphs.

High Temperature Reactor Project

The two main reactor designs being pursued in the high temperature reactor project are the Compact High Temperature Reactor (CHTR) and the 600 MWth Innovative High Temperature Reactor (IHTR).

CHTR is a prismatic bed, 100 kWth, lead-bismuth cooled reactor being developed to demonstrate technologies for supplying process heat at 1000 °C, to enable hydrogen production by splitting water. Reactor physics design for ^{233}U -Th as well as enriched ^{235}U based fuel has been established. The

CHTR is modular in design. The reactor cross-sectional view and the schematic layout are shown in the Figs. 1 & 2 respectively. The reactor core consists of nineteen prismatic beryllium oxide (BeO) moderator blocks. These blocks contain centrally located graphite fuel tubes, which house fuel compacts consisting of TRISO coated particle fuel. The moderator blocks are surrounded by reflector blocks (partially graphite and partially BeO). The nuclear heat from the core is removed passively by natural circulation of the coolant between upper and lower plenums, upward through the fuel tubes and returning through the graphite downcomer tubes at the periphery. Many passive heat removal systems, including high temperature heat pipes, have been incorporated in the design.

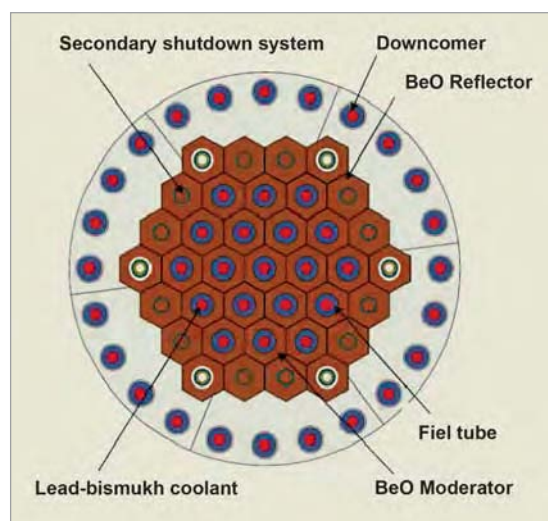


Fig. 1: CHTR cross-sectional view

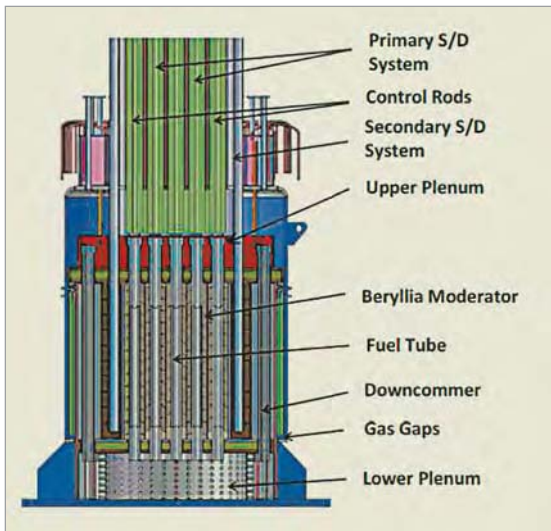


Fig. 2: Component layout

Development work for different systems is in progress in various divisions of BARC. For TRISO coated particle fuel, coatings have been prepared in Radiological laboratories on natural UO_2 kernels. Trials for fuel compact fabrication with ordered arrangement of surrogate particles with graphite matrix has been done and volumetric particle packing density of up to 47% has been achieved. Prototype of CHTR in-core components has been manufactured using graphite. Four carbon-carbon composite tubes in the shape of CHTR fuel tubes with bore for fuel compacts and coolant passage were made at the National Physical Laboratory (NPL), New Delhi and delivered to BARC. Material for the same is being characterised. Niobium based alloy, being considered as the metallic structural material for reactor shell and other components, has been developed indigenously at Nuclear Fuel Complex (NFC) with the help of BARC. Fabrication and assembly of components of a liquid metal loop using this alloy has been completed at NFC and the loop has been delivered at BARC. The CHTR development programme has been proposed in stages. In the first stage, a system with non-nuclear heating, consisting of surrogate materials, and operating at $\sim 550^\circ C$ would be setup in Trombay. Subsequently a critical facility with low power and

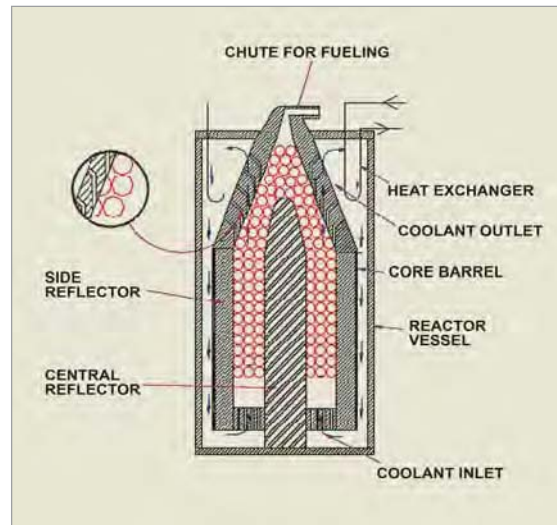


Fig. 3: The pebble bed IHTR

low temperature operation would be set up in Vizag. The same set-up would be finally operated at rated power and designated temperature. In the current conceptual design of CHTR, the core has primary shutdown system based on six absorber rods to be inserted in inner coolant channels and liquid poison injection of Indium in 12 BeO reflector holes acting as secondary shutdown system.

The IHTR-Core is being designed with 150000 pebbles floating in the coolant in annular core of 150cm thickness and graphite as moderator. The schematic of the pebble bed in IHTR core is shown in Fig.3. The fuel particles, called TRISO coated particles have a kernel of $250\ \mu m$ radius that contains the heavy metal ($^{233}UO_2 + ^{232}ThO_2$, where 7.6 wt % UO_2 of total heavy metal) and is surrounded by four carbon-based coating layers, forming a total outer radius of $450\ \mu m$. The proposed coolant consists of mixture of fluoride salts (FLiBe) which has a freezing point of $400^\circ C$ and a boiling point of $\sim 1400^\circ C$ at atmospheric pressure. Operating temperature of IHTR is about $1000^\circ C$. Presently the packing fraction of the pebbles in the core is being re-optimised to get desired negative coolant void reactivity characteristics.

Advanced Heavy Water Reactor (AHWR)

The Advanced Heavy Water Reactor (AHWR) is an innovative reactor designed for thorium utilization which uses boiling light water as coolant and heavy water as moderator. It is designed to produce 300 MW(e) power and will prove to be a technology demonstrator for the thorium fuel cycle. It is a vertical, pressure tube type reactor. The reactor incorporates a number of passive safety features and is associated with a fuel cycle having reduced environmental impact. At the same time, the reactor possesses several features, which are likely to reduce its capital and operating costs. The reactor is designed to produce 300 MW electrical power and 500 m³/day of desalinated water.

R&D Activities Associated with Reactor Physics Analysis of Advanced Reactors

Two different AHWR designs are being developed with thorium-plutonium and thorium-uranium cycles, in both closed and open cycle options. The plutonium topped version is designated as the reference AHWR design, AHWR-Ref and the LEU

topped variant is called as the AHWR-LEU. AHWR being the first-of-a-kind reactor, there are several multi-physics phenomena which are required to be simulated.

Several improvements in the existing core simulation tools have been implemented. Since the coolant is boiling, it introduces strong feedbacks to the core neutronics. Coolant conditions from thermal hydraulic studies were used to iterate the core power distribution till a convergence of about 0.1% is achieved. New codes based on different methodologies have also been developed to analyse the unique features of AHWR such as treatment of coolant void induced feedback along with burnup and temperature effects.

A 3D core simulation tool Analysis of Reactor transients in Cartesian and Hexagonal geometry (ARCH) based on diffusion theory has been developed and used extensively in both static and transient modes for the AHWR physics design. An integrated approach to safety calculations has been adopted through the PROMISIN project where the

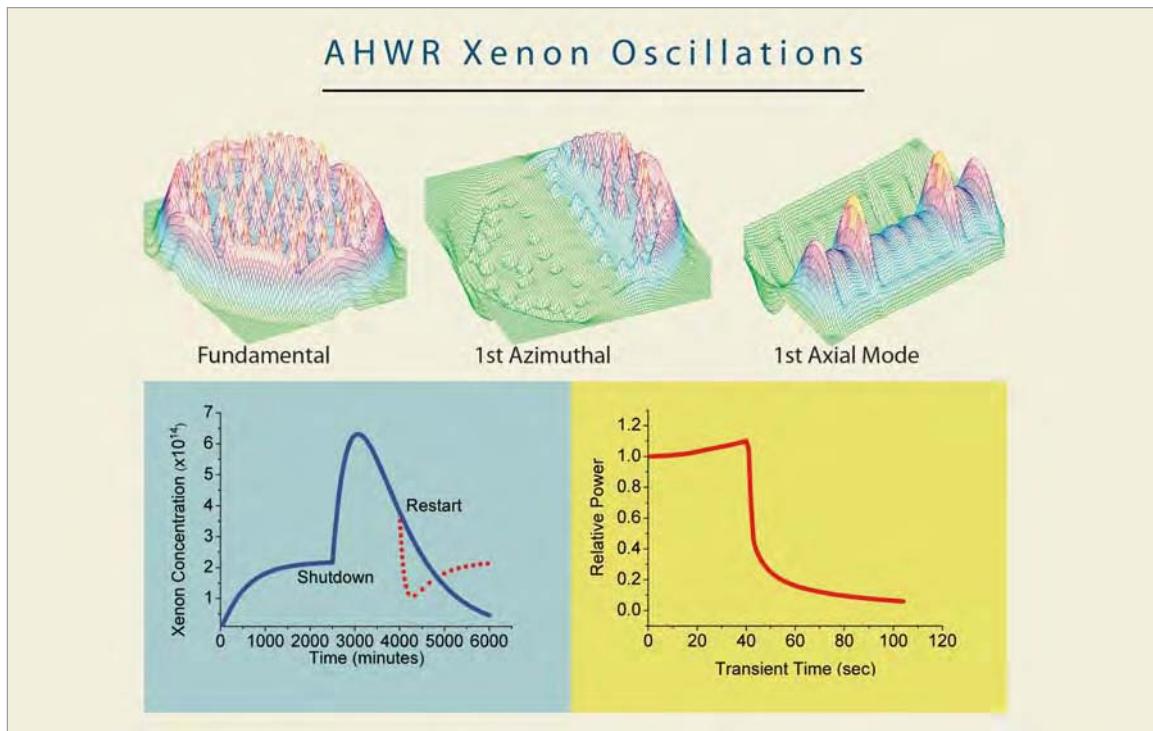


Fig. 4: Results of simulated transients for AHWR using ARCH

modelling the multi-physics phenomena through coupled neutronics and thermal hydraulics has been done. Also the AHWR core is large in diameter as compared to the active core height. Such large cores are prone to Xenon oscillations. As an example, the results of Loss of Regulation Accident (LORA), a xenon transient analysis with ARCH and xenon concentration after shutdown calculated from ARCH code are presented in Fig.4. Codes based on Monte Carlo techniques using continuous energy nuclear data codes are also being developed. The basic multi-group nuclear data set used in the physics design codes has also been updated with the isotopes of the thorium fuel cycle. The design codes have also been augmented with detailed fuel cycle analysis capabilities and development of fuel management schemes for the AHWR core with different types of fuels.

Physics Design of Advanced Heavy Water Reactor with Th-LEU fuel

The physics design of AHWR has been focussed on the Th-LEU fuel in an open cycle configuration. With ²³⁵U content of about 4.2%, discharge burnup of about 60GWd/T has been achieved. The equilibrium

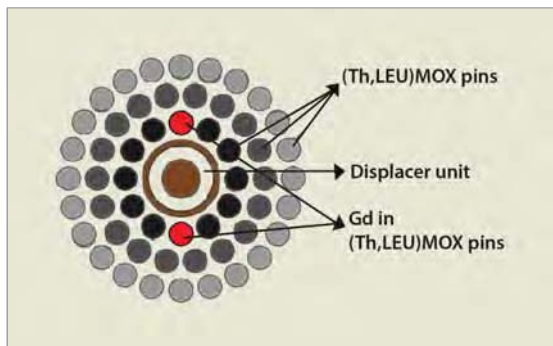


Fig. 5: AHWR equilibrium core cluster with Th-LEU fuel

fuel cluster is loaded with 30% LEU in ThO₂ in the inner 12 pins, 24% LEU in the middle ring of 18 pins and an average of 16% LEU in the outermost 24 pins. Gadolinium (Gd) is used as burnable poison in two pins on the inner ring, to suppress power ripples. The cross section of the fuel cluster is shown

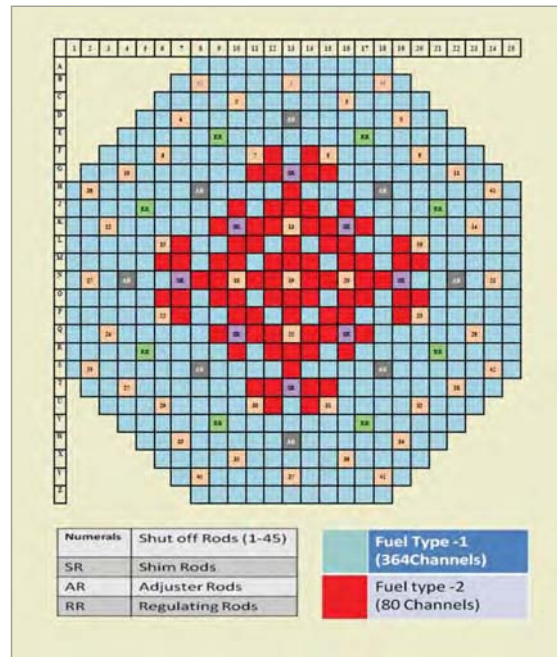


Fig. 6: Initial core loading pattern

in Fig. 5. The AHWR-LEU core, by design has enhanced safety and proliferation resistance characteristics. All the reactivity coefficients have been made negative. Power from Th/²³³U would be about 39%. The presence of ²³²U in discharged U and ²³⁸Pu in discharged Pu enhances its proliferation resistance characteristics. The AHWR-LEU fuel management has posed several challenges from managing a flat power/flux profile as the Gd burns to managing the in-core peaking at the empty reactivity device locations. The initial core of AHWR fuelled with Th-LEU is presented in Fig. 6. Several fuel management schemes through mini batch-fuelling are being studied as the core advances from initial to equilibrium phases. Presently, feasibility to remove in-core ECCS injection is being studied. Also the core is being re-optimised in order to get better shut down margins.

Earlier, a Plutonium topped core had been developed which operated in a closed fuel cycle producing about 65% from Th/²³³U fuel. The Pu content was adjusted to achieve self-sustenance in ²³³U. The enrichments of ²³³U and Pu are so chosen that the depletion of ²³³U in the (Th-²³³U) MOX pins is nearly

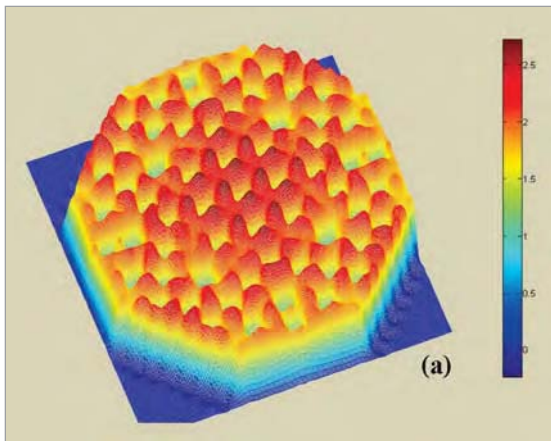
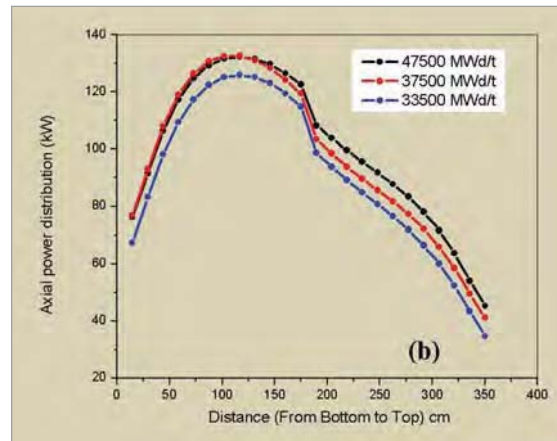


Fig. 7(a): Thermal flux distribution in AHWR,



(b): Axial flux distribution for a typical loading in AHWR after thermal hydraulic iterations

matched with the ^{233}U production in the (Th-Pu) MOX pins. The important feature of the AHWR core power distribution is that it has flat radial power characteristics (Fig. 7(a)) and a bottom peaked axial power distribution to get better thermal hydraulic margins (Fig. 7(b)).

Experimental Reactor Physics Activities: The Critical Facility went critical on 7th April, 2008. The observed critical height for the reference core configuration was 226.7 cm which agreed well with the estimated value of 226.5 cm. The core layout of the Reference core of AHWR-CF is shown in Fig. 8. Several experiments were performed which included, measurement of critical height for various cores, Calibration of reactivity devices, Neutron Spectrum measurement on central cluster, Cadmium ratio measurement at infinite dilution, Fine structure flux measurement inside the central lattice of Nat. Uranium and thorium clusters. The measured fine structure flux across the 19 pin nat. uranium fuel cluster loaded in the AHWR-CF is presented in Fig. 9.

Recently integral experiments with ThO_2 -U mixed pin cluster and ThO_2 -PuO₂ cluster (Fig. 10) were performed by loading them in the central E-5 and several other locations.

Experiments are being planned in the Sub Critical Reactor Coupled with 14 MeV Neutron Generator

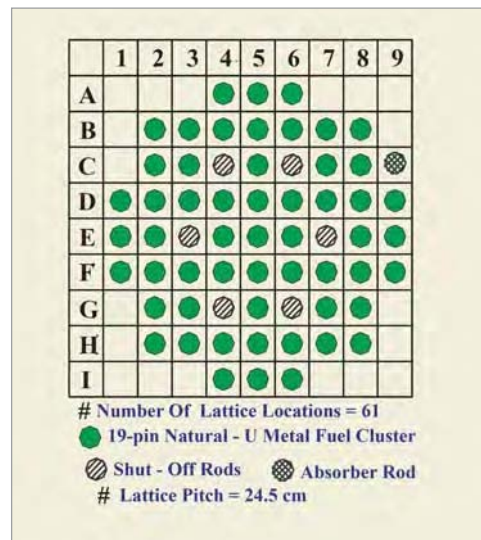


Fig. 8: Core layout of AHWR-CF

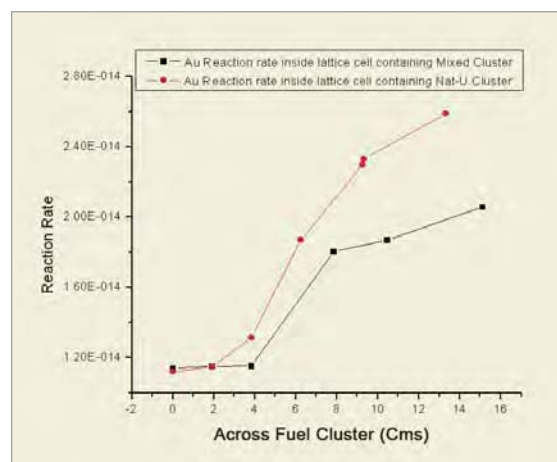


Fig. 9: Measured fine structure flux in NU and mixed pin cluster in AHWR-CF

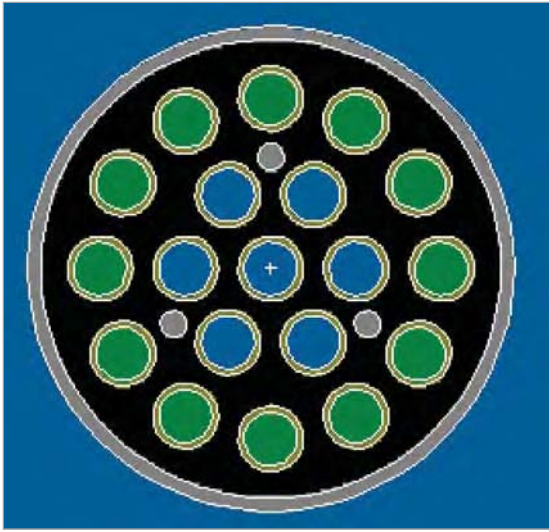


Fig.10: Mixed Pin (Nat. U-ThO₂) experimental cluster

for ADS related study. Presently, characterization of the neutron source, and estimation of Sub-critical multiplication factor has been done. Other experiments planned are measurement of Neutron flux distribution, neutron noise measurement buckling and neutron spectrum measurement.

Engineering studies of Advanced Heavy Water Reactor (AHWR)

Experimental Validation

Test facilities were built in the Reactor Engineering Division, BARC and academic institutes, to validate passive safety systems and First of A Kind (FOAK) features of the AHWR such as natural circulation core cooling; passive decay heat removal using isolation condensers (ICs); passive Emergency Core Cooling System (ECCS) injection during Loss of Coolant Accident (LOCA), Passive Containment Cooling System (PCCS) and Passive Containment Isolation System (PCIS).

These include setting up of natural circulation loops to gain insight of boiling two-phase natural circulation in single and multi channel configurations over a wide range of pressure, power and sub-cooling conditions. Test data from these facilities was also used for validation of in-house codes. To understand the effects of void reactivity feed back in natural circulation oscillations, one of the test facilities has incorporated void reactivity feed back by electrically simulating the power changes with change in void fraction.

Besides, an Integral Test Loop (ITL) has been set-up to simulate the start-up procedure, operational transients, LOCA, passive decay heat removal using ICs etc., in BARC. The schematic of the loop is shown in Fig. 11. ITL is a single-channel scaled test facility based on power-to-volume scaling philosophy. The facility has the same height of the natural circulation loop of MHTS as that of AHWR.

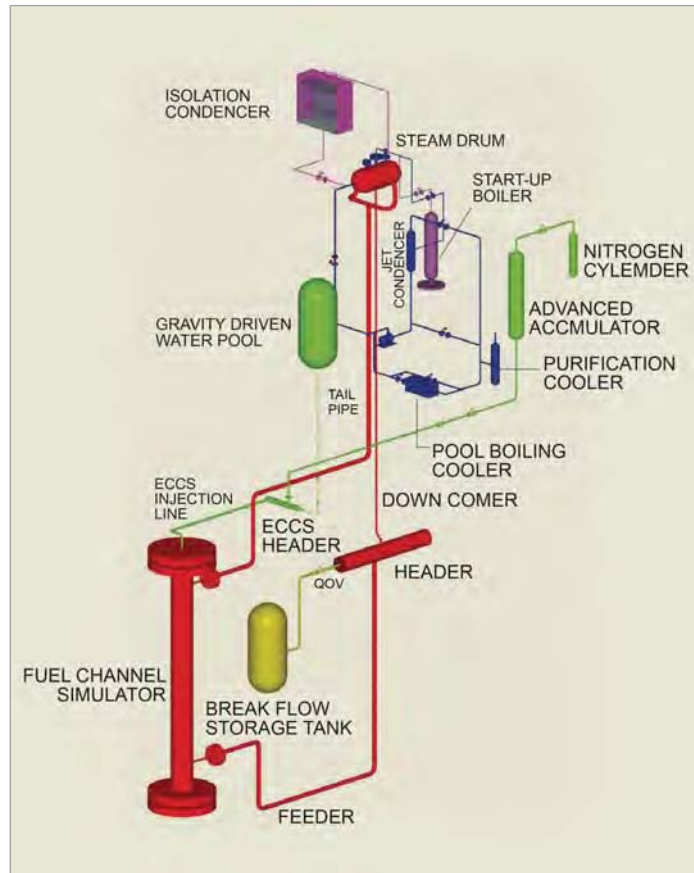


Fig. 11: Schematic of ITL

A directly heated type Fuel Rod Cluster Simulator (FRCS) is employed to simulate the core of the reactor (Fig. 12(a)). The two-phase mixture leaving the FRCS flows through the tailpipe (TP) to enter the steam drum (Fig. 12(b)), which is a horizontal vessel that facilitates the gravity based separation of steam and water. The steam leaving the drum condenses in the jet condenser (JC) and is pumped back as feedwater through a secondary feed pump (SFP) to the steam drum. The subcooled feedwater mixes with recirculation water in the steam drum and flows through a downcomer, a header and then through a feeder to enter the FRCS. A startup boiler (SB) is provided for pressurized startup to suppress the flow instabilities particularly at low pressure and low power. Pool Boiling Cooler (PBC) forms the ultimate heat sink for the facility. The facility also simulates the passive decay heat removal system comprising of IC submerged in water pool and emergency core cooling system comprising of ECCS header (ECCSH), injection line, advanced accumulator (AA), GDWP tank and a break flow storage tank (BFST) to accumulate the blow down mass. A quick opening valve (QOV) with an orifice is connected to header to simulate the instantaneous break of various sizes. The photographs of steam drum and fuel cluster rods installed in the actual loop are shown in the Fig. 12. This facility operates at full pressure, temperature and power conditions of AHWR and geometrically simulates one full size channel of AHWR. Steady state natural circulation behavior, start-up transients, thermal hydraulic stability, LOCA from 5 to 200 % and Station Blackout (SBO) conditions have been simulated in this facility. Critical Heat Flux (CHF) related experiments have been carried out in 3 MW_{th} Boiling Water Loop (BWL) and Freon loop at Indian Institute of Technology (IIT), Mumbai Experiments have revealed that adequate thermal margin exists in AHWR at 120 % full power. Separate effect test facilities have been built to validate PCCS and PCIS behavior of AHWR. To study the parallel channel instability and evaluate the thermal margin of AHWR, a new integral facility called Advanced

Thermal hydraulic Test Facility (ATTF) is being set-up at Tarapur.



Fig. 12(a): Directly heated type FRCS with bus bar connections



Fig. 12(b): Installed steam drum with tailpipe & downcomer connections for IFL

AHWR Fuel Development

As part of the fuel development programme for AHWR, irradiation studies on (Th-Pu) MOX and Th-LEU) MOX based fuel clusters are being carried out in DHRUVA reactor at regular fuel position. The

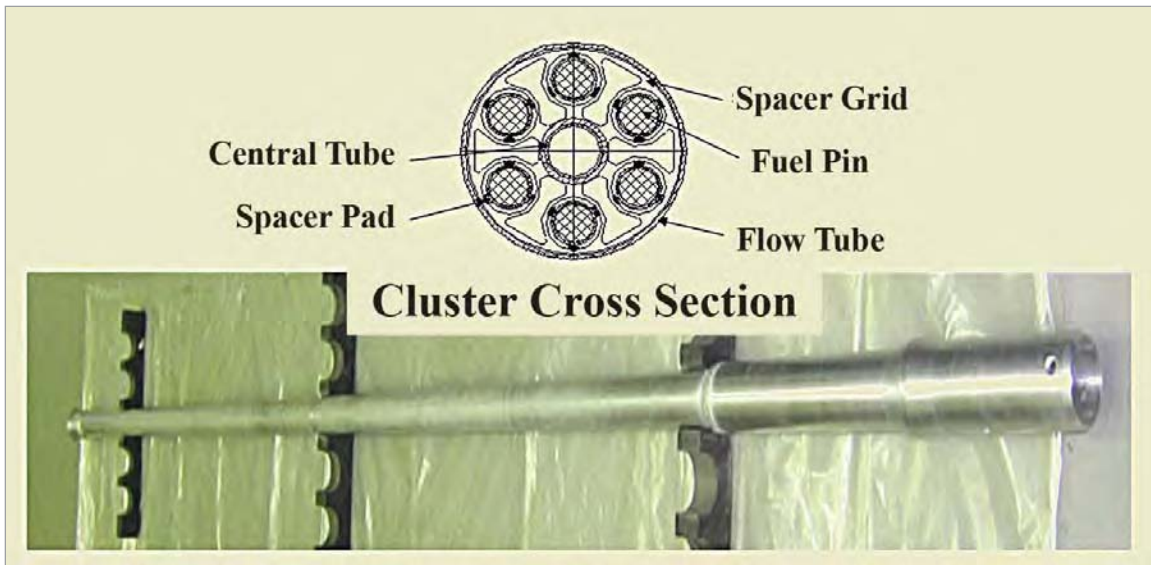


Fig. 13: Fuel cluster with AHWR type fuel pins for irradiation in Dhruva

AHWR fuel cluster design consisting of six fuel pins around a central spacer capture rod are assembled together by zircaloy and aluminium structural components. (Th-Pu) MOX based fuel cluster Fig.13 is presently under irradiation in Dhruva since June 2011.

Development of Fabrication Technology

Fabrication of integral nozzles by pull-out technology in nuclear components like steam drums, inlet header, end-fitting and pressure retaining components will have advantages over the conventional methods of fabrication. The development of this technology is being carried out

in collaboration with M/s Larsen & Toubro. A tubular component with integral nozzle fabricated using this technology is shown in Fig.14.

Core Safety Studies

Core Safety studies involve safety assessment of Advanced Indian nuclear power plants following operational, design basis and beyond design basis events covering all levels of defence in depth. It comprises of analytical evaluation, experimental program and uncertainty quantification. Studies are being carried out for reactors and experimental facilities.



Fig. 14: Component with nozzle pulled-out

The safety analyses for AHWR considering different categories of events and design improvements is summarized into a clad surface temperature vs. frequency plot as indicated in Fig. 15. It is seen that for all design basis events clad surface temperature does not exceed fuel failure criteria of 800 °C and for majority of events it does not exceed operational limit of 400 °C. It is also observed that peak clad temperature, during all these scenarios, is found to be well below the safety limits.

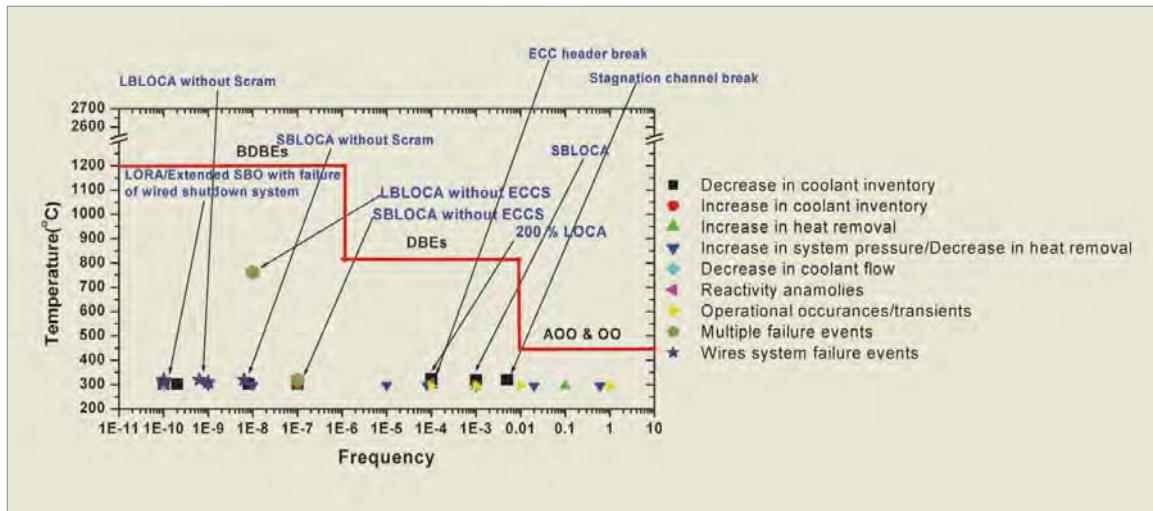


Fig. 15: Clad surface temperature vs. frequency plot

Experimental program caters to design basis and severe accident. Objective of experimental program for severe accident is development of failure Criteria, study of phenomena, fulfilment of validation matrix for advanced nuclear power plants with indigenous efforts augmented by national and international Collaborations, validation of codes and diagnostic system and development of severe accident management guidelines. AHWR experimental program caters to different stages of accident progression including severe accidents. Fig. 16 illustrates experimental facility for AHWR rewetting studies.

**Technology Developments
Development of Passive Valves & Devices**

The passive safety systems are being considered for numerous advanced reactor concepts. The motivation for use of passive safety systems is the potential for enhanced safety through increased system reliability.

The passive valves & devices are the key components of such passive safety systems. These passive valves function using only the process energy and hence

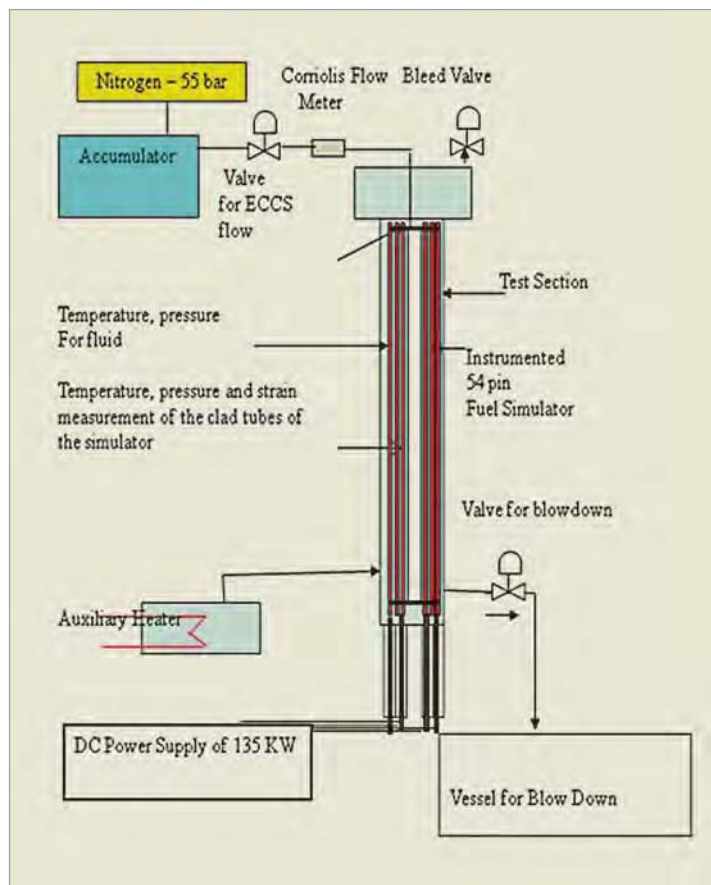


Fig. 16: Test setup for AHWR rewetting studies

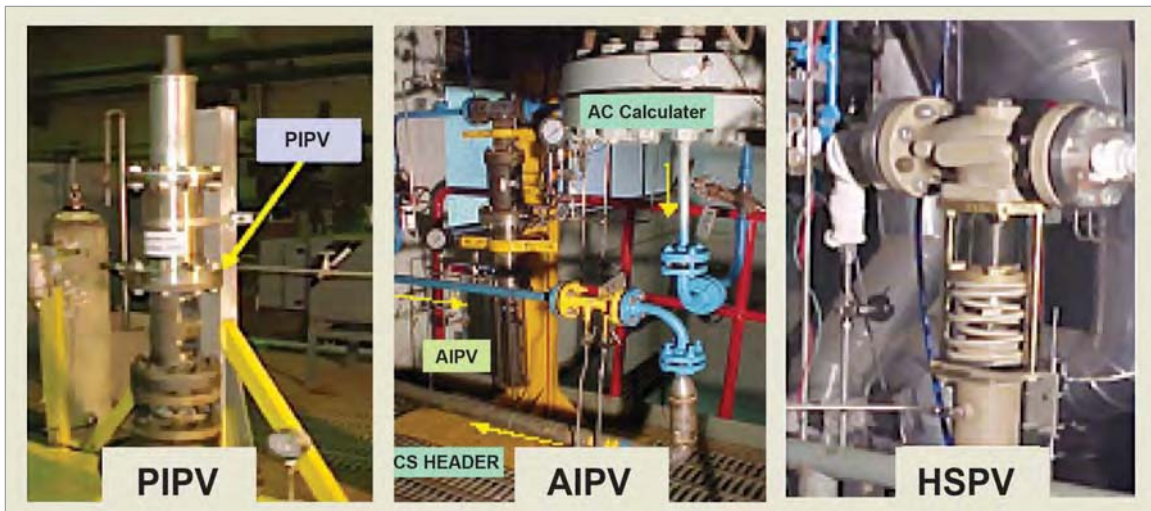


Fig. 17: Passive valves and devices being developed for AHWR

are considered a significant improvement over the current designs of valves actuating on external live signals or active sensors. Various passive valves & devices being Fig.17 for the Advanced Heavy Water Reactor (AHWR) are;

1. Hot shutdown passive valve (HSPV) for decay heat removal system.
2. Passive poison injection valve for PPIS (PIPV)
3. Passive accumulator isolation valve for ECCS accumulator (AIPV)
4. Pin actuated passive valve (PAPV).
5. One way rupture disk (OWRD)

Post Fukushima Assessment of AHWR

Under the postulated strong earthquake with/without Tsunami causing prolonged Station Black Out (SBO) for several days, the Reactor gets tripped on seismic signal. Heat is removed by Isolation Condensers immersed in Gravity Driven Water Pool (GDWP) containing 8000 m³ of water. GDWP water can remove decay heat for ~110 days with periodic containment venting allowed after 10 days.

Manufacturing and Performance Evaluation of AHWR Fuelling Machine

The AHWR fuelling machine (FM) is required to operate remotely to carry out 'On Power refuelling'



Fig. 18: AHWR fuelling machine

in reactor. The major sub-assemblies of the FM are ram assembly, magazine assembly snout assembly and separator assembly. RTD has conceptualized and carried out the detailed design of FM head and subsequently a prototype FM head was manufactured at MTAR Technologies Pvt. Ltd.,

Hyderabad as shown in Fig.18. The FM was manually tested in dry condition and operation was found satisfactory thus demonstrating the success achieved by sound design.

AHWR Probabilistic Safety Assessment

Level-1 Probabilistic Safety Assessment (PSA) has been carried out to identify the Postulated Initiating Events (PIEs) which may lead to Severe Core Damage (SCD) for the reactor. Major steps in Level-1 PSA are (i) Selection of initiating events (ii) Event Sequence Analysis (Physics, Fuel and Thermal hydraulic Analysis) (iii) Event Tree/ Fault Tree Analysis of Process and Safety Systems. Risk metric considered in Level-1 PSA is Core Damage Frequency (CDF). The Core Damage State is defined as the accident condition which results in peak clad temperature beyond 1473 K. Contribution to core damage from various initiating events is shown in Figure 19.

Level-2 PSA examines two enveloping severe accidents through a combination of probabilistic and deterministic approaches, in order to determine

the release of radionuclides from containment, including the physical processes that are involved in the loss of structural integrity of the reactor core. The two scenarios considered are (1) LOCAs in Inlet Header (spectrum of break sizes) & failure of both the wired shutdown system and (2) Main Steam Line Break (MSLB) outside containment & failure of both the wired shutdown system. Level-3 PSA analyses the transport of radionuclides through the environment and assesses the public health risk for the two scenarios considered. Consequences in terms of thyroid dose and effective dose to the individual located at various distances have been evaluated for the accident sequences arising out of 200% Steam line break outside containment. Doses are calculated for thyroid and bone marrow with different weather conditions. The maximum thyroid dose observed is 5.76 e-1 Sv at 0.5 km distance from plant. The exceedence frequencies are generated considering accident sequences arising out of LOCA case and failure of containment safety functions and MSLB with containment bypass. The graph for frequency of exceedence of a given

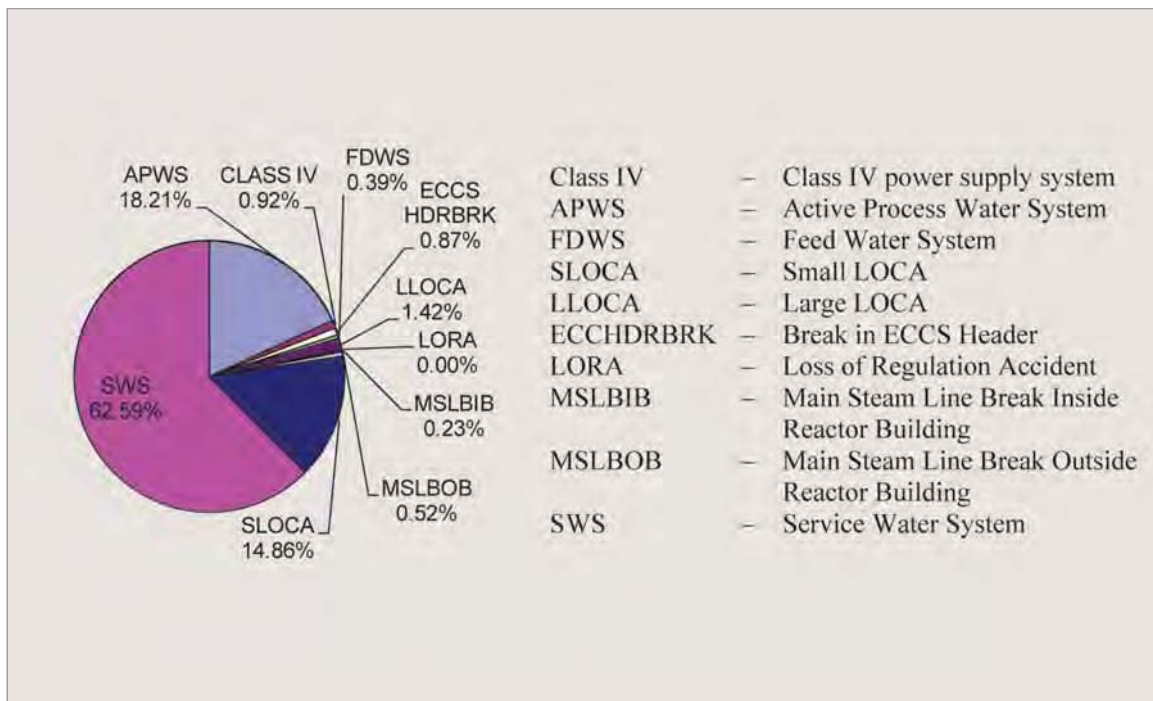


Fig. 19: Contribution to core damage from various initiating events

dose versus dose is shown in Figure 20(a). The very low frequency of exceedence values are indicative of the defence in depth employed in AHWR. The isodose curves for thyroid and bone marrow are generated for the seasons represented by weather conditions in January (dry weather) and July (wet conditions). Fig. 20(b) shows the Isodose curves for thyroid generated for the meteorological condition prevailing in the month of January.

Research to maintain the integrity and performance of Reactor Structures, Systems and Components.

Component Integrity

Integrity assessment of piping components is essential for safe and reliable operation of both conventional and nuclear power plants. It is especially important for nuclear power plants because of the application of leak-before-break (LBB) concept, which involves detailed integrity assessment of primary heat transport piping system with postulated cracks. The mechanical evaluation of pipe failures has evolved over time. While a considerable work has already been done in the past to develop integrity assessment procedure of cracked/un-cracked piping components, to address some of the issues in this area, a comprehensive *Component Integrity Test Program* was initiated at RSD, BARC. In this program, both theoretical and experimental investigations were undertaken to address various

issues related to the integrity assessment of pipes and elbows.

In the experimental investigations, fracture mechanics tests are carried out on cracked pipes and elbows subjected to bending moment and internal pressure at room temperature and at 300°C. Total 77 tests consisting of 33 pipes and 34 elbows of various sizes (200 - 400 mm diameter) with various crack configurations and sizes at different locations have been conducted. The tests demonstrated that: i. The number of cycles required for the postulated crack to reach through-wall is very large compared to the number of cycles anticipated during service, ii. Irrespective of the initial value, the aspect ratio of the crack when it becomes throughwall is limited to about 4.0 and iii. The maximum load sustained by the pipes having a through-wall crack is much more than the maximum load anticipated during service.

Tests on small tensile and Compact Tension (CT) and Three Point Bend (TPB) specimens, machined from the pipe of same material and heat, have also been performed to evaluate the actual stress-strain and fracture resistance properties of pipe/elbow material.

Numerical and analytical studies are performed on these tested specimens and components to compare the test results with the theoretical predictions and

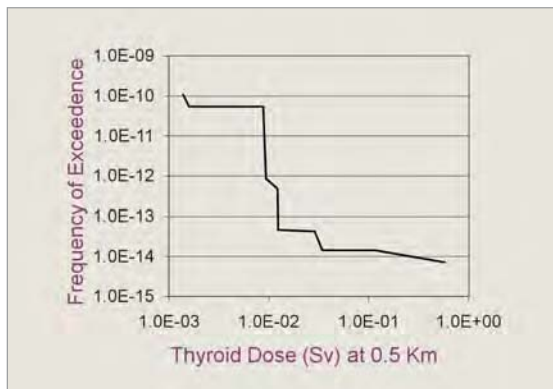


Fig. 20(a) : Frequency of exceedence versus dose

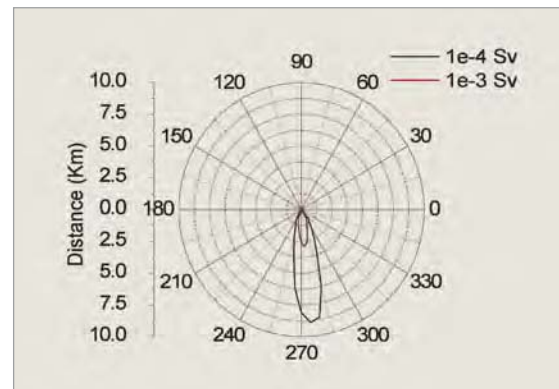


Fig. 20(b) isodose curve plotted for thyroid dose

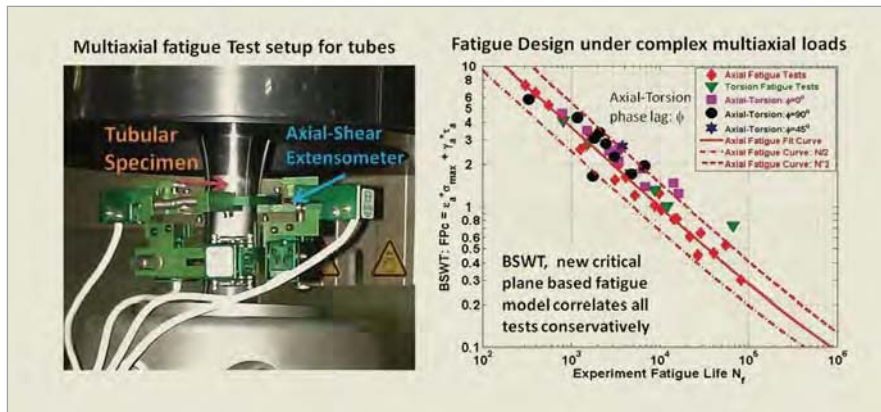


Fig. 21: Fatigue studies under multiaxial loading

also to study the role of stress triaxiality in the transferability of J-Resistance curve from specimen to component.

In another significant development work, new plastic collapse moment equations of both defect-free and cracked elbows, new limit load based generalized expressions of ' η_{pl} ' and ' γ ' to evaluate J-R curve from test results, new J and COD estimations schemes for circumferentially cracked elbows have been proposed and have received significant number of citations. Tests were conducted in several categories to study different degradation/ageing mechanisms and failure modes such as multiaxial fatigue degradation under multiaxial non-proportional cyclic loads Fig. 21; ratcheting of pressurized piping components; Low Temperature Sensitization (LTS) and Low Temperature

Embrittlement (LTE) of thermally aged stainless steel material and weldments; monotonic ductile fracture, fatigue crack growth Fig. 22, cyclic tearing/fracture of piping components Fig. 23. These tests were conducted under different loading conditions such as monotonic static loads, vibration loads, low magnitude cyclic load anticipated during normal operations, large magnitude.

cyclic load anticipated during a severe earthquake. Different types of loads such as axial, bending, internal pressure, torsion etc. and their combinations with different phase lags were considered to study the multiaxiality and non-proportionality effects on damage phenomenon. Tests were conducted on pipes / elbows of different sizes, without and with machined notches of different types (part through and through wall) and sizes at different location as

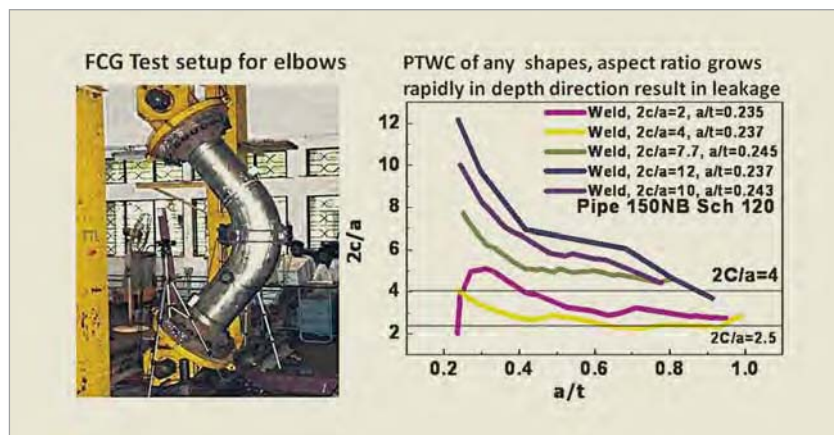


Fig. 22: Fatigue Crack Growth (FCG) studies on pipes / elbows

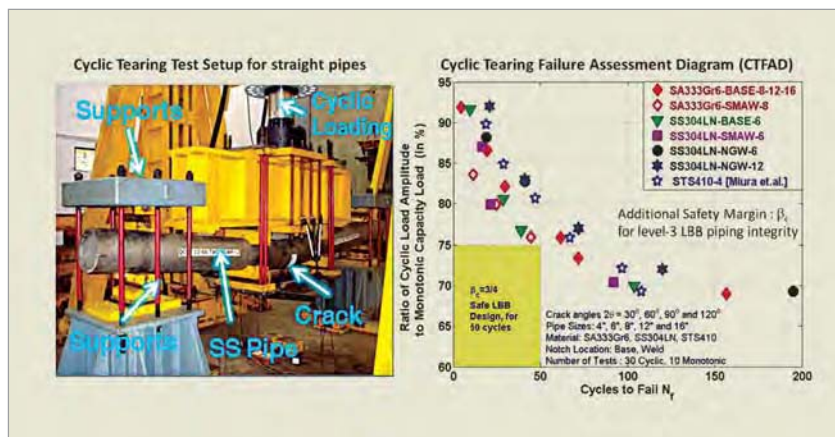


Fig. 23: Cyclic tearing studies on pipes

in base metal or in weld metal. Leak tests were also conducted on pipes with tight crack under operating pressure and temperature to assure the leakage size crack. The cyclic tearing tests led to development of a new criterion for cyclic tearing assessment which can easily be used for LBB demonstration against realistic failure mode.

Development of Facility to Conduct Drop Weight Tests for Determination of Nil-Ductility Transition Temperature (NDTT)

Conducting Drop Weight Test (DWT) to determine the Nil Ductility Transition Temperature (NDTT) of ferritic steels is mandatory as per ASME B&PVC specifications. The set-up as shown in Fig.24 is now fully commissioned and recently the setup was utilized in conducting NDTT tests in case of specimens obtained through two types of welding procedures, WPS789 and WPS794 concerned with ferritic steels, SA516 Gr.70 plate and SA508 Gr.4N Cl. 2 respectively.

Seismic Safety Studies of Structures, Systems and Components of Nuclear Facilities

For ensuring better seismic performance and economical design of SSCs under earthquake loading, dampers, energy absorbers, seismic base isolators are to be developed. Earlier, elasto-plastic dampers, lead extrusion dampers, friction dampers were developed and their efficacy was shown. Recently, semi active tuned liquid damper with

ferrous fluid was developed and it was shown experimentally and theoretically that it will improve the performance of structures against wind and earthquake loading.

Performance of the Piping System Subjected to Pressure and Seismic Excitation

In the design codes, conservative provisions were made considering monotonic plastic collapse and more recently the allowable were increased to reduce the conservatism. However, it is found essential to develop an explicit procedure to evaluate the performance levels as per the service demand. To meet this objective, a large number of tests were performed on piping systems and a performance based design procedure is evolved which will facilitate evaluation of the plastic deformations and application of appropriate limits as per the service

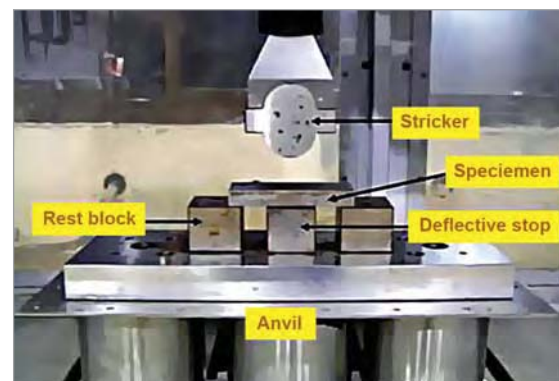


Fig. 24: Specimen for NDTT test

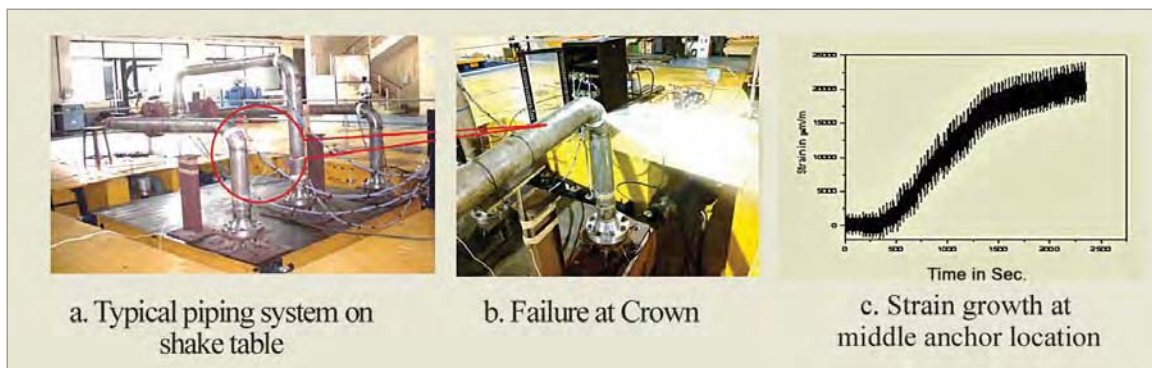


Fig. 25: Shake table tests on pressurised piping system

levels. Figure 25 shows a piping system, failure at crown and strain growth at crown.

Remarks

- Two reactor designs being pursued in the high temperature reactor project are discussed. Details of various activities related to Compact High Temperature Reactor (CHTR) are presented.
- Physics details of Advanced Heavy Water Reactor (AHWR) including LEU core are presented. Experimental reactor physics activities carried out in AHWR critical facility are discussed.
- AHWR engineering studies such as passive system features, simulation of start up procedures, operating transients in ITL and core safety aspects have been discussed
- Technology developments on fuel, fabrication of components such as fuelling machine etc related to the advanced reactors are explained briefly. Reactor structural and systems integrity studies (experimental and theoretical) and AHWR PSA studies are also briefly explained.

Acknowledgements

The author would like to express his appreciation to all the contributors from Reactor Physics Design Division, Reactor Engineering Division, Reactor Safety Division and Refuelling Technology Division.

References

- R.K. Sinha and Dulera I.V., Carbon Based Materials – Applications in High Temperature Nuclear Reactors, *Indian Journal of Engineering and Material Sciences*, Vol. 17, October 2010, pp 321-326.
- Krishnani P.D., "Fuel Cycle Flexibility in Advanced Heavy Water Reactor with the Use of Th-LEU Fuel", FHWR 2011, Ottawa, Canada, October 2–5, 2011.
- Mukhopadhyay D., et.al., "Level -1,-2, and -3 PSA for AHWR", BARC/2008/E/024, 2008.
- A. Ravikiran, P. N. Dubey, M. K. Agrawal, G. R. Reddy and K. K. Vaze, "Evaluation of Inelastic Seismic Response of a Piping System Using a Modified Iterative Response Spectrum Method" *International Journal of Pressure Vessel Technology*, 2013.
- Srivastava A., Lele H.G., Ghosh A.K., Kushwaha H.S., Uncertainty analysis of LBLOCA for Advanced Heavy Water Reactor, *Annals of Nuclear Energy*, Volume 35, Issue 2, February 2008.
- H. G. Lele, et. al. "Safety Assessment of Passive features of Advanced Heavy Water Reactor", International Conference on Future of HWRs, October 02-05, 2011, Ottawa, Ontario, Canada.

Uncertainty Quantification of Contaminant Transport Through Geological Repository using 2D Monte Carlo Simulation

D. Datta, M.Pandey, Brij Kumar and P.S. Sharma
Health Physics Division

Abstract

The safety of a radioactive waste or spent nuclear fuel repository is related to its capacity to confine radioactivity and isolate it from the biosphere. The most likely process leading to the release of radionuclides from a radioactive waste repository in a geological formation is the transport by groundwater. Entry of radionuclide into the biosphere after traveling through geosphere may possess a risk per year to the people living in the vicinity of the site. Therefore, this study has been developed to assess the risk in presence of the uncertainty of the parameters that constitute the governing model for describing the migration of the radionuclide through geological repository. The risk addressed here is due to drinking of water possibly contaminated with the migrated nuclide. Double Monte Carlo simulation is applied for modeling and the basic reason is due to the uncertainties of the bounds of the parameter of the specified distribution function. The paper demonstrates the simulation by an example problem in which migration of I-129 radionuclide released from waste disposal facility and migrated through a geological repository to a biosphere is focused.

Introduction

Subsurface contamination by leakage and spill of radioactive liquid effluent from any nuclear industry has resulted in many environmental concerns for a period of many years. Environmental risks of such contamination need to be analyzed to provide support for decisions related to remediation of the contamination problems. The safety of a radioactive waste or spent nuclear fuel repository is related to its capacity to confine radioactivity and isolate it from the biosphere. The most likely process that can lead to the release of radionuclides from a repository to the geosphere is transport by groundwater. Consequently, waste disposal-related safety analyses must assess the importance of the migration of radionuclides (i.e., their mobility) in the conservative assumption of leaching by groundwater (i.e., after the destruction of the engineered barriers). However, many models and relevant field studies have recognized that the contaminant fate in subsurface is substantially

influenced by uncertainties inherent in natural porous media, path length of the geosphere travelled by the radionuclide, fractional release rate, retardation factor and containment period. Presence of uncertainty not only increases the computational load but also provides a best estimate approach of safe design of a geological repository. Moreover, uncertainty of the parameters of the specified probability distribution (e.g., mean and standard deviation of a normal probability distribution) that characterizes the model parameters also yields a bound of the uncertainty and this bound can be very helpful while making any decision related to design of the waste package and its disposal into the geological repository. Mathematical models used for carrying out this time dependent risk assessment (risk analysis of a waste repository) include parameters having values varying within some ranges. Literature study shows that traditional 1D Monte Carlo simulation has been applied to estimate

the risk in presence of uncertainty. Examples of this kind of approach of risk assessment are elsewhere found [1]. In this context, the assessment and presentation of the effects of uncertainty are widely recognized as important parts of analyses for such complex systems [1]. Generally, most of the earlier studies used the stochastic approaches to accommodate the uncertainties associated with contaminant transport models [2-3]. This paper presents the double Monte Carlo based modeling of contaminant migration through geological repository. The outcome of this study is the assessment of time dependent risk to the public through the drinking of groundwater contaminated by the migrated water-borne radionuclide. In this modeling very often, the parameters of the probability distribution itself are expressed in the form of range or interval which is due to lack of proper analysis of the experimental data. This demands the double Monte Carlo simulation and the result of this simulation is expressed in terms of bounds generally attributed as lower cumulative probability and upper cumulative probability [4-5].

The physical processes which are responsible for migration of the contaminant include dispersion, advection, adsorption and decay. Time profile of the risk along with its two bounds is presented in this paper. The structure of the paper is as follows. Section 2.0 describes the double Monte Carlo simulation and sampling scheme required to generate the random numbers from the specific probability distribution. Section 3.0 presents the problem statement considered for the purpose of modeling. Numerical results of the outcome of this modeling are presented in section 4.0 and finally conclusion is presented in section 5.0.

2D Monte Carlo Method

The Monte Carlo method is a numerical solution to a problem that models objects interacting with other objects or their environment based upon simple object-object or object environment relationships. It represents an attempt to model nature through

direct simulation of the essential dynamics of the system in question. In this sense the Monte Carlo method is essentially simple in its approach - a solution to a macroscopic system through simulation of its microscopic interactions. A solution is determined by random sampling of the relationships, or the microscopic interactions, until the result converges. Thus, the mechanics of executing a solution involves repetitive action or calculation. To the extent that many microscopic interactions can be modeled mathematically, the repetitive solution can be executed on a computer. However, the Monte Carlo method predates the computer and is not essential to carry out a solution although in most cases computers make the determination of a solution much faster. There are many examples of the use of the Monte Carlo method [5] that can be stated in short as simple random sampling of the uncertain parameters with respect to the specific probability distribution. Latin hypercube sampling [5] is applied here as the main sampling scheme.

Illustration with Example

Suppose our sample model is as follows:

$Z = (X + Y)/(X \cdot Y)$, where x and y are uncertain parameters due to their randomness. Uncertainty of these parameters is assumed as follows:

$X = N([\mu_1, \mu_2], [\sigma_1, \sigma_2])$ and

$Y = U([a_1, a_2], [b_1, b_2])$.

Let the values of all these constants be:

$\mu_1 = 10, \mu_2 = 20, \sigma_1 = 0.2, \sigma_2 = 0.5;$

$a_1 = 100, a_2 = 150, b_1 = 300, b_2 = 400;$

Sampling strategy in double Monte Carlo is as follows:

Sample values of X and Y are generated using the following scheme as:

$X_1 = N(\mu_1, \sigma_1), X_2 = N(\mu_2, \sigma_1), X_3 = N(\mu_2, \sigma_1)$ and

$X_4 = N(\mu_2, \sigma_2)$

$Y_1 = U(a_1, b_1), Y_2 = U(a_2, b_1),$

$Y_3 = U(a_1, b_2)$ and $Y_4 = U(a_2, b_2)$

Construct a temporary matrix, say XX as $XX = [X_1, X_2, X_3, X_4]$. Compute the minimum and maximum of each rows of XX matrix.

Cumulative probability distribution with minimum values of each row of XX will be termed as lower cumulative probability of X and the same with maximum values of each row of XX will be termed as upper cumulative probability of X. Repetition of the similar task with $Y_1, Y_2, Y_3,$ and Y_4 will generate the lower and upper cumulative probability of Y. Now substituting the simulated min-max values of X and Y we have the following values of the model output as

$$Z_1 = (\min(X) + \min(Y)) / (\min(X) * \min(Y));$$

$$Z_2 = (\min(X) + \max(Y)) / (\min(X) * \max(Y));$$

$$Z_3 = (\max(X) + \min(Y)) / (\max(X) * \min(Y));$$

$$Z_4 = (\max(X) + \max(Y)) / (\max(X) * \max(Y));$$

Construct a temporary matrix ZZ with Z_1, Z_2, Z_3 and Z_4 . Compute the minimum and maximum values of each row of ZZ and labeled them as Zmin and Zmax. Cumulative probability distribution of Zmin and Zmax can be now constructed and labeled as lower and upper cumulative probability of the model Z. 2.5th, 50th and 95th percentile from lower and upper cumulative probability will provide the uncertainty band of the model output Z. The outcome of the complete simulation is as depicted in Figs.1-3.

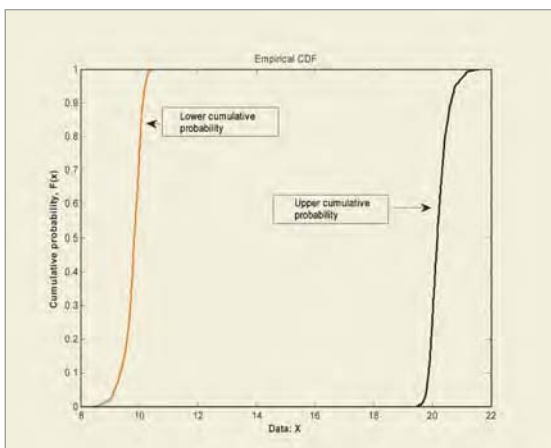


Fig. 1: Lower and upper cumulative probability of uncertain variable, X

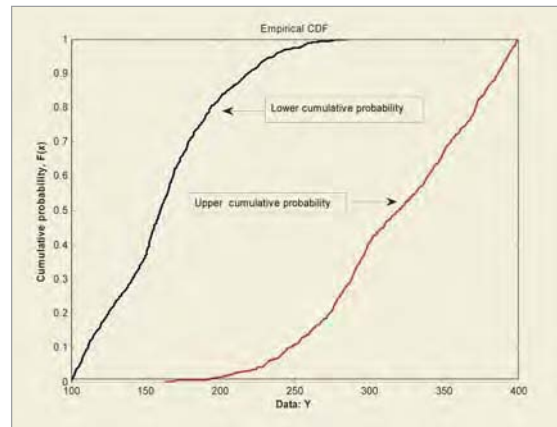


Fig. 2: Lower and upper cumulative probability of uncertain variable, Y

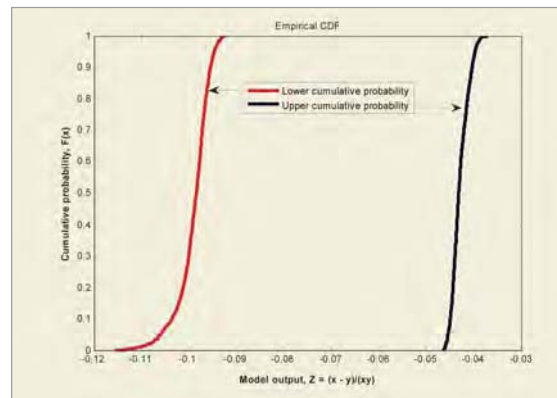


Fig. 3: Cumulative probability (lower and Upper) of Model output, Z

Problem Formulation

Double Monte Carlo simulation [5-6] based modeling has been applied to estimate the time dependent radiological risk to the human with respect to the migration of water-borne radionuclide through a geological repository. Accordingly the scenario considered in the model tracks the one dimensional migration of typical water borne radionuclide through two geo-spherical layers characterized by different hydro geological properties. Statement of the problem is as follows:

The processes being considered in the model are radioactive decay, dispersion, advection and chemical reaction between the migrating radionuclide and porous medium. Radioactive waste (conditioned) contained within a steel canister is disposed in the

form of a package in the geological repository, which can be represented as point source for the purpose of modeling. The migration of the radionuclide through the geosphere is the core of the present modeling. The governing equation covering all the processes mentioned is represented as

$$R \frac{\partial C(x,t)}{\partial t} = v d \frac{\partial^2 C(x,t)}{\partial x^2} - v \frac{\partial C(x,t)}{\partial x} - \lambda R C(x,t) \quad (1)$$

where, $C(x, t)$ = concentration of radionuclide at position x , in the geosphere at time t , R = retardation factor, v = water travel velocity in the geosphere layer (m/y), d = dispersion length in the geosphere layer (m), and λ = decay constant of the radionuclide in per year. The modeling of the biosphere is expressed via risk to the human from the ingestion of the drinking water containing the migrating radionuclide [7-9]. This biosphere modeling is given by accordingly,

$$\text{Risk (}/\text{yr)} = C(l, t) * B \quad (2)$$

where, B = biosphere risk factor evaluated from the drinking capacity of each individual in a year. The model for computing the biosphere risk factor can be given as

$$B = \frac{w}{W} \varepsilon \quad (3)$$

where, w = water ingestion rate (m^3/y), W = stream flow rate (m^3/y) and ε = risk factor (y).

The aim of this problem is to quantify the probability bounds of risk (y/yr) with random uncertain input parameters.

Solution:

Equation (1) has been solved analytically by using Green's function method with proper initial and boundary condition and the final solution [7-9] of $C(L, t)$ is written as

$$C(L, t) = 0.5 * C_0 * B * k * \exp(-\theta + \mu - \zeta - \eta) * \xi \quad (4)$$

where, C_0 = initial inventory of the radionuclide in the repository,

$$\theta = \lambda(t + T), \quad \mu = L / 2d, \quad \zeta = RL^2 / (4dv t), \quad \eta = vt / (4dR), \quad \text{and } T = \text{containment period (y)}.$$

The factor ξ is as follows:

$$\xi = [\phi(x_1) + \phi(x_2)], \quad \phi(x) = \exp(x^2) * \text{erfc}(x),$$

$$x_1 = (\zeta)^{1/2} + (\eta - \lambda t)^{1/2}, \quad \text{and } x_2 = (\zeta)^{1/2} - (\eta - \lambda t)^{1/2}$$

The uncertain input parameters of this model are:

= fractional release rate (y),

T = Containment period (y),

R = retardation factor,

L = geosphere path length (m),

d = dispersivity (m^2/y),

v = groundwater velocity (m/y)

Computational Issues

Uncertain input parameters are characterized by the specific probability distribution suggested by the domain experts. Experts also provide the bounds of the parameters of their probability distributions. Probability distributions representing the uncertainty of the input parameters are of two types: (a) log-uniform and (b) uniform. Accordingly sample values of the specific input parameters following the double Monte Carlo simulation are generated. Each random uncertain input parameter is expressed in terms of a probability bound addressed by lower and upper cumulative probability. Substitutions of these bounds in the model with the fixed value of the deterministic input parameters yield the probability bounds (lower and upper) of the risk. Uncertainty of the model output in this case is expressed in terms of these probability bounds. The function may be complex and is known as Faddeeva function [9]. Hence computation of this function has been carried out by following an algorithm given in [10]. Computation of the error function with complex argument is the computational issue of the factor ξ of equation (4). Lower and upper bounds of the estimated risk at different time have been computed. 50th percentile values from lower and upper cumulative probability of the time dependent risk are used as the mean risk at any specific time.

Numerical Results

Uncertain input parameters of the model as presented in Eq.(1-4) are: (a) leach rate, k (y), (b) retardation factor, R , (c) water travel velocity,

v (m/y), (d) containment period, T (y), (e) path length, L (m) travelled by the radionuclide within geosphere before coming to biosphere, and (f) the stream flow rate, W (m³/y). Probability distribution of all these uncertain parameters is suggested by experts. As per expert’s opinion, leach rate is log-uniformly distributed, but the limits of the log uniform distribution cannot be precisely specified and that is the reason, the limits of the leach rate distribution are provided by the experts in the form of an interval. Similarly, retardation factor is uniformly distributed and the limits (lower and upper) are again given as an interval. So, random sample values of leach rate and the retardation factor has been generated using double Monte Carlo simulation (section 2.1). Probability distribution of the water travel velocity, stream water velocity, containment period are considered as log uniform as per expert’s opinion. Geosphere path length is taken as uniform distribution.

The deterministic parameters are given in Table 1. Probabilistic uncertain parameters having lower and upper bounds in terms of an interval (as illustrated in section 2.1) are called as type II uncertain parameters. Parametric uncertainty of type II parameters of the model is as shown in Table 2. Parametric uncertainty of all type 1 probabilistic input parameters are presented in Table 3. A sample size of 1000 on the basis of Latin hypercube sampling has been used for simulation business.

Table 1: Deterministic input Parameters

Parameter Description	Values
C_0 (Bq)	3.7E10
d (m)	20
λ (y ⁻¹)	4.414E-8
w (m ³ /y)	0.73
ϵ (/Bq)	2.18E-10

Table 2: Type-II Probabilistic Parameters

Input	Distribution	Lower Bound		Higher bound	
		Low	High	Low	High
λ	Log-uniform	10 ⁻⁵	10 ⁻⁴	10 ⁻³	10 ⁻²
R	Uniform	1	3	5	10

Table 3: Uncertainty distribution of Type I Probabilistic Parameters

Parameters	Distribution	Lower limit	Upper limit
T (y)	Log-uniform	100	1000
v (m/y)	Log-uniform	10 ⁻³	10 ⁻²
L (m)	Uniform	100	500
W (m ³ /y)	Log-uniform	10 ⁵	10 ⁷

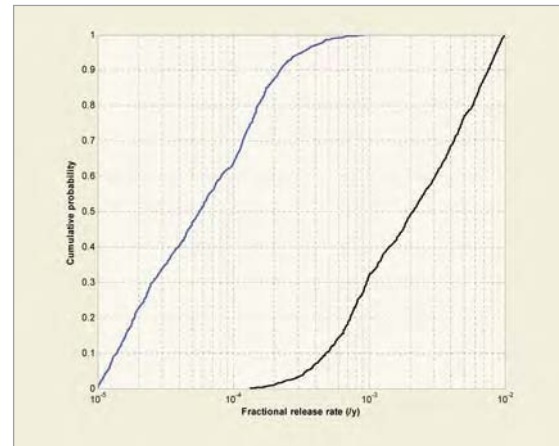


Fig. 4: Lower and upper cumulative probability of leach rate, λ (y)

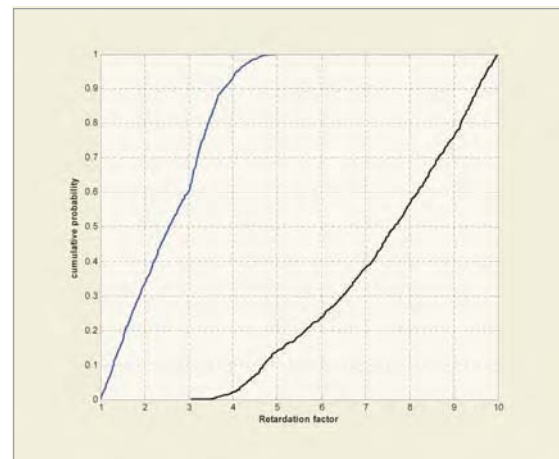


Fig. 5: Lower and upper cumulative probability of retardation factor, R

The lower and upper cumulative probabilities of double Monte Carlo simulated samples of leach rate and retardation factor are as shown in Figs 4 and 5. The histograms of type I probabilistic parameters T , v and L are as shown in Figs. 6-8.

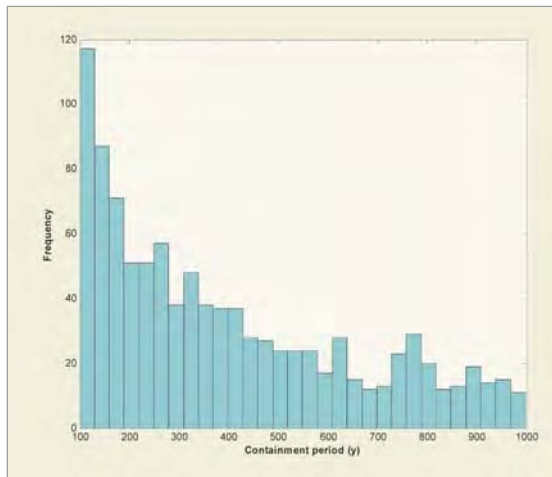


Fig. 6: Frequency distribution of containment period, $T(y)$

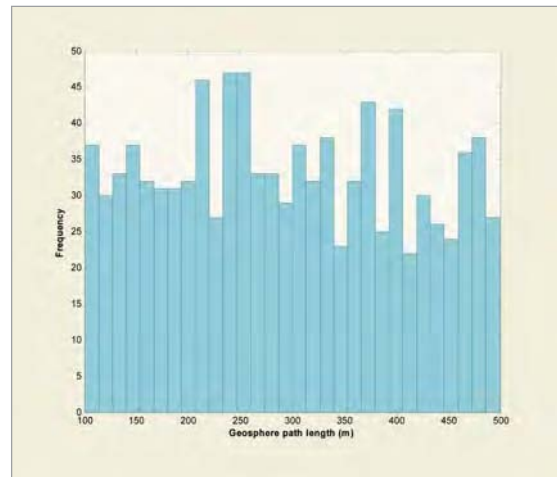


Fig. 8: Frequency distribution of geosphere path length

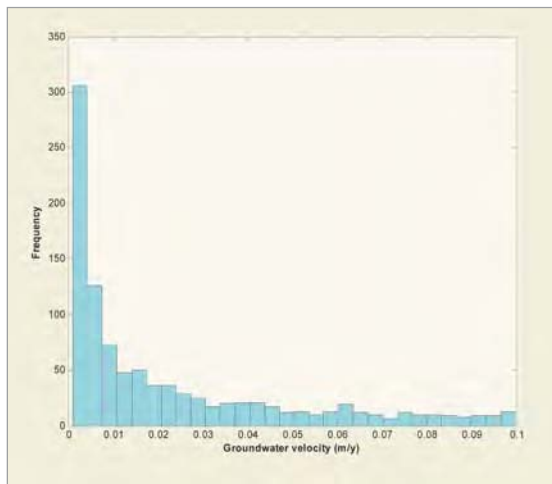


Fig. 7: Frequency distribution of groundwater velocity, n (m/y)

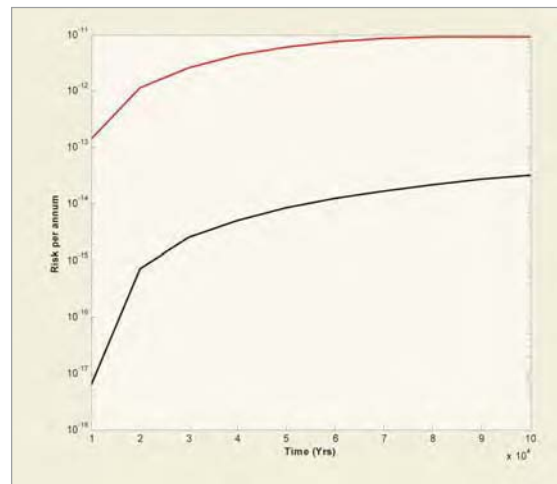


Fig. 9: Profile of the lower and upper bound of the time dependent risk per annum

Probability distribution of the time dependent risk through ingestion of water-borne radionuclide migrated through geological and biosphere is generated for a time interval of 10^4 y – 10^6 y by using the uncertainty distribution as shown in Figs. 4-8. Lower and upper cumulative probability distribution of the estimated time independent risk are used to compute the corresponding mean value of the risk at each observation time. The profile of the lower and upper bounds of the time dependent risk is presented in Fig. 9.

Bounds of risk per annum at each time can be easily predicted by drawing a line parallel to the ordinate at a specific time. Therefore, bounds of risk at that

specific time will be the intersection points of the line drawn and the lower and upper bound risk profile. It can be concluded from Fig. 9 that for the present problem, the interval of risk at time, $t = 40000$ y is found as $[4.0E-14, 3.5E-12]$ per year. Time profile of intervals of risk in a similar way can be easily generated to make some effective decisions on the issue of safe disposal of radioactive waste.

Conclusions

Risk assessment using Monte Carlo simulation is known as probabilistic risk assessment that requires careful interpretation when the spread of the variables represents uncertainty due to scarcity of

data rather than a genuine and measurable random distribution. Specific problems arise when the risk is dominated by a specific probability distribution of one of the parameter with a particular combination of other parameter values, as frequently occurs in assessments of nuclear waste repositories. In these circumstances, traditional methods may be computationally inefficient and, in any case, their results tend to accentuate the arbitrariness of much of the input data. Not only that, imprecise information of the parameters of a probability distribution will modify the spread of the output and hence in this context, double Monte Carlo simulation has been applied. In this paper, double Monte Carlo simulation based modeling of transport of radionuclide through a geological repository has been presented. Double Monte Carlo based modeling addresses the type II probabilistic parameters. Type II parameters play a major role in the simulation. Probability distributions of uncertain parameters are taken by expert's opinion. Presence of bounds of the risk can provide in making the decisions about the performance of the geological repository. That is to say that if the geological repository is perfect, it will restrict to migrate the radionuclide into the biosphere

References

1. NCRP (National Council on Radiation Protection and Measurements), A guide for uncertainty analysis in dose and risk assessments related to environmental contamination. NCRP Commentary No. 14, Bethesda, MD: National Council on Radiation Protection and Measurements; 1996.
2. Chen, Z., Huang, G.H., Chakma, A., "Integrated Environmental Risk Assessment for Petroleum-contaminated Sites – A north American case study", *Water Science and Technology*, vol. 38, pp. 131-138, 1998.
3. Helton, J.C., "Uncertainty and sensitivity analysis techniques for use in performance assessment for radioactive waste disposal", *Rel. Eng. System Safety*, vol. 42, pp. 327-367, 1993.
4. Datta, D., and H.S. Kushwaha, *Fundamental Statistics for Uncertainty Analysis, Uncertainty Modeling and Analysis*, Bhabha Atomic Research Centre, Trombay, Mumbai, 400085, (Editor: H.S. Kushwaha), pp. 1-48, 2009, ISBN: 978-81-907216-0-8.
5. Datta, D., *Statistics of Monte Carlo Methods Used in Radiation Transport Calculation, Applications of Monte Carlo Methods in Nuclear Science and Engineering*, Bhabha Atomic Research Centre, Trombay, Mumbai, 400085, (Editor: H.S. Kushwaha), April, 2009, ISBN: 978-81-8372-047-2
6. Vose, D., *Quantitative risk analysis - A guide to Monte Carlo simulation modeling*, Wiley, New York, 1996.
7. Robinson, P.C. and D.R. Hodgkinson, "Exact Solutions for radionuclide Transport in the Presence of Uncertainties", UK Atomic Energy Agency Report No. AERE R 12125, 1986.
8. Mishra S., "Sensitivity Analysis with correlated inputs- An Environmental Risk Assessment Example", Paper Presented in the Proceedings of the Crystal Ball User Conference, 2004.
9. Prado, P., T. Homma and A. Saltelli, "Radionuclide migration in the Geosphere, A 1D advective and dispersive transport module for use in probabilistic assessment codes", *Radioactive Waste Management and Nuclear Fuel Cycle*, vol. 16(1), pp. 49-68, 1991.
10. Abramowitz M and Stegun I A 1965 *Handbook of Mathematical Functions* (New York: Dover).

Development and Application of Radiotracer Technique for Online Leak Detection in High Pressure Heat Exchangers

H.J.Pant, V.K.Sharma, Sunil Goswami, J.S.Samantray and Gursharan Singh

Isotope Applications Division

Abstract

A radiotracer technique for online leak detection in high-pressure heat exchanger systems have been developed and successfully applied in various process industries in India. Bromine-82 as dibromobiphenyl is used as a radiotracer for leak detection in heat exchangers involving flow of organic fluids. The radiotracer is injected into high pressure side of the heat exchanger system and monitored at strategically selected locations in low pressure side using NaI(Tl) scintillation detectors connected to a preset data acquisition system. The tracer concentration curves monitored as a function of time are analyzed to identify the leaking heat exchanger(s). A number of leak detection investigations have been carried out since year 2001 leading to high economical benefits to the industry. This paper discusses principle of leak detection in high-pressure heat exchanger systems using radiotracer technique with two specific case studies.

Introduction

A leak is an undesirable interconnection between isolated parts of a system or between two systems and is suspected if there is any abnormal behavior of a system, such as loss of pressure, contamination of product or loss of process efficiency. A leak in a system can occur due to an unintended crack, corrosion or porosity, hole in an enveloping wall, loosening of bolts/joints and cracking of gaskets. After suspecting a leak(s) in a system, it is essential to confirm and identify the leaking system(s) at the earliest to avoid deterioration of product quality, loss of process efficiency, risk in safety and environmental hazards.

A heat exchanger (HX) is commonly used equipment in petroleum, petrochemical and chemical process industry. During the course of operation of these exchangers, occurrence of leakage is a common problem. Maintenance and servicing of HXs in industry is a difficult and expensive task necessitating hiring of a specialized agency. Therefore, it is necessary to confirm and identify the leaking HXs before planning shutdown and hiring a specialized agency for repair.

Online conventional analytical techniques are generally used to confirm and identify the leaking exchanger(s) provided sampling points are available at the inlets and outlets of individual heat exchangers. But a bank of heat exchangers that operate at high temperature and pressure usually do not have any sampling points at the inlet and outlet of the individual HXs because of safety reasons and thus analytical techniques cannot be applied for leak detection. There are other conventional techniques such as hydrostatic pressure test, chemical reagent test, bubble test, dye penetrant test, acoustic emission technique and helium tracer test for leak detection in industrial systems including heat exchangers. However, these techniques cannot be used online and thus require shutdown of the plant. Shutting down of the plant and applying conventional techniques is a cumbersome and time consuming procedure leading to substantial revenue loss to the industry.

Radiotracer techniques are widely used for leak detection in buried pipelines, measurement of flow parameters such as flow rates, residence time distribution, mixing/blending time in chemical reactors, sediment transport investigation in Ports,

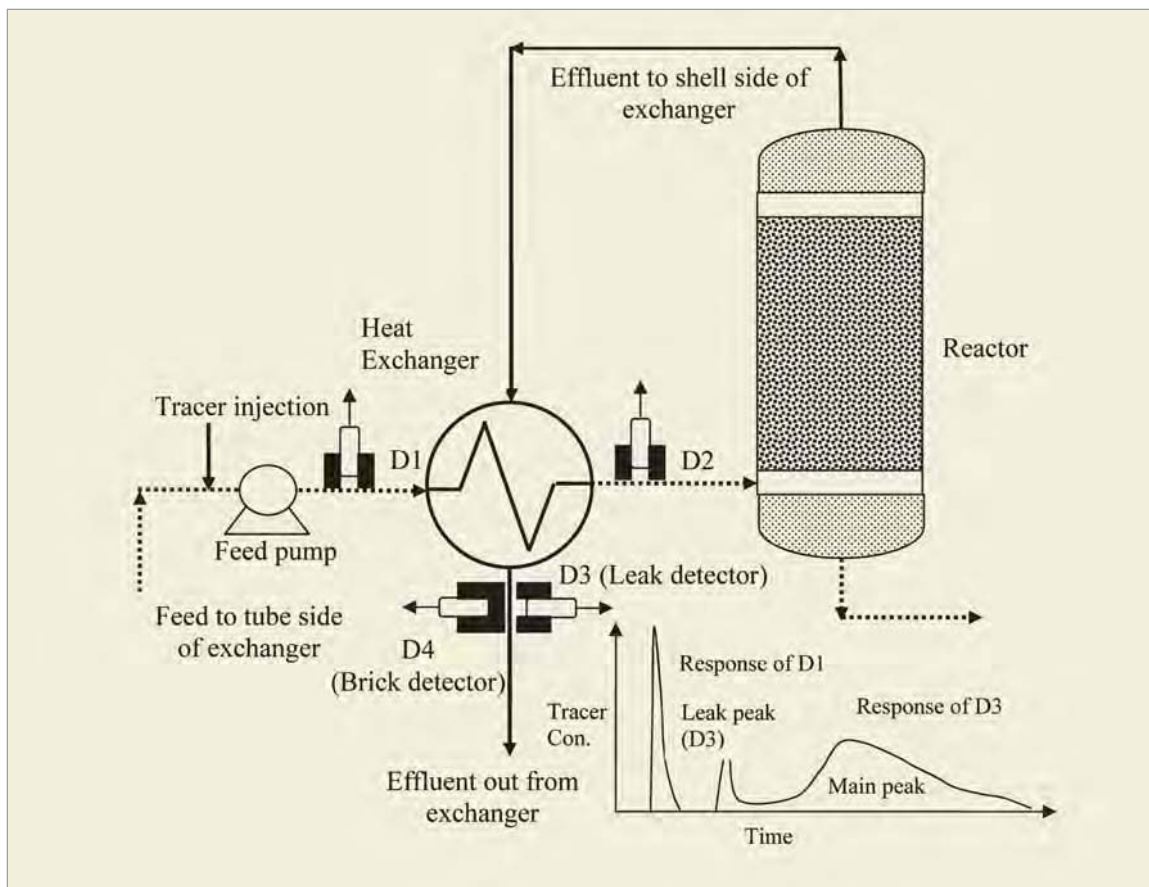


Fig. 1: Schematic diagram showing principle of radiotracer technique for online leak detection in heat exchangers

dispersion of effluents/pollutants in coastal waters and investigation of dynamics of fluids in oil fields. Radiotracer techniques have a number of advantages (over conventional tracer techniques) such as online detection, high detection sensitivity, availability of wide range of compatible radiotracers for different phases, ease of application to different situations and often do not have any competitive alternatives. The Isotope Applications Division, BARC has developed and applied a number of radiotracer techniques in Industry. Isotope Applications Division, BARC has alone carried out over 350 large-scale radiotracer investigations to benefit Indian Industry. At the request from different industries in India, development of online leak detection technique for HXs was undertaken by Isotope Applications Division, BARC in 2001. The technique was developed, standardized and applied in different

type of HXs. This paper discusses principle of radiotracer technique with two different case studies.

Principle of the Radiotracer Technique

The principle of leak detection in heat exchangers is based on differential pressure between two parts or components of the system and is shown in Fig. 1. If there occurs a leak in a heat exchanger, the fluid from high pressure side will leak into low pressure side. In shell-tube type heat exchangers in petroleum refineries, the cold feed is pumped to the tube side of the reactor and is required to be heated up before entering into the reactor, whereas the effluent from the reactor is fed through the shell-side the exchanger. The effluent flowing out of the reactor is at high temperature and transfers heat to the feed flowing through the tube side. In a feed-effluent exchanger, the feed stream (tube side) is at a high pressure than the effluent stream (shell side) and

therefore any leakage in the exchanger will be reflected in effluent side.

In radiotracer technique, a suitable radiotracer in an appropriate quantity is injected into the feed side (tube side) and monitored at the inlet and outlet of the tube side and outlet of the shell side (effluent stream) using three independent collimated scintillation detectors D1, D2 and D3, respectively as shown in Fig.1. The tracer concentration curve recorded by detector D1, usually called as 'injection detector' confirms injection of radiotracer into the tube side and time of injection. The detector D2 will provide residence time distribution curve of feed in tube side. However, any leakage in the exchanger will be reflected in tracer concentration curve recorded by detector D3 mounted at shell outlet of the exchanger, usually called as 'leak detector'. The curve recorded by detector D3 as shown in Fig.1, has two distinct tracer peaks. First peak preceding is due to leakage in the heat exchanger and is recorded immediately after inlet tracer concentration curve as the leaked tracer bypasses the reactor. Whereas, the second peak (main peak) is due to flow of tracer through the reactor and is referred residence time distribution of the reactor. The absence of leak peak in the curve indicates no leakage in the exchanger. There is always possibility of 'leak detector' recording false signals other than due to leakage if not shielded properly and thus misleading the results. Therefore an additional detector D4 called as 'brick detector' is also mounted at the shell outlet of the exchanger that monitors background radiations and stray/false radiations other than due to leakage. The signal recorded by 'brick detector' avoids ambiguity in leak detection due to stray/false signal.

Development of the Technique

Implementation of the radiotracer technique requires selection of a compatible radiotracer for the investigation in hand, its production, packaging, transportation to the experimental site, injection into the system, detection of radiotracer at strategically

selected locations and analysis of the data. Bromine-82 (^{82}Br) as dibromobiphenyl and as ammonium bromide is most suitable radiotracer for tracing organic and aqueous phase respectively, in leak detection investigations. The activity required varies from 40-100 mCi (1.5-3.7GBq) per test. The required radiotracers are produced in DHRUVA reactor at Trombay and transported to the experimental site in type approved lead containers / packages by Board of Radiation and Isotope Technology (BRIT), Mumbai with prior approval of Atomic Energy Regulatory Board (AERB), Mumbai. Necessary approval for conducting the investigation is obtained from the Radiation Safety Systems Division (RSSD), BARC and Atomic Energy Regulatory Board (AERB), Mumbai. At the site, the radiotracer is instantaneously injected into the system using a suitable injection system as



Fig. 2: A typical tracer injection system



Fig. 3: Collimated scintillation detector

shown in Fig. 2. The radiotracer is monitored at strategically selected locations using collimated scintillation detectors (size: 2 inch x 2 inch, Make: Amcrys, Ukraine) as connected to an indigenously developed multi-input data acquisition system (MIDAS). A typical collimated detector and MIDAS are shown in Fig. 3 and Fig. 4, respectively. The number of monitoring locations (detector) depends upon number of HXs in the system. Usually in a

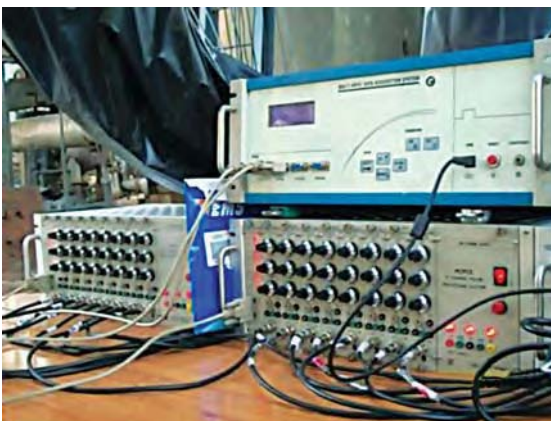


Fig. 4: Multi-input data acquisition system (MIDAS)



Fig. 5: A typical heat exchanger system in a refinery

single heat exchanger, three monitoring locations (detectors) are used. The MIDAS is coupled to a computer and can be programmed to monitor tracer concentration at a preset time interval. The acquired tracer concentration data monitored as a function of time is saved and analyzed to identify the leaking HX(s).

More than eleven radiotracer investigations have been carried out successfully by Isotope Applications Division, BARC during May 2002 to November 2011

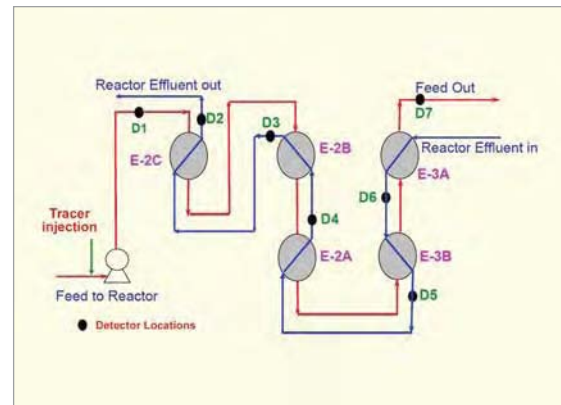


Fig. 6: Schematic diagram of the heat exchanger system and location of the detectors

in different petroleum refineries and petro-chemical industries in India. Types of HXs for which leak-detection was taken up were shell-tube type, rod-baffle type and welded-plate type. Two case studies are discussed in detail.

Table 1: Process and operating parameters in Shell-tube type heat exchangers

Exchanger	Shell Side						Tube Side					
	Fluid	Flow rate (Kg/hr)		Temp ($^{\circ}$ C)		Pressure (Kg/cm 2 g)	Fluid	Flow rate (Kg/hr)		Temp ($^{\circ}$ C)		Pressure (Kg/cm 2 g)
		Liquid	Vapour	In	Out			Liquid	Vapour	In	Out	
E-2 A/B/C	Feed	75739	5350	70	227	95	Effluent	64999	24172	268	158	83
E-3 A/B	Feed	72822	8267	227	356	94	Effluent	59568	29603	318	268	82

Case Studies

Leak detection in shell-tube type heat exchangers

A hydrocracker plant at M/s Indian Oil Corporation, Guwahati Refinery, Guwahati, Assam is meant for conversion of fresh feed (vacuum oil gas) to diesel. The plant consists of a furnace, hydrocracker (packed bed reactor) and a high-pressure heat exchanger system consisting of a number of heat exchangers connected in series. Plant engineers suspected leakage in the heat exchanger system because of presence of high level of sulphur in the final product. A radiotracer investigation was carried out to confirm leakage and identify leaking heat exchanger(s) in the heat exchanger system. A photograph of the heat exchanger system and schematic diagram of experimental setup showing radiation detectors for tracer monitoring are shown in Fig. 5 and Fig. 6, respectively. The process and operating conditions during the tracer tests are given in Table 1. ^{82}Br as dibromobiphenyl was used as a radiotracer. Two tests were conducted in April 2006 and about 1.85 GBq (50 mCi) activity was used in each test. The radiotracer was instantaneously injected at the suction end of the feed pump (shell side) and monitored at seven different strategically selected locations using collimated NaI(Tl) scintillation detectors (D1-D7) as shown in Fig. 3. Detector D1 (injection detector) and detector D7 record tracer concentration at the feed inlet and outlet respectively; and provide information about time of entry and exit of radiotracer from feed side of the exchanger, respectively. Leak detectors D2, D3, D4, D5 and D6 installed at tube outlets will record peaks due to leakages in the heat exchangers. In case of no leak in any of the heat exchangers, these detectors

will record only the background radiation levels. Fig. 7 shows a typical tracer concentration curves recorded in one of the tests. Peaks recorded by 'leak detectors' (D2, D3, D4, D5, D6) indicate existence of leaks in the heat exchanger system. The leaking exchangers could be identified based on the time of appearance of the peaks. First peak recorded by detector D2 appears later than the peaks recorded by detector D3. This implies that there is no leakage in E-2C and the peak recorded by D2 is due to leakage in exchange E-2B. Similarly, the subsequent peaks recorded by detector D2 were due to leakage in other upstream exchangers. If there would have been leakage in E-2A, detector D4 would have recorded peak prior to D5 and D6. However this was not observed. This eliminates possibility of occurrence of leak in E-2B. The peaks recorded by detector D5 and D6 clearly shows occurrence of leakage in exchanger E-3B and E-3A, respectively. Subsequent peaks recorded by detector D2, D3 and D4 are due to leak in exchanger E-3B. The extent of leakage in exchanger E-2A detected by D6 was low and the same could not be reflected in subsequent detectors due to dilution of radiotracer. Thus it was concluded that exchanger E-2B, E-3A and E-3B were found to be leaking.

In order to quantify the leak rates, the area of peak recorded by inlet detector i.e. detector D1 and the area of peaks recorded by "leak detector" were compared and the leak rates were estimated using the following relation.

$$\text{Leak rate (\%)} = \frac{\text{Area of leak peak}}{\text{Area of input peak}} \times 100 \quad (1)$$

The estimated leak rates in individual heat exchangers are given in Table 2. The total leak rate will be the

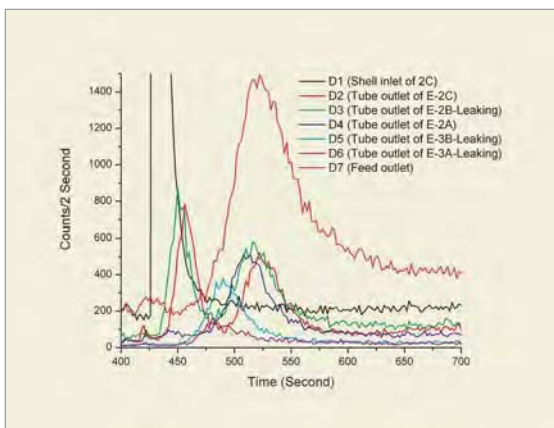


Fig. 7: A typical plot showing tracer concentration curves recorded by detectors

sum of individual leak rates. The mean total leak rate was found to be about 22.2 %. The total leak rate estimated by sulphur balance method in laboratory was found to be about 21 %.

Based on the results of the investigation carried out in April, 2006, shutdown of the plant was planned and necessary repair work was undertaken. The leakage in three exchangers was visually confirmed. After plugging the leaks, the plant was put back into normal operation. The analytical tests carried out for sulphur content in different product streams after restarting the plant showed sulphur content less than the design value (20 ppm). This indicated that the leaks in all the three heat exchangers were plugged.

Table 2: Leak rates in heat exchangers

Run No	Leak rates in individual heat exchangers (%)				Total leak rate (%)
	E-2B	E-2A	E-3B	E-3A	
1	3.7	4.7	7.7	9.4	25.5
2	7.2	8.6	6.6	9.0	31.4
3	5.0	6.7	7.7	10.4	29.8
Mean	5.3	6.7	7.3	9.6	28.9

Leak detection in a welded plate type heat exchanger system

A Diesel Hydrotreating (DHDT) unit at M/s IOCL Panipat Refinery, Panipat is designed to process a

hot blend of diesel streams and to produce a diesel of a specific quality characterized by higher cetane number and low sulfur content (30 ppm wt). The unit comprises of two parallel trains, each comprising of a reactor feed/effluent exchanger, a heater, two reactors and a stripper feed preheater connected in series; and can process 50% of the total feed. The heat exchanger system in each train consists of two independent reactor feed/effluent exchangers (E1 & E2) as shown in Fig. 8. The exchangers are not of conventional shell-tube type exchangers but welded-plate type exchangers of Alfa Laval Packinox make. Each heat exchanger consists of a bundle of a number of explosion formed, corrugated, metal sheets stacked on top of each other, separated at the edges by a spacer and contained within a pressure vessel. The two fluids are distributed in the heat exchanger bundle through header boxes mounted on both sides of the exchanger and flow between the plates of the exchanger where the heat exchange takes place. The heat exchangers are mounted vertically and operate in counter-current flow mode. The hot effluent from the reactors is equally divided into two streams and fed to the effluent side of each heat exchanger. The effluent transfers heat to the feed while flowing down from top to bottom and gets cooled. Similarly, feed is pumped through a common feed line which subsequently splits into two equal streams and flows to individual exchangers. The cold feed enters the heat exchangers from bottom and flows upward as it gets heated. During the normal operation, the total flow rate of feed and effluent are about 490 tons/hr and 540 tons/hr, respectively. Whereas the pressure in feed and effluent sides are about 127 kg/cm²g and 110 kg/cm²g, respectively. Four bellows are provided to compensate for differential thermal expansion between the hot stainless steel bundle and the pressure vessel. Since the bundle has no gaskets to soften and leak, the exchanger can be operated at temperatures as high as 550°C. During routine laboratory analysis, the sulfur content in the product (hydrotreated diesel) was found to

be high (>200 ppm). Even on increasing the weighted average bed temperature (WABT) of the reactors, there was no reduction in sulfur content in the product, indicating that the high sulfur content is not due to reduction of catalyst activity. After eliminating all the possibilities, leakage in either or both the feed/effluent exchangers was suspected to be source of product contamination.

Since the reactor feed/effluent exchangers (E1/E2) operates at high-pressure and there were no sample points available at the inlet and outlet of both the exchangers, confirmation of leak by analytical methods was not possible. Initially a Furfural test was conducted to confirm the leakage in the system. The Furfural tracer test confirmed the leakage in the heat exchanger system but again it was not possible to identify the leaking exchanger(s). Therefore, at the request of Indian Oil Corporation Limited, Panipat Refinery, a radiotracer investigation was carried out to identify the leaking heat exchanger(s).

In order to implement a radiotracer investigation with increased possibility of detection of even minor leaks and minimum radiation hazards, it was decided to operate the DHDT unit at about 30 % lower capacity than the normal conditions. In addition to this, the temperature of the feed was also reduced to minimize the production of vapor phase and hence enhancing possibility of detection of minor leakage(s). All the bypass and recirculation lines were also closed during the tracer test. The operating conditions during the tracer test of the heat exchanger system are given in Table 3. The radiotracer, having activity of about 100 mCi

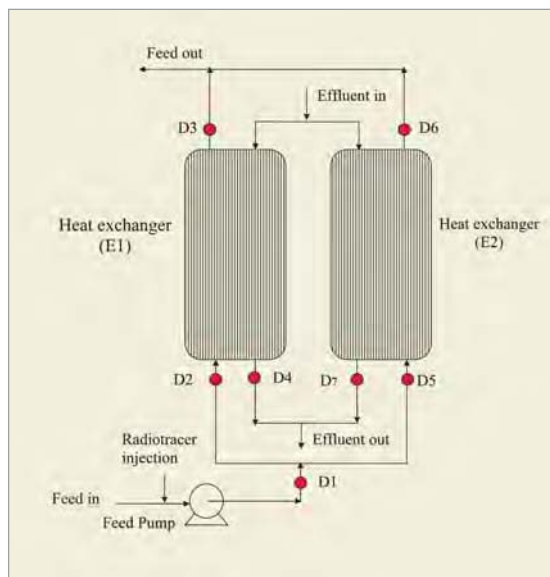


Fig. 8: Schematic diagram of heat exchanger system and tracer monitoring locations

(3.7 GBq), was instantaneously injected into the suction end of the feed pump using a specially fabricated injection system. Therefore, 50 mCi (1.85 GBq) activity will be eventually injected into feed side of each exchanger. The radiotracer was monitored at seven different strategically selected locations using collimated 2 inch x 2 inch NaI(Tl) scintillation detectors. The radiotracer concentration was monitored on the common feed line, the individual feed inlets & feed outlets and the effluent outlets of the two heat exchangers (E1 & E2) as shown in Fig.8. All the detectors were connected to a computer controlled data acquisition system (DAS); set to record tracer concentration at an interval of one second. If there exit a leakage in either or both the exchangers, the differential

Table 3: Actual process and operating conditions in heat exchanger system during radiotracer test

Exchanger	Feed side				Effluent side					
	Fluid	Flow rate (tons/hr)	Temp. (°C)		Inlet Pressure (kg/cm ² g)	Fluid	Flow rate (tons/hr)	Temp. (°C)		Inlet Pressure (kg/cm ² g)
			In	Out				In	Out	
E1	Reactor Feed (HC+H ₂ +H ₂ S+H ₂ O)	183	88	286	123	Reactor Effluent (HC+H ₂ +H ₂ S+H ₂ O+NH ₃)	207	322	202	113
E2	Reactor Feed (HC+H ₂ +H ₂ S+H ₂ O)	181	88	294	121	Reactor Effluent (HC+H ₂ +H ₂ S+H ₂ O+NH ₃)	204	319	195	112

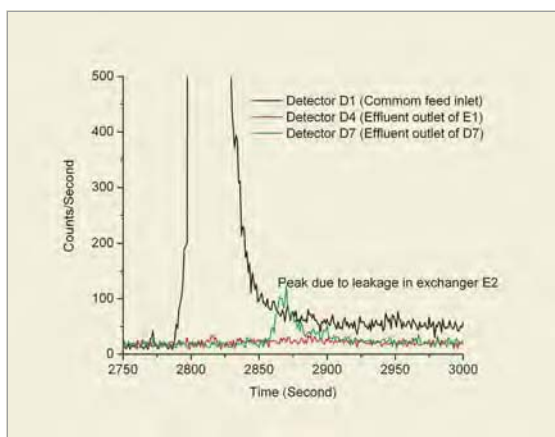


Fig.9: Tracer concentration curves recorded by detectors

pressure of 10 kg/cm²g will cause leakage from feed to effluent side, and get detected by detector D4 and D7 mounted on counter-currently flowing effluent streams. Fig. 9 show tracer concentration curve recorded by three different detectors mounted at common feed line and effluent outlets of the two heat exchangers indicating absence of leakage in exchanger E1 and presence of leakage in exchanger E2. Thus based on the study it was concluded that out of the two exchangers, only one exchanger i.e. E2 was found to be leaking. It was not possible to quantify the leak rate because of possibility of significant loss of radiotracer due to adsorption of radiotracer within the exchangers.

Based on the results of the investigation, shutdown of the plant was planned and necessary remedial measures were initiated. During the shutdown, the leakage in exchanger E2 was confirmed and leak rate was estimated using off-line Furfural tracer test and was found to be about 3% .

Conclusions

Radiotracer technique is an ideal technique for online leak detection in high-pressure heat exchangers. The technique has been developed, standardized and successfully applied to detect leakages in different types of heat exchangers in various refineries in India. Each online leak detection investigation carried out in refineries reduces the unnecessary shutdown time by a period of 10-15 days thus leading to high economic benefits to the industry. The potential of the technique and economical benefits grown out of the applications of the technique have been recognized by Indian industry and is now being used routinely on commercial basis.

References

1. Charlton, J.S.,(Eds.), Radioisotope Tracer Techniques for Problem Solving in Industrial Plants, Leonard Hill (1986), 320p.
2. Pant, H.J., Sharma, V.K. and Singh, Gursharan, Leak detection in a high pressure heat exchanger system using radiotracer technique, Proceedings of Thirteenth Annual Conference of Indian Nuclear Society (INSAC-2002) on Nuclear Technology-Catalyst for National Development, Bhabha Atomic Research Centre, Mumbai, India, October 9-11, 2002, pp.3.
3. International Atomic Energy Agency, Leak Detection in Heat Exchangers and Underground Pipelines Using Radiotracers, Training Course Series 38, IAEA, Vienna (2009).

Design & Development of Weld Inspection Manipulator for Reactor Pressure Vessel of TAPS-1

H. Chatterjee, J.P. Singh, R. Ranjon, M.P. Kulkarni and R.J. Patel
Refuelling Technology Division

Abstract

The reactor pressure vessel (RPV) of TAPS-1 BWR contains six longitudinal and four circumferential welds. Periodical in-service inspection of these weld joints has been a regulatory issue pending for long. In the 22nd refuelling outage in July 2012 the inspection of L1-1, L1-2 longitudinal welds as well as their junctions with C1 circumferential weld were proposed to be done using ultrasonic technique. Approaching these welds from OD side of the RPV is a difficult and tedious task. Therefore it was decided to examine these welds from ID side of the RPV by filling the cavity with water and approaching the RPV from top. No technology was locally available to take the probes at a depth of 10-12 m under water. NPCIL approached RTD, BARC to develop an underwater manipulator to accomplish this task. RTD took up this work as a challenge and came out with the design of manipulator. The weld inspection manipulator (WIM) was fabricated on a war foot basis, tested and successfully implemented in the reactor for the first time in TAPS history. The entire activity was completed in three months time. This article gives the details of design, manufacturing, performance testing, qualification trials and implementation of WIM in the reactor. Ultrasonic testing techniques were developed by QAD, BARC which are not covered in this article.

Introduction

The RPV of TAPS-1 is made of SA 302 grade B low alloy steel 3916 mm in outer diameter and 124 mm thick. It is internally clad with 5.6 mm thick SS 308L austenitic stainless steel weld deposits. There are six longitudinal and four circumferential welds in the RPV as shown in Figs. 1 and 2. The vessel welds are to be inspected periodically as a part of regulatory requirement. These welds cannot be approached for inspection from outside of the vessel due to the presence of thermal shield and from inside due to vessel internals. However during planned shut-down of the reactor the drier and separator assemblies are removed from the RPV top shell. As a result L1-1, L1-2 and their junctions with C1 become accessible for inspection from inside of the vessel.

Weld Inspection Manipulator has been developed to assess the integrity of L1-1 and L1-2 weld joints as well as their junctions with C1. During inspection the manipulator is lowered under-water along a

longitudinal weld to its lowest location. The manipulator then clings on to the RPV wall using permanent magnets and can move on the vessel along the weld using refuelling grapple. The motorized weld cleaning brush attached to the manipulator can be traversed laterally using cross travel at any location of the weld to clean the deposited materials on the heat affected zone (HAZ) of that location. Thus by operating sequentially the grapple for vertical motion and cross travel for transverse motion the entire weld and its HAZ can be cleaned.

Subsequently the weld cleaning brush is replaced by probe holders and the entire weld and its HAZ can be scanned using the motions of grapple and cross travel.

Design Details

The weld inspection manipulator has to perform four important functions namely: (i) clinging on to RPV wall, attaching to or detaching from RPV wall and moving on the RPV wall along a longitudinal

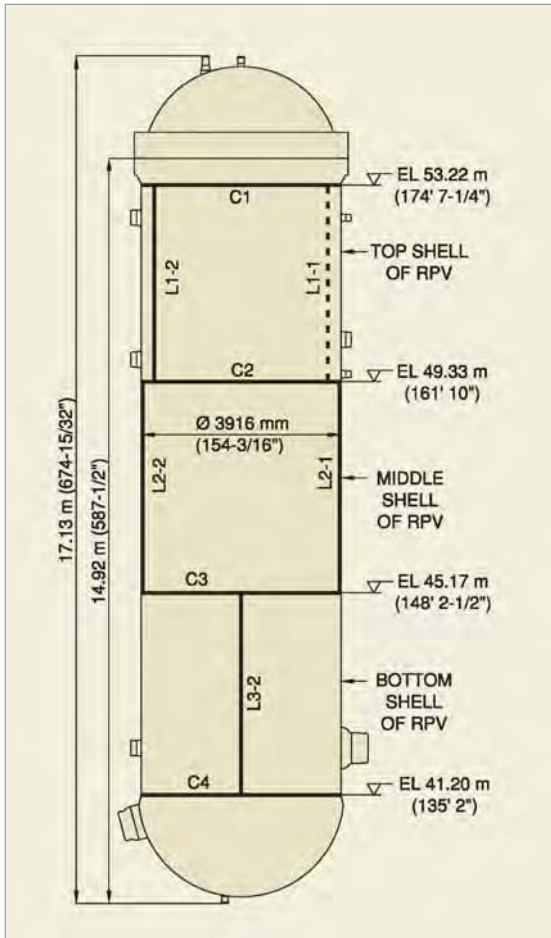


Fig. 1: Schematic of reactor pressure vessel of TAPS 1

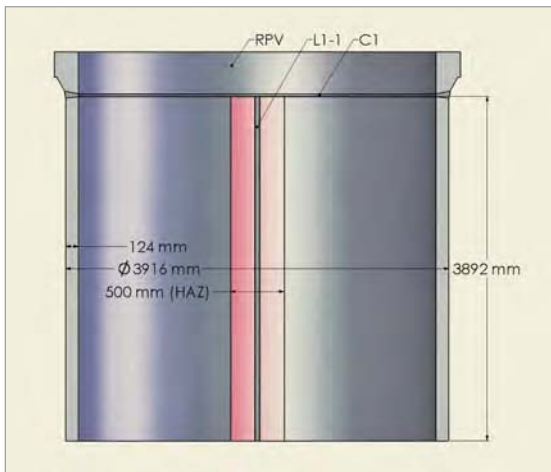


Fig. 2: RPV top shell. clad removed to show C1 and L1-1 welds

weld (ii) transverse motion of probe holder or weld cleaning brush across the HAZ (iii) weld cleaning and (iv) UT scanning of welds. Accordingly there are four major subassemblies to perform these

functions: (a) main body (b) cross travel assembly (c) weld cleaning assembly and (d) probe holder assembly as described below:

Main Body

It consists of a triangular SS 304 platform 975 mm high, 740 mm wide and 16 mm thick about which all other components of WIM are configured (Fig. 3). The typical triangular shape allows it to be mounted on three wheels which impart enhanced stability on the RPV surface and minimum lateral traction during moving on the RPV. Three cut-outs on its surface are meant to make it light weight. The SS 304 bail attached to the platform is similar to the bail of TAPS fuel assembly to make it compatible to refuelling grapples for handling. The seating face below the bail is meant for parking WIM using gantry at the gantry operated manipulator (GOM) stand in the fuel storage pool of the reactor building. From there it is picked up by the grapples and shifted to the cavity interconnected with it. Three wheels are mounted on the platform by taking into account the curvature of the RPV. Aluminum has

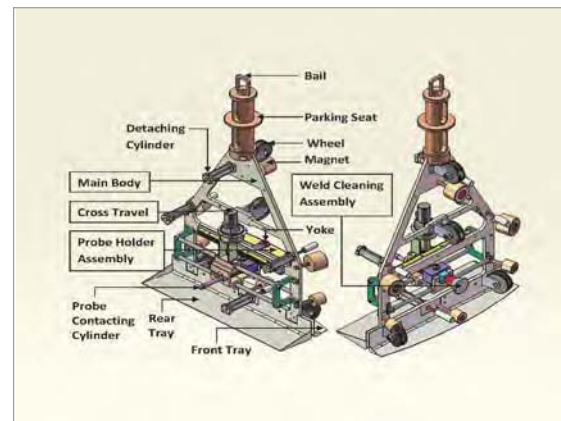


Fig. 3: CAD model of weld inspection manipulator

been chosen as the wheel material. Due to its softness as compared to SS, the RPV clad surface is protected from any scratch marks during moving of WIM in addition to its other advantages like light weight and corrosion resistance.

An additional fourth wheel has been provided at the centre of the platform to facilitate inspection of the region where L1-1 or L1-2 joint meets C1. At

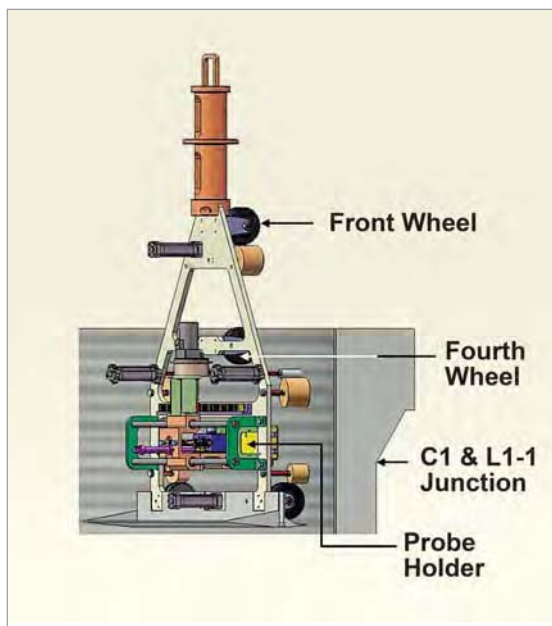


Fig. 4: Role of additional fourth wheel

this time the front wheel moves out of the RPV and the fourth wheel provides support to the platform as shown in Fig. 4.

Neodymium Iron Boron permanent magnets have been mounted at six locations of the platform for clinging WIM onto the RPV. These magnets have highest energy product and excellent retentivity among other commercially available grades. Thus a large pull force is provided by a small size of the magnet which is especially advantageous for light weight applications. The poor corrosion resistance due to the presence of large quantity of Fe is circumvented by providing epoxy coating around the magnet. When WIM moves on the RPV the gap between front face of these magnets and RPV clad is 1-2 mm. Together these magnets provide a pull-force of approximately 30 kg on RPV which is sufficient to keep WIM clinging onto the RPV during inspection or cleaning.

Four pneumatic cylinders are used to detach WIM from RPV. All fasteners are

locked by tack welds or locktite but to prevent any accidental fall of WIM hardware into the RPV, trays have been provided. The scheme for operating pneumatic cylinders for WIM operation is shown in Fig. 5.

Four cylinders are used for detaching WIM from the RPV as and when required. Lever operated directional control valve (DCV) will keep these retracted under normal condition. During extending the piston for detaching WIM, flow control valve (FCV) with metered-out connection will avoid any impact on the RPV.

Cross Travel

It consists of an SS 304 cross travel guide block with bronze bush free to move horizontally on three SS 304 guide rods Fig. 6. An SS 304 rack is screwed on to WIM platform. The cross travel guide block carries an SS 304 enclosure containing a 30 W brushless DC motor with gear head and a rotary potentiometer. The enclosure is kept under 2 bar (g) air pressure to avoid water-leakage into it from the RPV Fig.5.

The DC motor drives an SS 304 pinion which engages with rack and causes transverse motion of the cross travel guide block at 2.5-100 mm/s.

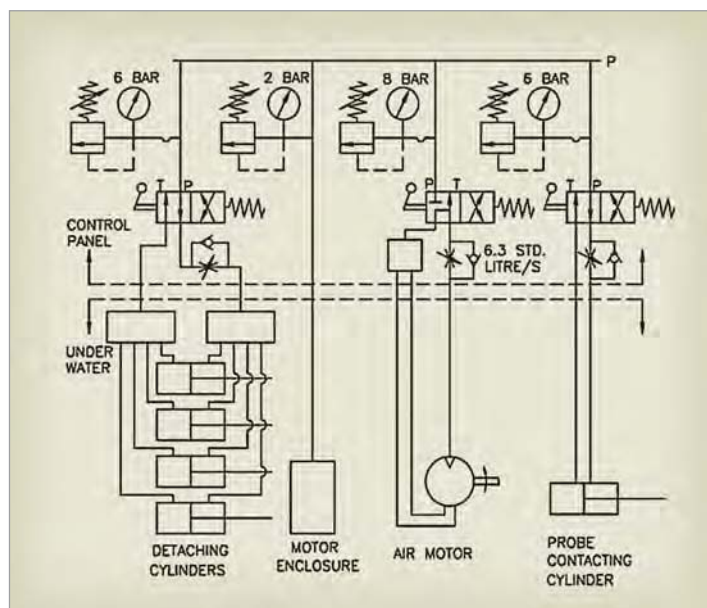


Fig. 5: Pneumatic scheme for WIM operation

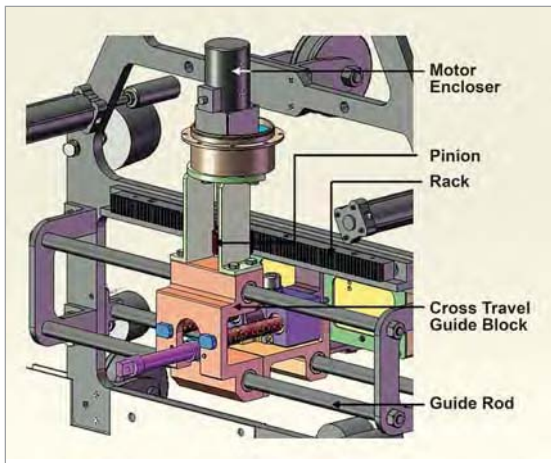


Fig. 6: Cross travel assembly

The position of the cross travel is sensed by potentiometer with an accuracy of 1.7 mm. The velocity of the cross travel is regulated by PC based control scheme Fig. 7. Operator interface software (OIS) program facilitates operation in four modes selectable by operator as a) speed & direction control through Joystick b) Direction control through joystick and speed setting through OIS c) Both speed & direction control through OIS d) Intermittent operation (start/stop timing configurable) through OIS. A USB based data acquisition system acquires control signal from a joystick. The signal is processed through control logic programmed in personnel computer in order to generate required output to motor driver through data acquisition card. The DC motor is equipped with built-in EM brake which is

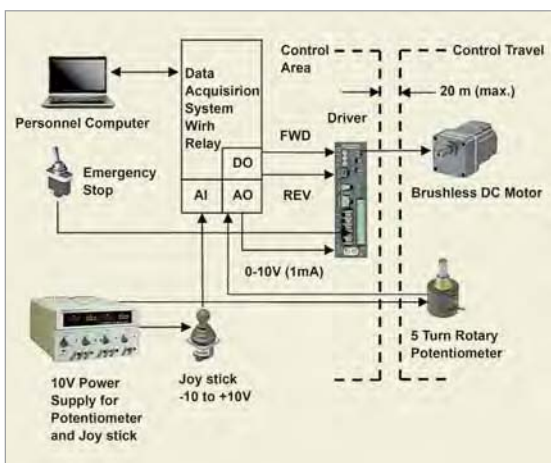


Fig. 7: Schematic of cross travel control scheme

released whenever motor starts and actuated whenever it stops without any external command. Protection logic is implemented in the control program to prohibit movement of cross travel at extreme ends. The motor driver has inbuilt protection feature for over torque condition. A backup hard-wired control scheme is provided to perform all the above functions in case the data acquisition system or software is not available.

Weld Cleaning Assembly

This consists of an SS air motor 90 W, 100 rpm and a weld cleaning brush with stainless steel body and Nylon 6-12 bristles which are fitted on to the WIM main body after removing the end-effector assembly Fig. 8. The pneumatic cylinder presses the brush against the weld joint to be cleaned. While the air motor rotates the brush, the cross travel is indexed horizontally in steps of 10-15 mm from one end and the refuelling grapppler pulls the WIM vertically up to clean a horizontal strip of the HAZ.

Thus by the combination of cross travel and refuelling grapppler the entire 500 mm HAZ can be cleaned. The pneumatic scheme for probe contacting cylinder and air motor is shown in Fig. 5.

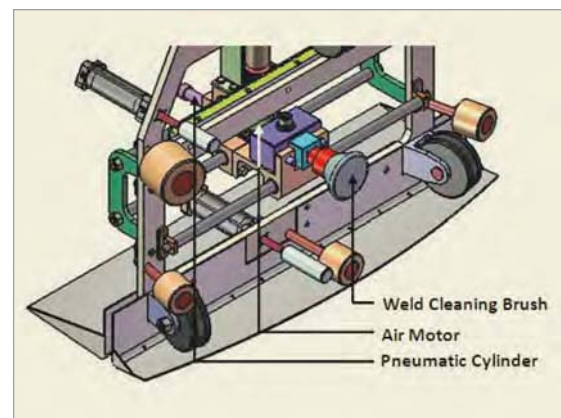


Fig. 8: Weld cleaning assembly

Probe Holder Assembly:

It is an assembly of probe holder and yoke. It is of two types: horizontal end effector is for detecting vertical weld defects Fig. 9(a). Vertical end-effector is for detecting horizontal weld defects Fig. 9(b).

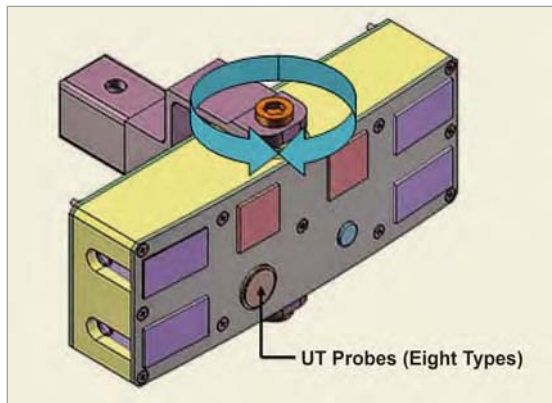


Fig. 9(a): Horizontal probe holder assembly

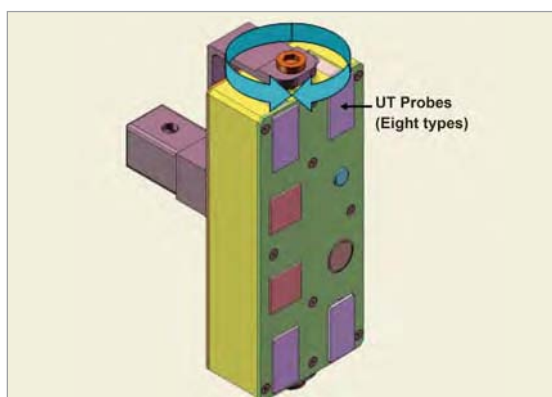


Fig. 9(b): Vertical probe holder assembly

The probe holder, made of Nylon 6-12 due to its low water absorption property, has its front face shaped to the curvature of RPV for perfect contact. It can freely swivel about the yoke pin and automatically adjust its contact with the RPV irrespective of the position of the cross travel guide block.

It houses 8 UT probes for flaw detection each for a peculiar purpose. The individual probes are spring loaded so that each of them is in complete contact with RPV Fig. 10. The contact between probe holder and RPV is made using a pneumatic cylinder. Development of UT technique and selection of UT probes were done by QAD, BARC.

Test set-up of WIM

As the test setup for functional testing of WIM had to play a vital role throughout the entire activity, its fabrication was taken up prior to the fabrication of WIM.

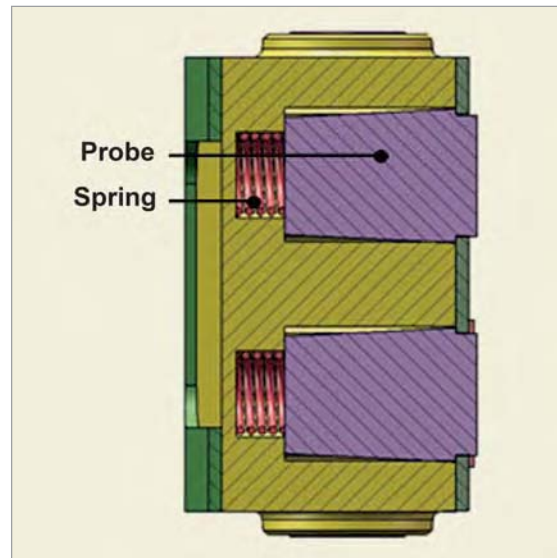


Fig. 10: Probes with individual springs

It was made by bending two plates to simulate the RPV and clad respectively. The plate representing clad was backed by the plate representing RPV and both plates were supported on a vertical support structure as shown in Fig. 11(a) and (b). Each plate is 2.5 m high, 1.28 m wide and 6 mm thick. Standard notches were machined at several locations of the SS 304 clad which acted as reference notches for demonstrating the notch sensing capability of WIM using UT probes.



Fig. 11(a): WIM with test setup



Fig. 11(b): WIM with cross travel and probe holder

Fabrication and Testing

Precision machining components of WIM like guide-rods, motor enclosure, probe holder etc. were made on CNC machine. All bought out components were delivered within four weeks. Fig. 12 (a) to (d) shows some of the important components of WIM. Performance testing of WIM was carried out in the supplier’s premises. All functional aspects like clinging on test setup wall using magnetic force,



(d)

Fig. 12: (a) Air motor with weld cleaning brush, (b) DC motor with potentiometer, (c): Horizontal probe holder, (d): WIM control panel

moving on test setup wall, pressing the probe holder against test setup wall by probe contacting cylinders, horizontal scanning of HAZ by cross travel, cleaning action of brush by air motor, sensing the reference notches by UT probes and detaching from the walls by advancing the detaching cylinders were successfully demonstrated.

Qualification Trials at AAFR, TAPS-1

WIM was shifted to the Additional Away From Reactor (AAFR) fuel storage pool of TAPS 1&2 for qualification trials. AAFR has facilities like refuelling grapple for handling WIM and Gantry Operated Manipulator (GOM) stand for parking WIM in the pool Fig. 13. These facilitate handling and testing of WIM in reactor simulated conditions. The capabilities of WIM for weld inspection were demonstrated by immersing WIM in the pool

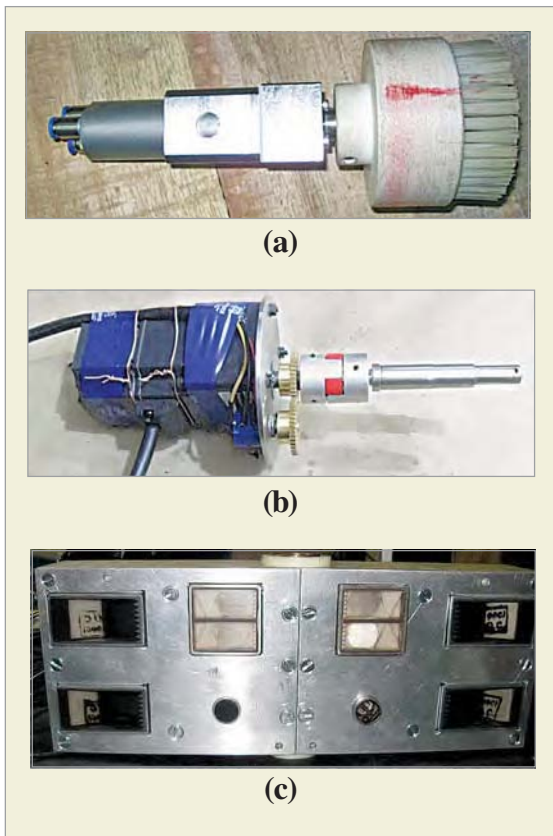


Fig. 13: AAFR fuel storage pool of TAPS 1&2

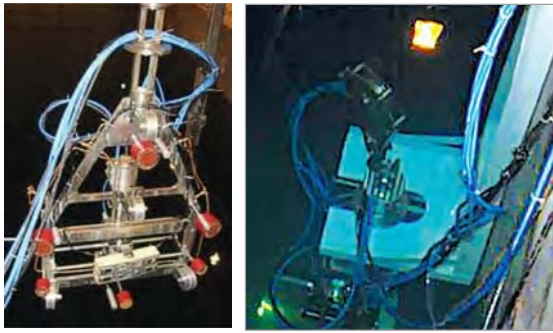


Fig. 14: WIM lowered to AAFR pool (left), WIM parked on GOM stand (Right)

Fig. 14 with the same test setup as used in the supplier's premises and reference standard notches were successfully detected.

During this activity it was observed that an unacceptable level of electromagnetic noise was induced in the UT probes whenever the DC motor of cross travel was running. This problem was addressed by running the cross-travel intermittently in steps of 3-4 mm. Probes were calibrated using calibration blocks having standard notches and simulating RPV clad surface.

Deployment in the Reactor

WIM was finally deployed to the reactor for implementation. Welds L1-1, L1-2 and their HAZ were cleaned by weld cleaning brush. UT scanning of these welds and their junction with C1 were successfully carried out Fig. 15 & 16. During weld inspection it was found that the RPV clad surface has waviness of the order of 2-3 mm which resulted in intermittent contact between probes and RPV clad surface. It takes about 5 hrs for cleaning a longitudinal weld, 8 hrs for scanning by vertical probe holder and 16 hrs for scanning by horizontal probe holder.

Data acquisition during RPV inspection was done by QAD, BARC. During cleaning of the circumferential-longitudinal weld junction the Vessel Flange Protectors which protrude a little inside the RPV and are made up of carbon steel were found to obstruct the inspection by attracting the magnets. This problem was solved by replacing them by SS 304 flange protectors.



Fig. 15: WIM performing weld cleaning

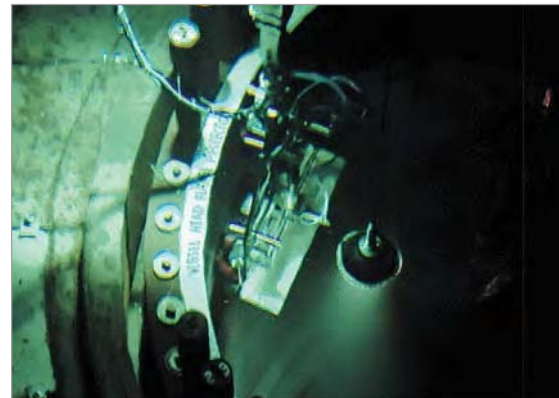


Fig. 16: WIM performing weld inspection using horizontal probe holder

Conclusion

Weld inspection of reactor pressure vessel (RPV) of TAPS 1&2 has been a long pending regulatory requirement. In the 22nd refuelling outage of July 2012 weld inspection of the welds L1-1, L1-2 as well as their junctions with C1 has been successfully carried out from inside the RPV of TAPS-1. Weld Inspection Manipulator was especially designed and fabricated in a short span of three months for this purpose. This development is the first of its kind inspection for BWR RPV. This has helped the site to fulfill its commitment of RPV weld inspection for the first time in TAPS history. WIM may be employed for cleaning and inspection of all accessible areas of the vessel from inside.

Machinery Protection System for Large Rotating Machines

Sanjay K. Jain, M. Kalra, Gaurav and D. A. Roy
 Reactor Control Division

Abstract

For vibration monitoring and protection of large rotating machines like turbines, large motors, etc, a DSP based Machinery Protection System (MPS) has been designed and developed jointly by BARC and ECIL. The system is designed to protect the rotating machines from catastrophic failures due to excessive vibration. The system provides continuous, online monitoring of vibration and related signals and meets the requirements of API 670 standard for machinery protection systems.

Introduction

Health of large rotating machinery gets reflected in the vibration signals collected from the rotating and supporting structures. Using this vibration data, it is possible to detect any impending trouble in the machine so that preventive action can be taken in time and catastrophic failures can be avoided. Continuous vibration monitoring can provide quick warning against excessive vibration and prompt the operator to take remedial action. An on-line vibration monitoring and protection system thus plays an

important role in ensuring safety and economics of the plant.

With the aim to address this need for such an on-line system having state-of-art features configurable for individual plant requirements, the indigenous development of a Digital Signal Processor (DSP) based Machinery Protection System (MPS) was initiated by RCnD, BARC as a joint effort along with ECIL, Hyderabad under an MOU between BARC and ECIL.

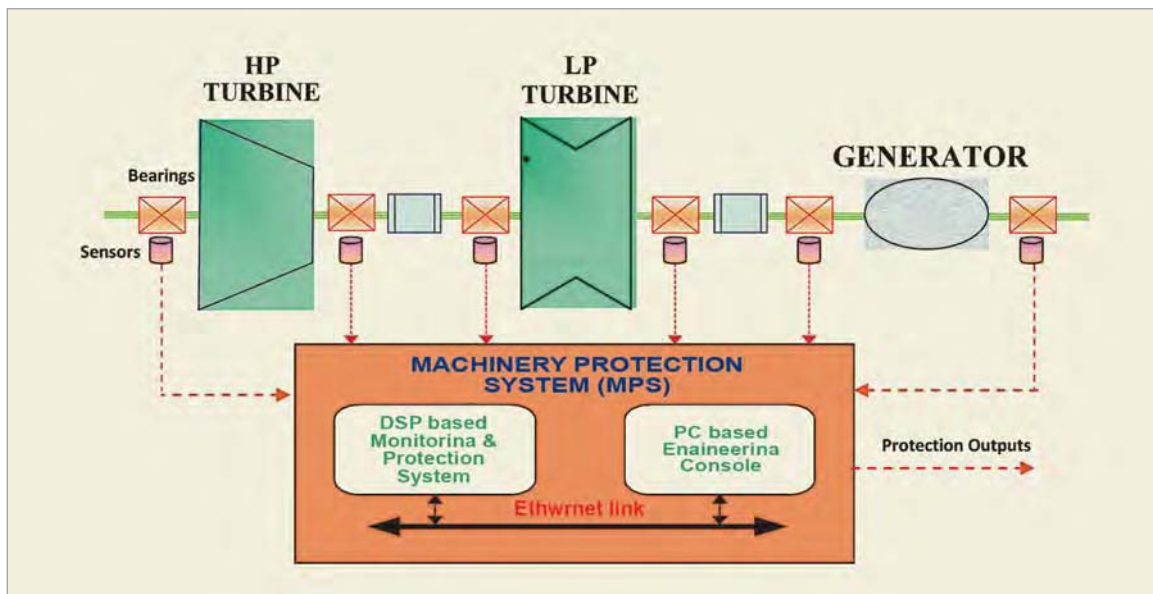


Fig. 1: Machinery protection system

The main components of the system (Fig.1) are the front-end instrumentation consisting of transducers (for vibration, speed and process parameters) and signal conditioning, DSP based data acquisition and protection module and back-end PC-based monitoring and configuration station. The main objective of the system is to monitor all the vibration signals to detect any deviation from normal levels and to provide alarm and trip signals in case the deviations are beyond certain set limits.

System Description

The Machinery Protection System (MPS) acquires a number of dynamic input signals (like vibration, displacement, eccentricity etc.) and speed input signals from field and on detecting excessive vibration levels it provides alert signal to operator and generates contact outputs to shutdown (trip) the machine. The system can be configured to measure the following parameters:

1. Absolute Vibration (Accelerometer, Velocity Sensor)
2. Relative Shaft Vibration (Radial Measurement)
3. Absolute Shaft Vibration (Accelerometer, Proximity Sensor)
4. Shaft Position (Axial or Radial)
5. Shaft Eccentricity
6. Absolute Expansion (Casing expansion or Overall thermal expansion)
7. Relative expansion (between the rotor and the stator)

Measurement of the above parameters requires acquisition of the signals, signal validation and necessary signal processing. The signal processing and monitoring functions include:

- Processing of all dynamic channels to extract signal parameters like RMS, peak and peak-to-peak values
- Sensor health checking to monitor for broken lines or faulty components of sensors.

- Alarm processing with programmable ALARM and TRIP limits and programmable time delays and hysteresis.

Protection is achieved by generating contact output to trip (shutdown) the machine when any of the above measured parameter exceeds the set TRIP limit. The system also generates analog outputs for monitoring purpose. It sends relevant information on Ethernet for display to operator on a PC based Engineering Console. The Engineering Console also provides facility to configure various input parameters and their trip settings.

System Architecture

The Machinery Protection System (MPS) consists of an embedded system installed in 19" bin and a PC-based Engineering Console (EC), which are connected through Ethernet. The embedded system is of modular construction and is user configurable through the Engineering Console. The embedded system acquires various dynamic signals like vibration signal, displacement signals etc. and if any of these signals crosses the ALARM (alert) limit, it generates a digital alarm output and if the measured value crosses the TRIP (danger) limit then it generates a trip contact output which is used to protect/shutdown the machinery.

Apart from the protection function the embedded system also sends the acquired data to the Engineering Console for monitoring, analysis and display. The engineering console is used to configure the embedded system, to analyze the data received from embedded system and also to display the data

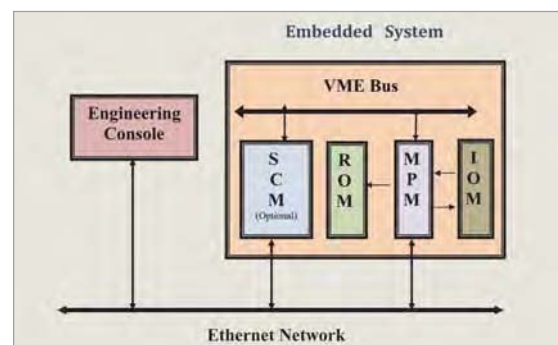


Fig. 2: Block diagram of MPS

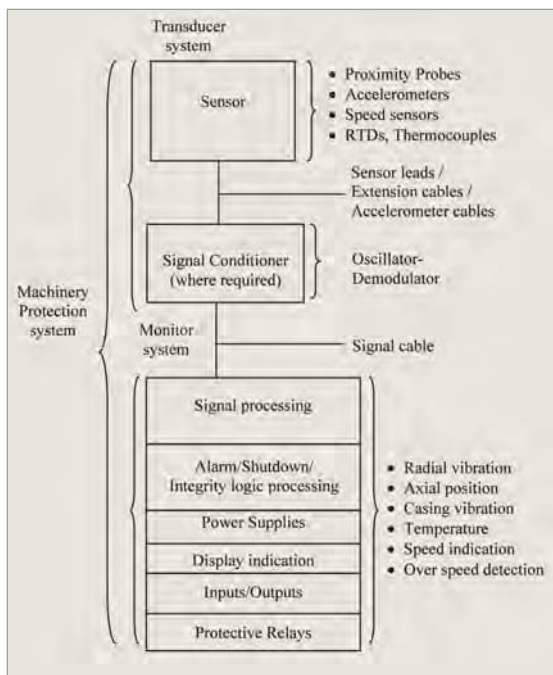


Fig. 3. Machinery protection system as per API standard 670

in different formats. The block diagram of Machinery Protection System is shown in Fig. 2.

The Embedded System consists of various hardware modules performing signal conditioning, data acquisition, signal processing and protection functions. These modules are fabricated as standard 6U cards interfaced with VME bus and installed in the 19" bin. The design of the system follows the guidelines given in the API Standard 670 for Machinery Protection Systems Fig. 3.

Embedded System Hardware

The Embedded System consists of following modules.

- Machinery Protection Module (MPM)
- Input Output Module (IOM)
- Relay Output Module (ROM)
- Power Supply Module (PSM)
- System Controller Module (SCM)

The arrangement of these modules as installed in a 19" bin with the front and rear view of the system bin is given in Fig. 4 and Fig. 5 respectively. A pair of MPM and IOM is connected back-to-back on the motherboard of 19" bin.

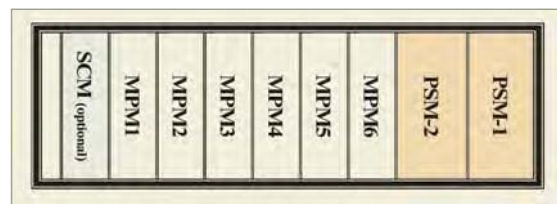


Fig. 4: Front view of embedded system of MPS.

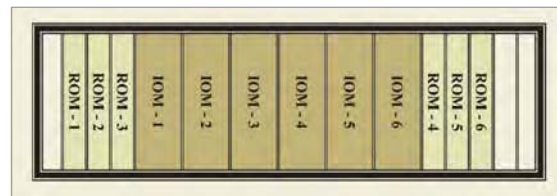


Fig. 5: Rear view of embedded system of MPS.

Machinery Protection Module (MPM)

The MPM acquires analog signals, processes the acquired inputs using a DSP and if any parameter exceeds the set alarm limit, it generates alarm. If the parameter exceeds the set trip limit then it generates a trip signal to the machinery. This module consists of DSP, Microcontroller, Memory, communication controller and other peripherals. The system configuration from the Engineering Console can be downloaded to MPM through onboard communication (Ethernet) controller. The MPM also sends the processed data to the Engineering Console through onboard Ethernet. This module can be used as standalone protection unit for small systems. Maximum of six MPMs can be accommodated in one MPS Bin.

The main features of MPM are:

- It can process 4 Dynamic (Vibration) channels and 2 Speed Channels.
- It can acquire signal from DC to 3.5 KHz as per the requirement.
- It performs digital filtering using DSP with configurable filter parameters.
- It performs signal processing functions like integration and rectification and provides signal parameters like peak, RMS.
- It monitors signal parameters for alarm and trip conditions and generates Alarm/trip with configurable Time delay and Hysteresis.

- It can process Dual channel to measure input parameters from two sensors in split range mode.
- It checks Sensor and Channel healthiness.
- It supports features like Danger bypass and Trip multiply.
- It gives LED indications on front facia for alarm/trip, sensor failure, MPM board failure and Power failure.
- It gives Raw buffered input signals on front facia through connectors for external monitoring and analysis.
- MPM is Hot swappable, so faulty module can be easily replaced online with healthy module.



Fig. 6: Machinery protection module (MPM) and Input output module (IOM) of MPS

Input Output Module forms the input output interface of MPS. IOMs are plugged in to the back planes mounted on the rear side of the MPS. MPM and IOM module are shown in Fig. 6. Interface between IOM and MPM is through backplane as shown in Fig.7. The inputs and outputs of the MPS are terminated on the screw terminals provided on the facia of IOM. This module provides signal conditioning for various sensors. This module also provides the power supplies to various transducers. Depending upon the type of transducer, power supplies can be selected using jumpers provided on the board. There is provision for over voltage

protection and short circuit protection on input and output side. Maximum of six IOM can be used in one MPS bin.

The main features of IOM are:

- Each IOM can be interfaced with 4 Dynamic (Vibration) and 2 Speed Sensors.
- Input signal range is -18V to +18V.
- It provides built-in power supply to various types of the sensors.
- Signal conditioning features include programmable gain and Programmable Supply to Sensors.
- It has provision to test each channel through reference input.
- It generates processed analog output (0-5V/4-20mA) for dynamic and speed sensors as well as pulsed output for speed sensors.
- It generates open collector outputs for driving relays of ROM on alarm and trip conditions.
- IOM is a Hot swappable module.

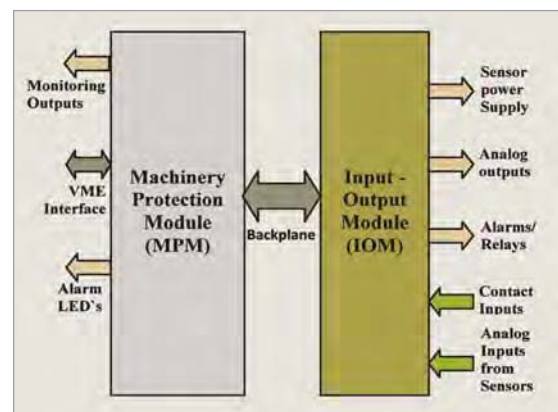


Fig. 7: Interface diagram of MPM and IOM

Relay Output Module provides relay outputs for alert and trip (danger) conditions. This board consists of 16 relays and one pair of contacts of each relay is available on the screw terminal mounted on the facia of the board. ROMs are plugged in to the back planes mounted on the rear side of the MPS as shown in Fig. 5. The relays in ROM are driven by the open collector signals generated in IOM and available in the back plane. These relay outputs can be dynamically configured from the Engineering Console. Maximum of six ROMs can be used in one MPS bin.

Power Supply Module (PSM) provides the power at required voltages to the modules as well as to the sensors connected to the system. The MPS can operate either from a single PSM or from dual-redundant current sharing PSMs. Each of the power supplies provides a contact output, which is fed to the terminal of IOM to show the health status of power supply. Indication of power supply 'ON' status is provided on the front facia of MPM.

System Controller Module (SCM) (optional) acts as an optional interface between the embedded system and engineering console to provide user configurability, data analysis and system diagnostics. It is a VME bus based CPU module with onboard Memory, Real time Clock, Watchdog and Ethernet. This module receives the configuration from the Engineering Console on Ethernet and forwards the configuration information to the respective Machinery Protection Modules on the VME bus.

The SCM can receive the processed data from the MPMs, perform additional analysis and processing functions, if required, and send the data to the Engineering Console for display. In case of failure of any channel the SCM can be used for dynamic re-routing of signals to spare healthy channels.

PC based Engineering Console (EC) is used for configuring the MPS and it also acts as a display station for MPS. It displays the data received from MPS in different formats like tabular, bar graph, trend etc. It also displays the alert/trip, diagnostic and various system states in message and LED display format.

The EC provides following functionality for MPS:

- Real time display of signal parameters (RMS and peak values) in bar-graph and tabular format with data update rate of 1 second (Fig.8).
- Colour coded visual indication of signal parameter crossing alarm/danger limits along with messages.
- Long term trend display of RMS values of parameters and viewing of real-time trend, real-time frequency spectrum, waterfall and orbit

plots Figs.9 & 10.

- Configuration function for changing alterable parameters like signal range, alarm trip/limits under password control.
- Creation of data files of parameters for further analysis.
- Display of status/indication for Communication link, Sensor, Channel health.
- Viewing, logging and time stamping of diagnostics messages and printing of signal plots, diagnostic messages and parameter change log and history.

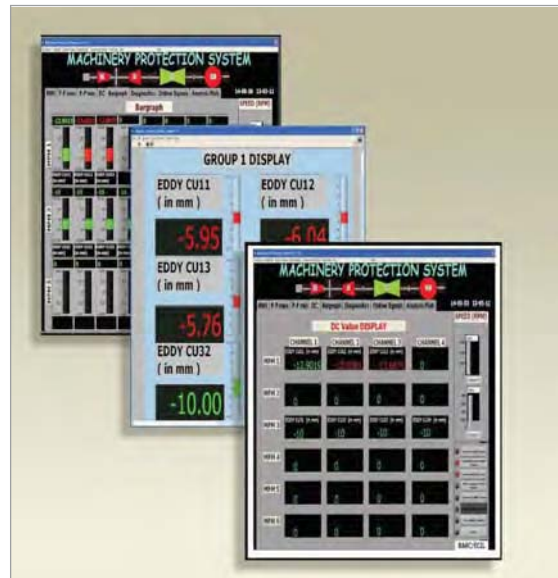


Fig. 8: Graphical user interface for MPS.



Fig. 9: Various analysis plots on GUI of MPS.

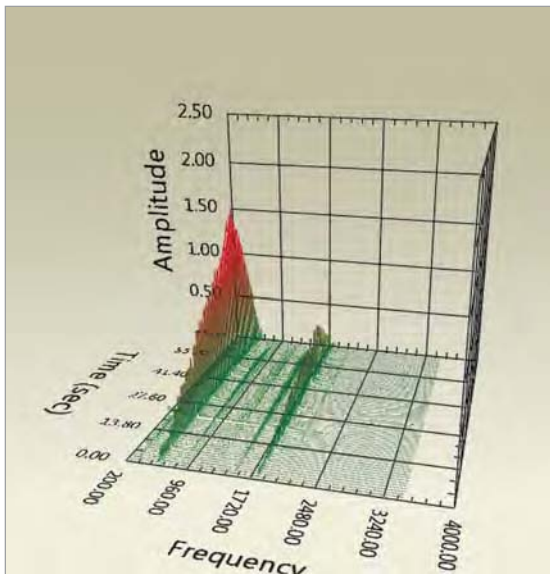


Fig. 10: Water fall plot

Special features, Interlocks and Display Functions

The system provides the following special features and interlocks:

Trip multiply feature There is a provision to multiply the values of alarm and trip threshold with a multiplication factor, and this is achieved by reading the status of a contact input implemented through a key switch. There is a provision to enable/disable the Trip Multiply feature from Engineering Console. The multiplication factor for trip multiply is configurable through Engineering Console.

Danger bypass (DB) interlock A Danger Bypass key switch is provided as a contact input to bypass the trip outputs. If the Danger Bypass input is true, system does not generate contact outputs for trip (danger) condition whereas it continues to generate the LED indications.

Display features The Engineering console provides an integrated display capable of displaying all measured vibration parameters, alarm (alert) and trip (danger) setpoints, DC gap voltages (for radial shaft vibration and axial position) and speed measurements. Displays of all vibration channels have a minimum resolution of 2% of full scale while

the speed channels have a resolution of 1 rpm. The displays are updated once every second.

Dynamically Re-routing feature System has provision of Dynamic signal bus and relay signal bus on the backplane. It is possible to suppress faulty channel operation automatically (through the SCM) and dynamically re-allocate the input sensor signal or relay output signal to spare healthy channels through the backplane without affecting the system operation.

Redundancy feature Redundancy in power supplies allows continued system operation even in the condition of failure of one power supply module.

Diagnostic features MPS provides various diagnostic features to ensure correct operation of the system. The main diagnostic features are listed below:

- The system checks healthiness of connected sensors. On detection of faulty sensors, it gives LED indication on MPM front facia and a contact output and also displays a message and LED indications on EC.
- Machinery protection module (MPM) checks the health state of its components and gives contact output and indication on the facia.
- MPM has inbuilt watchdog timer which checks the software flow of the program.
- System has a provision of user-invoked test signal inputs, which are applied to each channel to check their healthiness.

System Integration and Testing

The design and development of the system has been completed. Documentation in the form of Design Manual and User Manual has been prepared. The system was integrated into a 19" bin along with power supply modules and sensors and acceptance testing (functional and environmental) was successfully completed at Turbovisory Lab (Fig.-11) of ECIL, Hyderabad. The system has now been shifted for field trials at one of the NTPC plants near Delhi.



Fig. 11: Testing of MPS at ECIL

Conclusion

With the above development, an indigenous, state-of-art and user-configurable system is available to meet the requirements of machinery protection in various power plants and industries. The system will be manufactured and marketed by ECIL who will also provide long term maintenance support. This indigenous development will help in reducing the dependence on imported systems.

Acknowledgement

The authors express thanks to Shri Y. S. Mayya, Head, RCnD, Shri C.K.Pithawa, Associate Director (E&I) and Head, ED, BARC, Shri G. P. Srivastava, Director, (E&I Group), BARC for their constant encouragement and support for this project. The authors are also thankful to Shri R.V.Reddy, DGM, CAD, ECIL and Shri B. Kannaiah, Sr DGM,

CAD R&D, ECIL for their wholehearted support during development, fabrication and testing of the system.

References

1. Jain, Sanjay K, et al, Design Manual of Machinery Protection System, Rev0, Mumbai, Jan 2009.
2. Roy, D.A , et al, "Development of Machinery Protection System", International Conference on Vibration Problems, BESU, Howrah, Jan 2007.
3. Jain, Sanjay K, et al, "Machinery Protection System", Plant Maintenance Summit, FICCI, Bengaluru, May 2011.
4. Gaurav, et al, "Embedded PC based controller for use in VME bus based Data Acquisition System", PCaPAC-2012, VECC, Kolkata, Dec 2012.

Development of DSP Based Signal Acquisition and Processing System for Extrinsic Fabry-Perot Interferometric (EFPI) Fiber Optic Sensors

Ashwin Rathod, Shivam Mishra and Shrinkhla Ghildiyal

Precision Engineering Division
and

Sushil Bahuguna, Sangeeta Dhage and S. Mukhopadhyay

Control Instrumentation Division

Introduction

The advent of fiber optic sensors has brought numerous potential advantages over conventional electrical signal based sensors, such as small size and weight, immunity to electromagnetic interference, lack of sparking hazard, larger bandwidth, easy interface with data communication system, higher accuracy and resolution, and high multiplexing potentials. Along with this, the low optical loss of the fibers makes it possible to locate sensors far from the signal processing electronics. Their ability to withstand high level of radiation, temperature and pressure makes them ideal for applications in harsh environments. The optical fiber sensing proves to be a remarkably versatile approach in the field of measurement.

Indigenous development of Fiber Optic Sensors based on EFPI principle has been carried out for Pressure (Gauge), Temperature and Low Pressure (Absolute) transducers. The article presents the development of a DSP based signal acquisition and processing system for Extrinsic Fabry-Perot Interferometric (EFPI) sensors, jointly by Precision Engineering Division and Control Instrumentation Division. It describes the basic concepts of EFPI sensors and the algorithm used to estimate its cavity length. The hardware configuration and the implementation issues are covered in detail. The experimental results of an EFPI temperature sensor interfaced with this hardware have also been presented.

Fiber Optic Sensing

In an EFPI sensor, two mirrors (either or both mirrors could be ends of fibers, separated by an air cavity or any dielectric material other than fiber) form the interferometer. The distance between the two mirrors is called the cavity length or gap length. Fiber optic white-light interferometry (WLI) has been widely used to measure the cavity length of an EFPI. This technique allows absolute and unambiguous measurements over a wide range and is insensitive to the light source instability. WLI uses a broad band light source to illuminate the sensor and a spectrometer senses the optical signal. A change in the physical parameter, to be measured, causes a calibrated change in the cavity length of the EFPI. Hence the primary objective is to get an accurate and reliable measure (calibration) of cavity length. By using different transduction principles, different type of EFPI sensors can be developed.

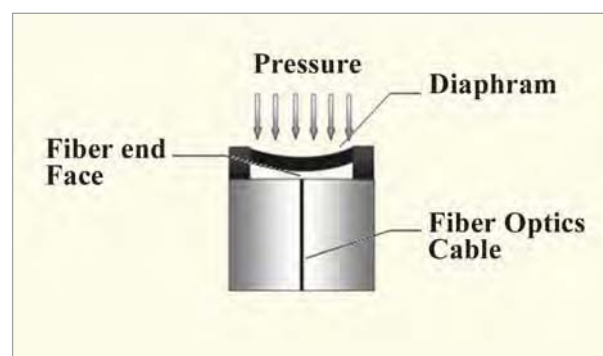


Fig. 1: EFPI configuration formed using a fiber end and a diaphragm.

Fig. 1 shows an EFPI pressure sensor. The diaphragm indicated has its inner surface polished using nano finishing, forming one of the EFPI mirrors, while the fiber end face forms the second. Increase in pressure causes the diaphragm to deflect, changing the cavity length of the EFPI. By measuring the cavity length the pressure can be determined. On similar lines thermal expansion of an element can be used to cause transduction in an EFPI temperature sensor.

Cavity length Measurement

The interference spectrum acquired from the spectrometer needs to be demodulated to compute the cavity length (or gap length) of the EFPI sensor. As the physical parameter to be measured cause a direct change in the cavity length, the measurement of cavity length gives the estimation of the measurand as shown in Fig. 2. Such a system is not unique to one type of sensing. They remain generic to all EFPI sensors measuring any physical parameter. The basic principle is to be able to let the physical parameter, to be measured, bring about a change in the cavity length that can be calibrated in terms of the physical parameters.

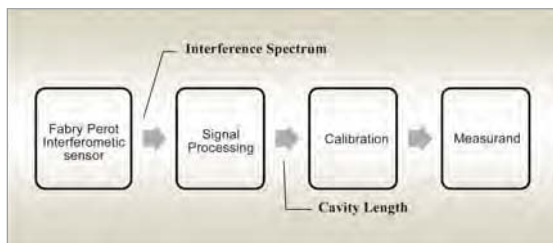


Fig. 2: Signal processing for EFPI sensors

The sensor system shown in Fig. 3 consists of a broad band light source (Tungsten halogen lamp or SLED) that transmits light to the sensor via a fiber optic cable. The reflected interference signal, coupled back in to the fiber returns to an optical splitter. The splitter sends a portion of the light to a spectrometer. The spectrometer uses a CCD array to detect the incoming spectrum. The data from the CCD array can then be processed using a cavity length estimation algorithm explained in the next section to finally compute the cavity length.

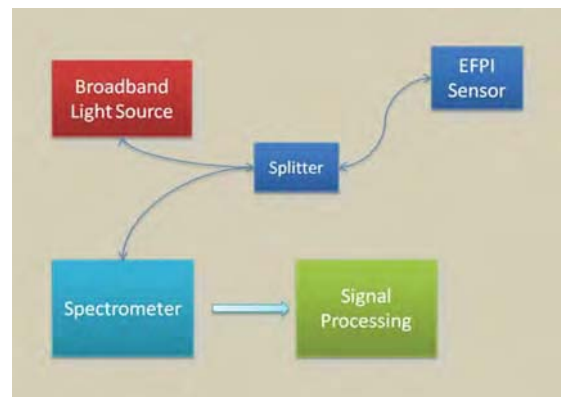


Fig. 3: Fiber optic sensor system

The cavity length estimation algorithm developed to compute the cavity length of the EFPI uses wavelet based denoising for pre-processing of the spectrum signal followed by Hibert transform to compute the instantaneous phase of the spectrum [1]. Least squares regression is used to compute the EFPI cavity length. The optimal length of the spectrum for cavity length computation can be determined from the study carried out in [1]. The algorithm mentioned requires extremely large number of mathematical computations and thus needs highly accelerated signal processing hardware for real time measurement with a considerably large sampling frequency.

Cavity Length Estimation Algorithm

The spectrum signal of an EFPI can be expressed as

$$x(\lambda) = a(\lambda) + b(\lambda) + \cos\left(\frac{4\pi}{\lambda} l + \pi\right) + c(\lambda) \quad (1)$$

where l is the cavity length and $2l$ is the total optical path difference; $a(\lambda)$ is the low frequency envelope present predominantly due to a combination of responses on various components of the system viz., light source, splitter, grating, CCD array; $b(\lambda)$ is the contrast which is influenced by the cavity length and the reflection of fiber ends and $c(\lambda)$ is noise. The constant phase π is added due to the reflection occurring on the second surface of the interferometer. Fig. 4 shows a typical optical spectrum signal acquired from an EFPI. In this particular experimental set up, the EFPI sensor has been formed using a single mode fiber (SMF) facing

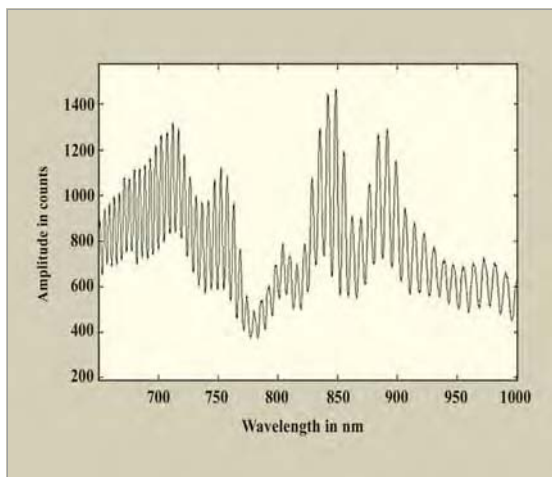


Fig. 4: Optical spectrum signal obtained from an EFPI using an optical spectrum

an Aluminium mirror. The Aluminium mirror surface has been finished using Diamond Turn Machining (DTM) having a surface finish of 10nm (peak to valley) approximately.

By using Discrete Wavelet Transform (DWT) the frequency content (measurement is in wavelength of the spectrum) of the signal could be analyzed at multiple resolutions or scales. The decomposition is carried out by passing the signal through a half band low pass filter at each scale followed by a half band high pass filter. The output of the low pass filter is called the approximate coefficient and the output of the high pass filter is called the detailed coefficient. Subsequently, each low pass filter output is down-sampled, obeying Nyquist's rate, as each of these signals is band limited ideally to half the frequency range. The above procedure, referred to as sub-band coding is repeated for the approximate coefficients to obtain further levels of decomposition. By appropriately thresholding the approximate and detailed coefficients and then combining them by the process of reconstruction (using inverse Wavelet Transform), the envelope and high frequency noise can be eliminated from the spectrum signal. In the present case, 8 level wavelet decomposition has been implemented for pre processing of spectrum signal. Instantaneous phase of the denoised spectrum signal can be obtained using Hilbert Transform.

$$\varphi(\lambda) = \left(\frac{4\pi}{\lambda} \right) l \quad (2)$$

Hilbert Transform is numerically implemented using Fast Fourier Transforms (FFT). The method involves transforming the signal in the frequency domain using FFT. Coefficients at positive frequency are doubled and those at negative frequency are reduced to zero. An inverse FFT of the modified frequency domain signal gives the analytic representation (an array of complex numbers) of the signal. The argument or the phase of the complex number gives the instantaneous phase. $\varphi(\lambda)$ thus computed is wrapped around $-\pi$ to π . An unwrapping algorithm is used to unwrap the phase. This unwrapped phase bears a linear relation with $(1/\lambda)$ as seen in (2), the absolute value of the slope of the line being equal to 4π times the cavity length.

In order to process a spectrum having a frame length of 1024 points, a total of 286,600 flops are needed for the present algorithm. The pixels of the CCD are currently read in a linear fashion imposing a restriction on the minimum time of 7.2 ms, required to digitize one full frame of spectrum data. DSP based dedicated hardware simultaneously manages 1) all house-keeping activities and 2) transfer of data to a permanent storage in 3.2 ms. Hence, time available for processing EFPI signal is only 4.0 ms. Sampling frequency however is decided by real time process requirements and may need to be increased, thereby reducing available processing time further. The DSP processor selected for the application is capable of executing 1.2 Giga flops and takes 0.25 ms to perform the total number of 286,600 floating point operations. It is evident that in order to meet the processing requirements in the stipulated time a dedicated DSP processor based hardware is essential for the application.

Signal Processing Hardware

As explained earlier the sensor system includes a light source, an EFPI sensor and a spectrometer connected using an optical splitter. The signal acquisition and processing system acquires the CCD output of the spectrometer, subsequently processing

it to compute the cavity length. Fig. 5 shows the block diagram of the EFPI sensor signal processing system.

The spectrometer shown, an original equipment manufacturer (OEM) device is a symmetrical Czerny-Turner design with a fiber optic entrance connector, collimating and focusing mirror, diffractive grating and linear CCD sensor. The signal acquisition and processing hardware consists of a floating point Digital Signal Processor (DSP) along with an FPGA. The FPGA generates control signals for CCD sensor in spectrometer and to the peripherals on board. The DSP processor acquires the spectrum frame, processes it online for the estimation of EFPI cavity length as per the cavity length estimation algorithm and transfers the processed results to the host computer for display of parameters.

The signal acquisition and processing tasks are made to run in parallel by implementing a FIFO on the FPGA. The analog signal from spectrometer is digitized on board by a 16 bit ADC and the output is stored in FIFO. After acquisition and storage of one full frame of signal in FIFO, an interrupt is generated for the DSP processor by the FPGA. DSP copies the data from FIFO and stores it in its internal RAM for further processing. As the FPGA controls the acquisition and fills the FIFO with next frame, the DSP processor processes an earlier frame. A flash memory provided on board is used to store important calibration data. An ethernet module communicates the computed cavity length along with raw and filtered spectrum to the host computer.

As shown in the detailed block diagram, the FPGA generates necessary control signals required to run the CCD sensor present in the spectrometer. The analog CCD output is shifted serially, pixel wise, and is digitized using the ADC at a rate of 500 kHz. The ADC works in sync with the CCD sensor using control signals also generated using the FPGA. The entire digitized spectrum frame is stored in a FIFO created within the FPGA.

The 200MHz DSP processor core used has the capability of single cycle execution of an instruction. The single instruction and multiple data (SIMD) structure of the DSP processor is used efficiently for faster implementation of processing algorithms. Floating point DSP processor features an enhanced Harvard architecture. With its separate program and data memory buses and on chip instruction cache, the processor can simultaneously fetch two operands and an instruction (from the cache), all in a single cycle. Processor core contains three independent, parallel computation units i.e. the arithmetic/logic unit (ALU), multiplier and shifter for maximizing the computational throughput. Wavelet filtering of spectrum signal uses large number of convolution operations. There are three basic operations in a convolution namely shift, multiply and accumulate. The multiply and accumulate (MAC) operation requires filter coefficients and signal samples to be stored in program data memory and data memory respectively or vice versa which would allow the operation to execute in a single cycle. The efficient utilization of DSP hardware for in-situ computation in MAC minimizes the execution time of the wavelet de-noising algorithm.

Prototype Development of Signal Processing

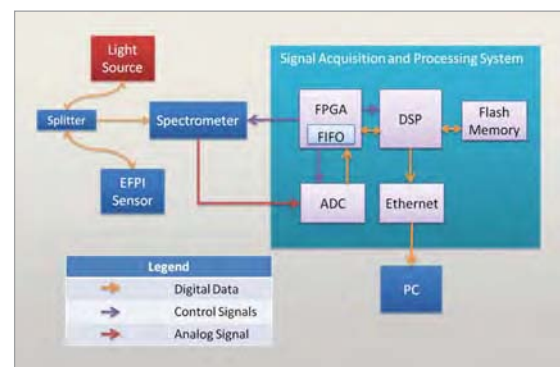


Fig. 5: Block diagram of EFPI signal processing system

System

Prototype development of the system includes the development of data acquisition and signal processing hardware and power supply card, implementation of signal processing algorithm on

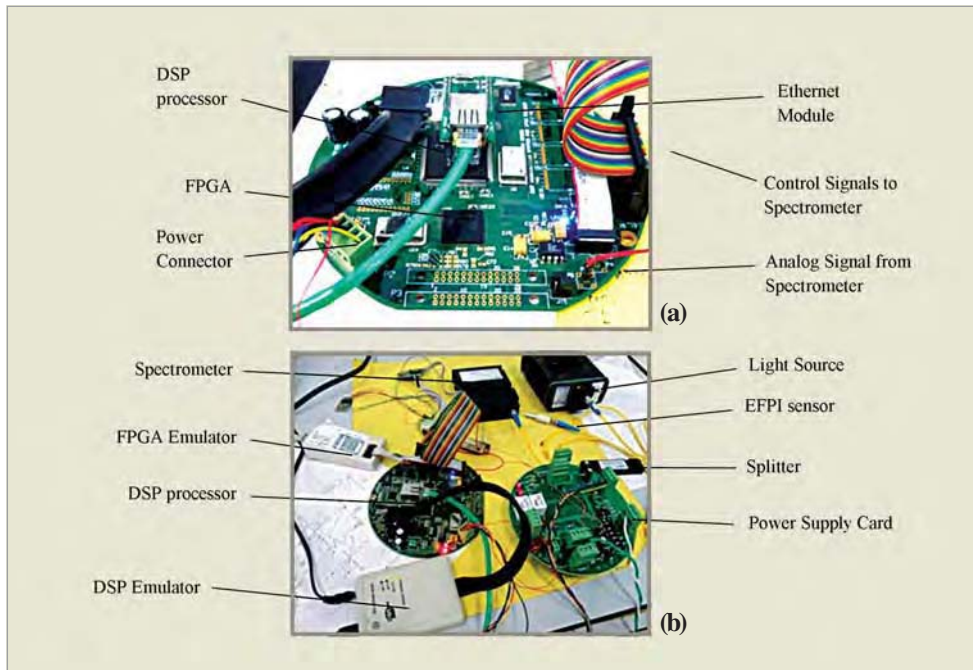


Fig. 6: Prototype hardware. (a) Signal processing and acquisition card. (b) Test setup

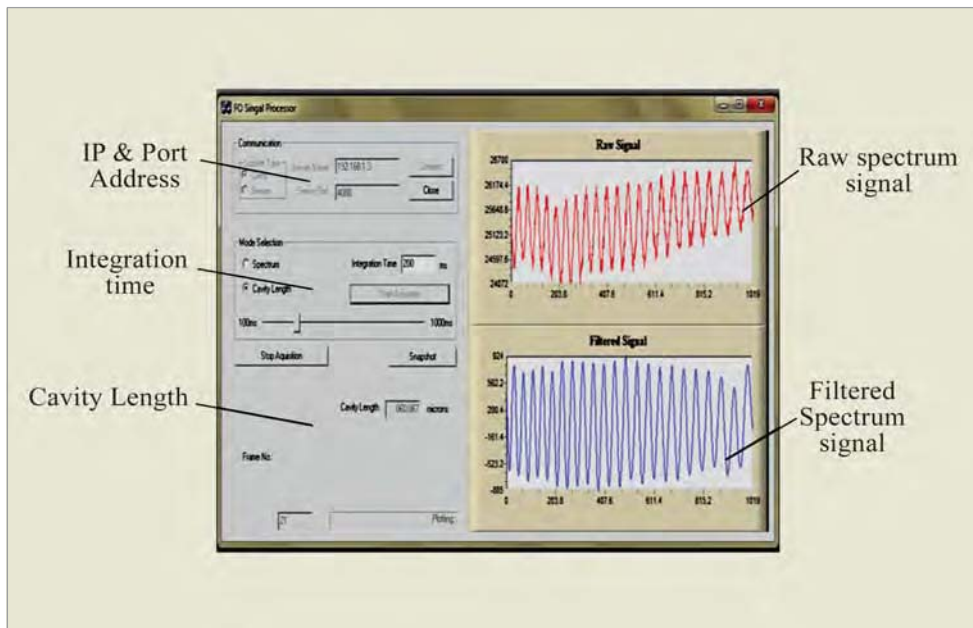


Fig. 7: Snapshot of the user interface

DSP-FPGA hardware, building a graphical user interface on host computer and system integration. Fig. 6 show the experimental setup which includes optical setup, DSP based signal acquisition and processing electronics, power supply, and necessary debugging emulator.

Fig. 7 shows the Graphical User Interface (GUI) displaying the cavity length of the EFPI, and raw and filtered spectrum on separate charts. The interface also allows the user to set the parameters needed by spectrometer. As seen in the figure, the left side of the GUI allows the setting of IP and Port

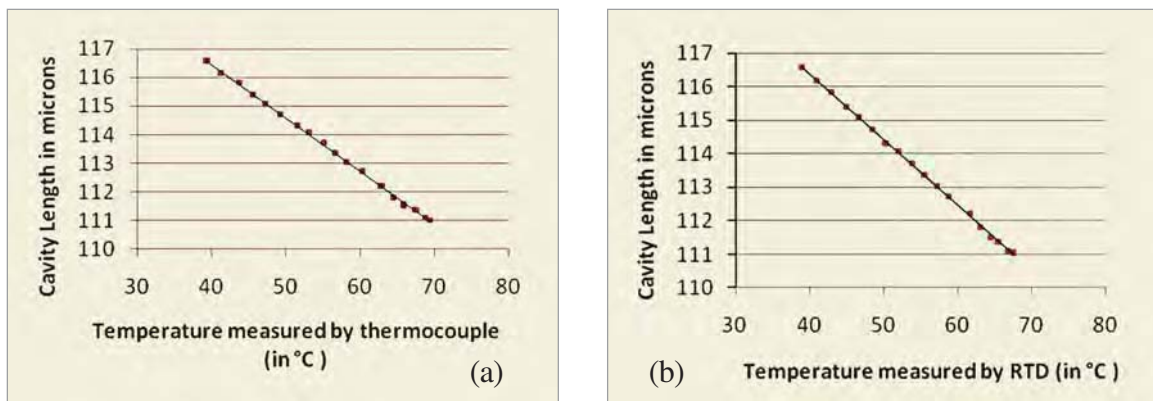


Fig. 8: Cavity length of EFPI temperature sensor versus (a) thermocouple and (b) RTD

address for communication with DSP hardware via the ethernet module. The Integration time can be set from 1 ms to 10000 ms. The cavity length is displayed in microns. The right side of the GUI shows the spectrum signal. The top chart show the raw spectrum signal from the spectrometer in red and the bottom chart shows the wavelet denoised signal with the pixel number on the X-Axis and the amplitude on the Y axis.

EFPI Application

A prototype extrinsic EFPI temperature sensor developed and fabricated at PED, BARC was interfaced with the acquisition and processing system. The thermal expansion of a metallic object placed in front of a fiber causes a change in the cavity length of the EFPI. Thus by estimating the cavity length, using processing hardware, the temperature could be computed. The sensor was tested and compared with conventional temperature sensors (thermocouple and RTD). The cavity length estimation algorithm was implemented on prototype DSP hardware for computation of cavity length. Fig. 8 shows the variation of the cavity length of the prototype EFPI temperature sensor as compared to the temperature measured by thermocouple and RTD.

These temperature sensors can prove to be extremely useful in providing real time temperature monitoring

of transformer winding temperature, owing to their immunity to EMI/RFI. Similarly they can be effective in temperature monitoring of generator winding, microwave and induction heating and various bio-medical equipments involving harsh RF-environments such MRI and NMR.

Conclusion

This article reports in-house implementation of EFPI sensor cavity length estimation on a DSP hardware. The DSP based processing hardware is not specific to any one type of sensor. It could be used to measure any external measurand by using the right transduction principle. This would prove to be a huge advantage while multiplexing sensors. Such systems would not be constrained to multiplexing different types of sensors in one unit, For example, temperature, pressure and accelerations sensors could be multiplexed in one acquisition and processing system. Development of the systems for actual deployment is in progress.

References

1. Rathod A., Mishra S., Ghildiyal S., Mukhopadhyay S. "Transform Domain Methods for Performance Enhancement of EFPI Sensor". *Sensors and Actuators A: Physical*, 189 (2013) 1-7

Report on DAE-BRNS 4th Interdisciplinary Symposium on Materials Chemistry (ISMC – 2012)

The DAE-BRNS 4th Interdisciplinary Symposium on Materials Chemistry (ISMC-2012), organized by Chemistry Division and Society for Materials Chemistry, was held at BARC during 11-15 December, 2012. With an overwhelming response from participants from India and abroad, the symposium was convened with 34 invited talks and about 500 contributed papers covering frontline research in diverse areas of material science such as nuclear materials, nanomaterials, thin films, devices and sensors, materials for energy conversion and storage, biomaterials, magnetic materials, catalysts, soft matter, carbon based materials, high purity materials, organic materials, computational materials chemistry and so on. The deliberations were focused on materials research programmes for harnessing power from nuclear fission, fossil fuels, hydrogen and other sources. The development of new

technologies based on nanomaterials for the above applications e.g. in separation science and sensors was discussed at large. Dr. Srikumar Banerjee, DAE Homi Bhabha Chair Professor and former Chairman, Atomic Energy Commission, in his keynote address highlighted the importance of materials chemistry in emerging technologies. In particular, he emphasized on materials for nuclear technology and environment.

Speakers from India and abroad delivered invited talks on a variety of topics such as nanotechnology-driven cancer therapy, materials issues in solar cells, functional materials, complex chemical hydrides for hydrogen storage, diamond thin films for electronics, non-linear dielectric nano-crystals, protonic-anionic mixed conduction ceramics, high performance electrolytes for solid oxide electrochemical cells, etc.



From Left to Right: Dr. A. K. Tyagi, Dr. D. Das, Dr. S. Banerjee, Dr. T. Mukerjee

A Brief Report on National Seminar-cum-Workshop on 'Water and Energy: Sustainability and Security for Future Needs'

The National seminar cum workshop on 'Water and Energy: Sustainability and Security for Future Needs', 'WAVE 2012' was organized at Dwarkadas J. Sanghvi College Of Engineering in Association with Indian Institute of Chemical Engineers- Mumbai Regional Center(IICHe-MRC) and Indian Desalination Association(InDA) on 27th& 28th September 2012 at D.J. Sanghvi College Of Engg, Vile-Parle,Mumbai-56.

Various dignitaries like Mr. V. K. Srivastava, Chairman of IICHe-MRC and Head, Thermal Desalination Section, BARC Mumbai; Dr P. K. Tewari, President of InDA and Head Desalination division, BARC Mumbai; Mr. D. P. Mishra, Past President of IICHe; Dr. D. J. Shah, founder principal of D.J.Sanghvi College of Engineering (DJSCE) ,Professor and

Former Dean of MPSTME; Dr Hari Vasudevan, Principal of DJSCE; Dr. V. Ramesh, Prof. of Chemical Engineering Department of DJSCE and Dr. (Mrs.) Alpana Mahapatra, Organizing Secretary of Seminar, Professor and former HOD of DJSCE, spoke about how sustainable development was the need of the hour and how this seminar was an interface for industry and academia interaction during the inaugural session. The vote of thanks of the inaugural session was proposed by Dr. (Mrs.) Alpana Mahapatra.

After the inauguration ceremony, invited talks by eminent speakers from BARC and several industries were delivered on various tones related to Water & Energy security.



Release of the souvenir and abstracts

Report on the IPA Theme Meeting on “Synergy in Physics and Industry, (SPI -2013)”

An IPA (Indian Physics Association) theme meeting entitled “Synergy in Physics and Industry (SPI-2013)” was organized by Bhabha Atomic Research Centre and held at the Multi purpose Hall, Training School Hostel, Anushaktinagar, Mumbai during Jan. 21-22, 2013. The purpose of the meeting was to discuss and suggest ways to enhance co-operation between physics research (and also research in other fields) in academic institutes (Government laboratories and universities) and industry so that academic institutes could meet the requirements of industry and industry may better absorb knowhow developed in academic institutes and use it for production. This meeting was primarily focused on the following four topics: (i) energy, (ii) automobiles, (iii) medical diagnostic and devices and (iv) plasma and micro-fabrication technology. The meeting comprised of three plenary talks and sixteen invited talks by eminent scientists and industry participants, and a poster session. In addition, there was a special panel discussion that was chaired by Prof. R. Chidambaram. (PSA to Govt. of India) and participated by eminent personalities from industry: Dr. A. K. Gupta (Pallonji Shapoorji), Dr. KVS N Raju (President, M/s Elico, Hyderabad) as well as academia: Dr. S. Mubashir, (DST), Dr. S. Kale, (BARC), Prof. R. Thekkedath (VC, Cochin university) and Dr. S. Kailas (BARC).

This meeting focused on discussions pertaining to the state-of-the-art affairs at both industry and academia and emphasized the need of having a strong interaction between research community, industry and law making agencies in such a way that their interests find a common expression.

Some of the specific suggestions for development of technology oriented industry that may take of modern day challenges for development of the country are as follows:

1. During the deliberations, it was proposed to develop a National level committee: This committee would be expected to look into the various possibilities of establishing synergy between the industry and the academia. It would look into the possibility of providing a platform enabling discussion and debate required to access both ‘know-how’ and ‘know-why’ that is crucial to realize all the three phases of product development namely design, development and delivery, and ultimately a technological leadership.
2. **Technology parks:** National level technology parks would be set up by the Government with advanced research facilities in select areas where both industry and academic researchers may work in close association.
3. **Academia driven consortiums:** A consortium where academia would provide major support in terms of knowhow and finance. In this consortium, the training of the already existing knowhow with academia/government may be imparted to the industry.
4. **Industry driven consortiums:** A consortium where industry would play dominant role would also be set up. In this consortium, industry would bring their scientific problems pertaining to the product development, which would be taken up by the academia.

BARC Scientists Honoured

Name of the Scientist : **A.K. Tyagi**
Affiliation: **Chemistry Division**
Award : Fellow, Indian Academy of Sciences (FASc)
Conferred by : Indian Academy of Sciences

Name of the Scientist : **H.N. Ghosh**
Affiliation : **Radiation and Photochemistry Division**
Name of the Award : Fellow, Indian Academy of Sciences (FASc)
Conferred by : Indian Academy of Sciences

Name of the Scientist : **Vinita Grover Gupta**
Affiliation : **Chemistry Division**
Name of the Award : INS Young Scientist Award
Conferred by : Indian Nuclear Society



V. R. Chavan
Metal Art Work

Published by:
Scientific Information Resource Division,
Bhabha Atomic Research Centre, Trombay, Mumbai 400 085, India

BARC Newsletter is also available at URL:<http://www.barc.gov.in>